LBL-169
c.2

RECEIVED
LIBRARY
RADIATION LABORATORY

DOCUMENTS SECTION

PRESSURE (UP TO 40 KBAR) AS A PARAMETER IN THE STUDY OF VIBRATIONAL EXCITON LEVELS AND CRYSTALLINE POTENTIALS OF MOLECULAR CRYSTALS: NAPHTHALENE AND N-PARAFFINS

Che-Kuang Wu
(Ph. D. thesis)

October 1971

AEC Contract No. W-7405-eng-48

TWO-WEEK LOAN COPY

This is a Library Circulating Copy which may be borrowed for two weeks. For a personal retention copy, call Tech. Info. Division, Ext. 5545

LAWRENCE BERKELEY LABORATORY
UNIVERSITY OF CALIFORNIA

LBL-169
c.2

25

DISCLAIMER

This document was prepared as an account of work sponsored by the United States Government. While this document is believed to contain correct information, neither the United States Government nor any agency thereof, nor the Regents of the University of California, nor any of their employees, makes any warranty, express or implied, or assumes any legal responsibility for the accuracy, completeness, or usefulness of any information, apparatus, product, or process disclosed, or represents that its use would not infringe privately owned rights. Reference herein to any specific commercial product, process, or service by its trade name, trademark, manufacturer, or otherwise, does not necessarily constitute or imply its endorsement, recommendation, or favoring by the United States Government or any agency thereof, or the Regents of the University of California. The views and opinions of authors expressed herein do not necessarily state or reflect those of the United States Government or any agency thereof or the Regents of the University of California.

Table of Contents

Abstract v

I. Introduction 1

II. Theory 4

A. Symmetry Consideration and Factor Group Analysis 4

B. The Perturbation of the Crystalline Force Field on the Internal Vibration 16

C. Internal Vibrational Energy Levels (vibrational exciton levels) of Molecular Crystals 23

D. Intensity 33

E. Selection Rules for Combinations and Overtones 36

F. Experimental Methods 37

III. Instrumentation 41

A. Pressure Devices 41

B. Optics 42

C. Pressure Scale and Presicion of the Measured Frequencies 46

IV. Experimental Results, Calculations and Discussions (Part I and Part II) 51

Part I.
Naphthalene

A. Blue and Red Shifts 51

B. Discussion of Non-Bonded Interatomic Potential 62

C. A Direct Observation of Resonance Phenomenon and Calculation of Unperturbed Levels as well as Coefficients of Mixing 63

D. Application of High Pressure Crystalline Data on Molecular Vibrational Assignment 78

Part II.
N-Paraffins and Polyethylene

A. Pressure Effects on the Spectra of N-Paraffins 81

1. Odd-Numbered N-Paraffins--n-$C_{23}H_{48}$ and n-$C_{29}H_{60}$ . . 93

2. A Comparison of Pressure Effects among Various Crystal Sturctures 103

B. Applications 114

1. Non-Bonded Hydrogen Repulsion Potential 116

2. Volume and Wave Vector Dependence of Gruneisen Parameters 121

Acknowledgments 133

Appendix

I. Overtone and Combination Transitions 134

II. An Estimation of the Separation of an Unresolved Doublet 137

References 139

PRESSURE (UP TO 40 KBAR) AS A PARAMETER IN THE STUDY OF VIBRATIONAL EXCITON LEVELS AND CRYSTALLINE POTENTIALS OF MOLECULAR CRYSTALS: NAPHTHALENE AND N-PARAFFINS

Che-Kuang Wu

Inorganic Materials Research Division, Lawrence Berkeley Laboratory
and Department of Chemistry; University of California,
Berkeley, California

ABSTRACT

An infrared spectrophotometer is modified for the quantitative study of high pressure spectra. The infrared absorption spectra of naphthalene, n-paraffins, ($C_{23}H_{48}$, $C_{24}H_{50}$, $C_{28}H_{58}$, $C_{29}H_{60}$) and polyethylene are measured to a pressure of 40 kbar. It is observed that at least two pairs of energy levels behave as if they are in resonance. It is possible that they are examples of Fermi resonance. The corresponding unperturbed energy levels as well as the coefficients of mixing at various pressures are calculated. Interaction force constants between non-bonded hydrogens, in the expression, $\beta = Ar^{-(B+2)}$, are calculated from the pressure dependence of factor group splittings of n-paraffin rocking modes. Microscopic Grueisen parameters of n-paraffins are obtained as a function of unit cell volume and chain wave vector. Many other aspects of pressure effects are observed and discussed. Additional experiments and theoretical studies are suggested.

A physical model is proposed to distinguish two types of dynamic crystalline forces as well as to illustrate how an intramolecular potential is perturbed by the crystalline potentials which cause pressure induced frequency shifts and factor group splittings.

I. INTRODUCTION

Exciton theory was first introduced by Frankel[1] in 1931 and was applied to the electronic levels of molecular crystals. Since then, there has been a great deal of work on this topic. To date, the theory has been discussed and expanded in books written by Davydov,[2] Craig and Walmsley,[3] Dexter and Knox,[4] and in review articles by Fox and Schnepp,[5] and McClure.[6]

The application of the theory to the vibrational levels of molecular crystal was initiated by Hornig.[7] Hexter[9] extended the electronic exciton theory to include the vibrational wave function. To date, there are excellent articles on this aspect of the theory by Hass,[10] Halford,[11] Duyckaerts,[12] Hexter,[13] Vedder and Hornig,[14] and Dows.[15]

In exciton theory, the crystalline energy levels are considered as those of the gas state perturbed by a crystalline potential. By carrying out a perturbation treatment (mathematically very complicated, since there are Avogadro number of molecules in the system to be considered), the frequency shift from the gas to the solid state is expressed as a function of a crystalline perturbation potential.

For the electronic energy levels of molecular crystal, great success in explaining the frequency shift of gas to solid was achieved by assuming that the crystalline force field is simply the dipole-dipole interaction force. Multipole interactions are taken into consideration in a refined treatment.

The perturbation potential used to explain the shift in electronic levels was applied to the vibrational energy levels with little success. Recently, it was shown that the short range repulsion force alone may account for the so-called factor group splitting for some of the

vibrational bands of the molecular crystals; paraffins,[55] ethane, CH_3Cl[41] and naphthalene.[42] However, the repulsive potential function alone can not explain the frequency shift of gas to solid for the corresponding energy levels.*

At the present time, several theoretical and experimental groups are attempting to understand the nature of the perturbation potential.

In the literature, the frequency shift and Davydov splitting are often described; the former, as due to a static crystalline potential and the latter as due to a dynamic crystalline potential. The use of the terminology "static crystalline potential" in this case is quite misleading, since it does not follow the usual definition, e.g. the static lattice potential defined in the Mei Grueneisen equation of state.

The presentation of section B and C in the chapter on theory is designed to clarify the misconception which arose from the loose usage of the terminology "static crystalline potential," as well as to gain further understanding in the physics of the crystalline perturbation on the intramolecular vibrations.

The crystalline potential is usually approximated by the sum of intermolecular pair potentials. The intermolecular pair potential is a power series of infinite terms. However, for a given intermolecular distance, the pair potential may usually be truncated to two terms. If one hypothetically decreases the density of a crystal continuously to that of a gas, the intermolecular distance of the nearest neighbor is changed from the unit cell dimension (or a fraction of it) to infinite.

---

*Various types of forces considered by Pimentel[43] in the matrix study may play a part in the crystalline force field of single crystals. Electrostatic dipole-dipole interaction forces have been worked out by Decius for a number of ionic crystals.[44]

The force is scanned through all values of the power series. It is obvious that in order to gain information on the intermolecular force, the knowledge of frequency for a given crystal structure as a function of density is necessary; that is, the mere knowledge of the frequencies of the gas and solid state at room pressure and temperature is insufficient. Since larger changes in unit cell dimensions can be achieved by varying pressure rather than temperature, high pressure studies of molecular crystals are thus desirable for obtaining information on the intermolecular force fields. This as well as several other applications of high pressure IR spectra are presented in Chapter IV.

In Chapter III an experimental set-up is described which makes a quantitative study of IR spectra, under very high pressure, using a Drickamer type NaCl cell possible for the first time.

II. THEORY

A. Symmetry Consideration and Factor Group Analysis

A crystal lattice can be constructed from a unit cell by the translation operation which carries any unit cell into any other. The unit cell is the smallest unit in which no atoms are equivalent under simple translations. However, some of the atoms in a unit cell may be equivalent under operations of the symmetry elements of a unit cell group. The unit cell group is isomorphous with one of the 32 point groups possible in crystals, but may contain such operations as screw axis or glide planes in addition to purely point operations. The space group is defined as the product of the operations of the unit cell group and those of the infinite group of translation. The space group is then an infinite group. However, if we define the translations which carry a point in a unit cell into the equivalent point in another cell as identity, the space group is reduced to the unit cell group. Thus the unit cell group is the factor group of the space group.

Any point in the lattice is a site, and in certain locations some symmetry element of the space group passes through the site. The point group of symmetry operations that leave the site invariant is called a site group. The site group must be a sub group of both the factor group and the molecular point group.

It is known from the theory of small vibrations that it is possible to find normal coordinates for any atomic system, such that both the kinetic and potential energy do not involve cross terms. In mathematical form, the kinetic energy T, and potential energy V, of the entire crystal may be written as

$$2T = \sum_{i}^{3ntN-6} \dot{Q}_i^{\,2} \qquad (1)$$

$$2V = \sum_{i}^{3ntN-6} \omega_i \, Q_i^{\,2} \tag{2}$$

Where n is the number of atoms per molecule, t molecules per unit cell, and N is the number of unit cells. In this case, the motion of the system (a molecular crystal here) can be resolved into the motions of a set of independent harmonic oscillators of angular frequency ω_i and normal coordinate Q_i. The vibrational wave function for the entire crystal is then

$$\Phi = \prod_{i}^{3ntN-6} \Psi_{v_i}(Q_i) \tag{3}$$

where $\Psi_{v_i}(Q_i)$ are given explicitly by

$$\Psi_{v_i}(Q_i) = \exp[-(\pi\omega_i/h)Q_i^{\,2}] \times H_{v_i}[(2\pi\omega_i/h)^{1/2}\, Q_i] \tag{4}$$

where H_{v_i} is the Hermit polynomial of degree v_i. The energy levels in the harmonic approximation are given by

$$E = \sum_{i} (v_i + \tfrac{1}{2})h\nu_i \; ; \quad v_i = 0,1,2 \cdots \tag{5}$$

Since T and V are to be invariant under all of the operations of the space group of the crystal, the coordinates Q_i must transform as an irreducible representation of the space group. The functions H_{v_i} are odd or even functions of Q_i according to whether v_i is odd or even. If Q_i belongs to a non-degenerate irreducible representation of the space group, the corresponding Ψ_{v_i} transforms either as Q_i or the totally symmetric representation of the space group according to whether v_i is odd or even. The vibrational ground state $\Phi_{\Sigma v_i=0}$ is non-degenerate and belongs to the totally symmetric irreducible representation of the space group even if there are degenerate as well as

non-degenerate normal modes.

For a pure vibrational spectrum, the electronic state remains unchanged. The vibrational transition probability is proportional to the square of the transition dipole moment.[16]

$$[\mu]_v^{v'} = \int \Phi_{v'}^* \, \mu \, \Phi_v \, d\tau \tag{6}$$

In this equation v and v' stand for the set of vibrational quantum numbers in the lower and upper state respectively. If one expands the dipole moment of the crystal μ in a power series of the normal coordinates, then

$$\mu = \mu_o + \sum_i \left(\frac{\partial \mu}{\partial Q_i}\right)_o Q_i + \cdots \tag{7}$$

When the higher terms in the development of Eq. (7) are neglected, upon substituting Eq. (7) into Eq. (6), we obtain

$$[\mu]_v^{v'} = \mu_o \int \Phi_v \Phi_{v'}^* \, d\tau + \sum_i \left(\frac{\partial \mu}{\partial Q_i}\right)_o \int \Phi_{v'}^* \, Q_i \Phi_v d\tau \tag{8}$$

The first term on the right vanishes if $v \neq v'$ since the vibrational eigenfunction of different states are orthogonal to one another. According to Eq. (3)

$$\int \Phi_{v'}^* \, Q_i \Phi_v d\tau = \prod_{j \neq i} \int \Psi_{v_j'}^* \, \Psi_{v_j} dQ_j \int \Psi_{v_i'}^* \, Q_i \Psi_{v_i} dQ_i \tag{9}$$

The integrals, $\int \Psi_{v_j'}^* \Psi_{v_j} dQ_j$, are different from zero only when $v_j = v_j'$, i.e. $\Delta v_j = 0$; while $\int \Psi_{v_i'}^* Q_i \Psi_{v_i} dQ_i$ is different from zero only when $\Delta v_i = \pm 1$. The transition energy is the same for all different v_i initial states and the intensities differ by Boltzman factor $\exp - E_{v_i}/kT$. Therefore, the allowed difference bands can not be observed experimentally. Thus, we shall see that when both electrical

anharmonicity [higher terms in Eq. (7)] and mechanical anharmonicity [higher terms in Eq. (2)] are neglected. Only fundamentals are allowed transitions.

Whether a certain fundamental ν_i of the crystal is IR active can be decided on whether $(\frac{\partial\mu}{\partial Q_i})_o$ is different from zero or whether the integral in Eq. (6) is non zero. Such an integral can exist only if the reducible representation of its integrand contains the totally symmetric representation of the space group.

Since translational operations leave any vector invarient, they do not change the magnitude and the orientation of μ. That is, the dipole moment of the crystal μ belongs to the totally symmetric representation of the translation group. Namely, it belongs to the unit cell group. It is a theorem of group theory that irreducible representations of the factor group, U, are also irreducible representations of the space group, S. In these particular irreducible representations, the elements of the invariant sub-group, T, are all given by identity. Consequently, the set of irreducible representations $\Gamma^s_{\mu_x}$, $\Gamma^s_{\mu_y}$, $\Gamma^s_{\mu_z}$ which are totally symmetric with respect to translation are given by

$$\Gamma^s(\mu) = \Gamma^u(\mu) \tag{10}$$

Therefore, in order for $[\mu]^{v'}_v$ to exist, $\Gamma^s(\Phi^*_{v'})\Gamma^u(\mu)\Gamma^s(\Phi_v)$ must contain A^s_1. We are interested especially in the case v=0 ($\Sigma v_i=0$), the representation of the initial state $\Gamma^s(\Phi_o)$ belongs to $A_1{}^s$ species and v'=1 ($\Sigma v_i' = 1$), the representation of the final state is $\Gamma^s(\Phi_{v'})=\Gamma^s(Q_i)$. This demands that

$$\Gamma^s(Q_i) \text{ belongs to } \Gamma^u(\mu) \tag{11}$$

That is, only those normal coordinates of the crystal which are totally symmetric with respect to translation may be active, and the selection rules are given by

$$\Gamma^u(Q_i) = \Gamma^u(\mu) \tag{12}$$

Therefore, to the harmonic approximation, the total number of the observed frequencies in the infrared and, in the Raman spectrum must be the same as the number and symmetry types determined by the molecules in a single unit cell.

The wave length of a photon in a medium of refractive index n=2, is one half of its vacuum value, and is of the order of 1 to 10 microns in the infrared. This is substantially infinite relative to unit cell dimension, so that for all practical purposes one can assume that the wave vector of an infrared photon K is equal to zero. In the process of transforming a photon into an excitation wave packet of the crystal, not only energy, but also momentum has to be conserved. That is, $K = k_{v'} - k_{v=0} = 0$. Since the ground state of a crystal belongs to the totally symmetric representation of the space group, the wave vector $k_{v=0}$ of the ground (initial) crystal state of the transition is simply zero. Therefore, the wave-vector of the excited state must be zero. This leads to the same conclusion as Eq. (12). Namely, only those normal coordinates of the crystal which are totally symmetric with respect to translation may be active in the infrared. Explicitly, we may write the infrared active modes as

$$Q_i(k=0) = \sum_{m=1}^{N} [q_i{}^u]_m \tag{13A}$$

Where $(q_i{}^u)_m$ is the <u>ith</u> normal coordinate of the <u>mth</u> unit cell. Physically, this motion is such that equivalent atoms of all unit cells are in phase.

The physics leading to Eq. (12) can easily be illustrated with a one dimensional model. For a one-dimensional crystal, the out of phase modes may be written as

$$Q_i(k) = \sum_m^N q_i^u \exp ikma \tag{13}$$

where a is the unit cell dimension. The dipole moment corresponding to this normal motion of the crystal could be written as

$$\mu_i(k) = \mu_{io} + \left(\frac{\partial\mu}{\partial Q_i}\right)_o Q_i(k) + \cdots \tag{14}$$

Substituting Eq. (13) into Eq. (14) and writing the time dependence of q_i^u explicitly, we have

$$\mu_i(k) = \mu_{io} + \left(\frac{\partial\mu}{\partial Q_i}\right)_o (q_i^u)^o \sum_m^N \exp i(kma+\omega_i t) + \cdots \tag{15}$$

At any instant, e.g., $t=t_o$, the second term in the right hand side can be represented graphically. For example $k = \frac{\pi}{6a}$ as

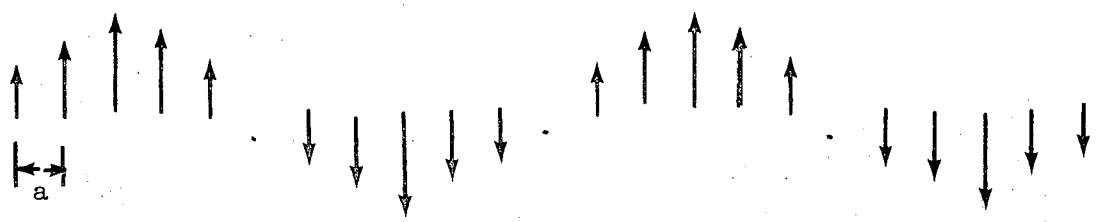

It is seen that to the harmonic approximation the time dependent part of $\mu_i(k)$ is practically zero at any instant unless the wave length of the normal coordinate of the crystal is the order of the crystal dimension which is in the order of 1 micron for the polycrystalline sample in the actual study. That is, unless the wave vector of the normal motion of the crystal is nearly zero, there is no change of dipole moment accompanying this normal motion of the crystal. Thus, there is no emission or absorption of radiation, according to classical electrodynmaics.

In order to find the spectroscopically active modes of the crystal, one needs to consider only the unit cell and thus, the unit cell group. The analysis below will be based on the relationship between the

representations of the various groups. It is always possible to write linear relations between the irreducible representations of the unit cell group and those of the site group. Irreducible representations which are so related are called corresponding irreducible representations. The correspondence may be determined in any specific case by comparing the character tables of the site group and the unit cell group. In this way, correlation charts[17] can be set up between the various site groups and the unit cell group. It is a simple matter then to proceed via these tables to analyze a given crystal structure for spectroscopic activity.

The determination of the spectroscopic activity of naphthalene will be used as an example.

Naphthalene Spectra

The crystal structure of naphthalene is described by the space group $P_{2_1/a}$ (C_{2h}^5), with two molecules per unit cell. The site symmetry is C_i. Figure 1 shows the unit cell and symmetry elements of the naphthalene crystal. The relative orientation of the molecular axis to the unit cell axis is analytically shown in Table 1. To analyze the spectrum, one makes use of the correlation connecting the molecular symmetry group (D_{2h}) with that of the site group (C_i), and connecting the site group with that point group isomorphous of the unit cell group (C_{2h}). The correlations are shown in Table 2. Also shown are the symmetry species of the translations (and thus, the dipole moments) along the x, y, z axis of the molecule (z is perpendicular to the molecular plane, y is the long axis; also see Fig. 1) and along the a, b, c, crystal axis. In the site group, translations are all A_u.

The normal coordinates and their symmetry classes as well as the fundamental frequencies of the gas state molecule are necessary for the

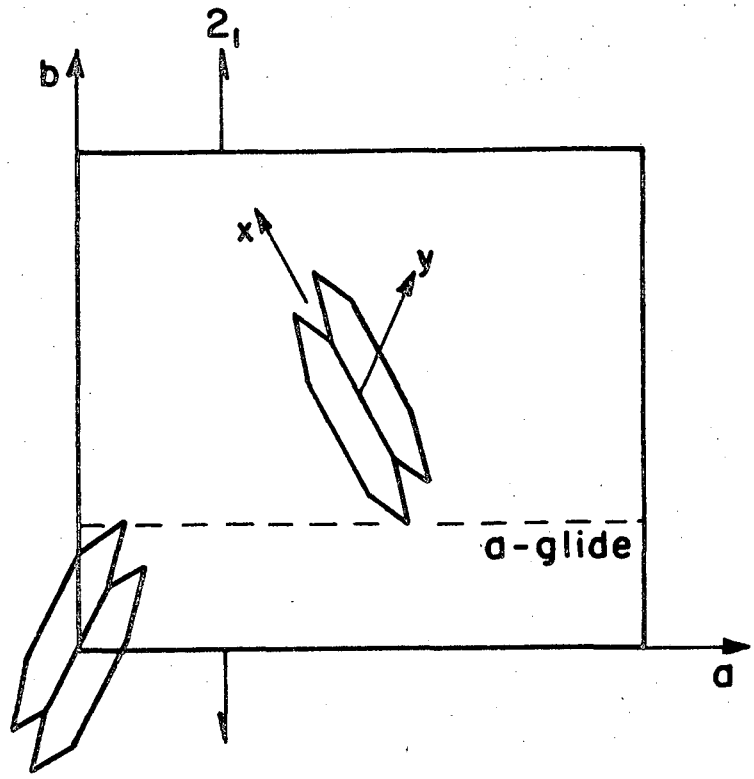

XBL 7110-7363

Fig. 1. Naphthalene has a monoclinic unit cell and has cell dimensions at room temperature and pressure as: a = 8.24Å b = 6.00Å c = 8.66Å β = 122.9° $\alpha = \gamma$ = 90° (the angle between b and c is denoted by α, between c and a by β, and b by γ). The two molecules in a unit cell which have coordinates (0 0 0) and (1/2 1/2 0), are interchanged by symmetry operations of screw axis 2_1 which lies along (1/4 b 0), and a-glide (a 1/4 c). [after D. P. Craig, Ref. 3].

Table 1. Directional cosine of the Naphthalene molecular axis in its crystal; cosines of the angle between the molecular axis and the monoclinic a and b axis and c', perpendicular to the ab plane.

	z	x	y
a	+0.8399	-0.3207	-0.4379
b	-0.4425	-0.8718	-0.2103
c'	+0.3143	-0.3704	-0.8741

(after Cruickshank, Reference 32)

Table 2. The correlation table for naphthalene.

Degrees of freedom	Molecular symmetry D_{2h}	Site symmetry C_i	Factor group symmetry C_{2h}	Degrees of freedom
	A_g		A_g	
	B_{1u}	A_g		
	B_{2g}		B_g	
	B_{3g}			
	A_u		A_u	b
z	B_{1u}	A_u		
x	B_{2u}		B_u	a,c
y	B_{3u}			

(After G. C. Pimentel, et al. Reference 34.)

study of the molecule in the solid state. These are available in the literature for naphthalene.[33] The condition for infrared activity in the gas phase is that the normal coordinates of the molecule have the symmetry of a component of the molecular dipole moment. Therefore, the inrared-active modes of the naphthalene molecule are those belonging to the classes, B_{1u}, B_{2u} and B_{3u} of the molecular point group.

The correlation table is simply the expression of the retention in the sub group (the site group, C_i) of a part of the symmetry elements of the group (either the unit cell group C_{2h} or the molecular point group D_{2h}). Thus, all of the symmetry classes that have the character -1 under the inversion operation in D_{2h} correlate with A_u of the site group. All those symmetry classes of the factor group, C_{2h}, which are asymmetric with respect to the inversion operation correlate with A_u of the site group.

Since the symmetry of a molecule in a crystal is actually that of the site, one simply correlates each molecular vibration with its proper class under C_i and predicts its spectral activity by using selection rules appropriate to C_i (i.e., that those vibrations falling under A_u will be infrared-active). The procedure to this point is called the site analysis.[18] For example, ν_8, γ_1 and δ_5 are of the symmetry classes b_{1g}, a_u and b_{2u} respectively in the isolated molecule. $\nu_8(b_{1g})$ is infrared inactive in the gas phase. In the crystal it falls under class A_g of the site group and remains inactive. $\gamma_1(a_u)$ is inactive in the gas phase. In the crystal, it belongs to class A_u of the site group and can be active. Its intensity will be expected to be low, since it can only be active because of the small crystal field perturbation. $\delta_5(b_{2u})$ is gas phase active. In the crystal it remains active. The result is obvious that any degenerate vibration

of a molecule which is in a site of a symmetry group C_1, C_2, C_i or D_2, may split, since there is no degenerate class in these groups. This splitting is the so-called site group splitting. Symmetry, of course, tells us nothing about the magnitude of the site group splitting. Site group splitting is a first order effect, and the change in intensity is second order. This will be discussed later in this chapter.

Having considered the effect of the lowering of symmetry due to the local field at the site, one must now take into account the fact that the coupling may occur between two naphthalene molecules of the unit cell, i.e., the factor group analysis.[8] This involves the construction of the symmetry coordinates q_α^u and q_β^u of the unit cell from the normal coordinates q_a and q_b of the molecules at the two sites of the cell. Considering only one normal motion of the molecules, we have

$$\begin{pmatrix} q_\alpha^u \\ q_\beta^u \end{pmatrix} = \begin{pmatrix} B_{\alpha a} & B_{\alpha b} \\ B_{\beta a} & B_{\beta b} \end{pmatrix} \begin{pmatrix} q_a \\ a_b \end{pmatrix} \tag{16}$$

B is a unitary matrix similar to the transformation matrix for the transformation of internal coordinates into symmetry coordinates in the theory of molecular vibrations.

The correlation table shows that for each A_u vibration of the molecules at the two C_i sites, there will be two unit cell vibrations, one each of species A_u and B_u. Of these unit cell vibrations, those in class A_u will be infrared active with the transition dipole parallel to the b axis. Those in class B_u will be infrared active with the transition dipole perpendicular to the b axis. The symmetry coordinates of the unit cell are obviously

$$q_\alpha^u = \frac{1}{\sqrt{2}} (q_a + q_b) \; ; \qquad q_\beta^u = \frac{1}{\sqrt{2}} (q_a - q_b) \tag{17}$$

Since q_α^u and q_β^u are orthonormal and so are q_a and q_b. The B matrix is, thus

$$B = \begin{pmatrix} 1 & 1 \\ 1 & -1 \end{pmatrix} \tag{18}$$

Equation (17) tells us that the molecule in site a vibrates either in phase with, or exactly 180° out of phase from the molecule in site b for the spectroscopic active modes of the crystal.

In summary, from symmetry considerations, site group and factor group splittings are expected in the spectra of molecular crystals. The major purpose of the next two sections is to illustrate the nature of the crystalline force field causing these splittings and the accompanying frequency shifts.

B. The Pertrubation of the Crystalline Force Field on the Internal Vibration

One may describe the displacement of the center of gravity of each ion or molecule as well as the displacement of the angles which define the orientation of a set of axis fixed to each molecule with respect to an axis fixed in the entire crystal by the coordinates S_j^i. Here the superscript and subscript represent the ith coordinate of the jth molecule. These coordinates are lattice coordinates, and they are analogous to the coordinates which define the translation and rotation of a free molecule. The distortion of the molecular configuration, relative to the center of gravity and body axis of the jth molecule is to be designated by the internal coordinates R_j^i. These are the internal coordinates in the same sense as in the usual molecular vibration problem.

In these coordinates, the potential energy of the solid is given by

$$V = V_o + \left(\sum_{ii'jj'}^{tN,tN\ 6,6} L_{jj'}^{ii'} S_j^i S_{j'}^{i'} + \sum_{ii'i''jj'j''} J_{jj'j''}^{ii'i''} S_j^i S_{j'}^{i'} S_{j''}^{i''} + \cdots \right)$$

$$+ \left(\sum_{ii'jj'}^{tN\ tN\ 3n-6,3n-6} M_{jj'}^{ii'} R_j^i R_{j'}^{i'} + \cdots \right)$$

$$+ \left(\sum_{ii'jj'}^{tN\ tN\ 3n-6,6} N_{jj'}^{ii'} R_j^i S_{j'}^{i'} + \cdots \right) \qquad (19)$$

where L, J, M, and N are force constants. Since S_j^i and R_j^i are not normal coordinates of the crystal, cross terms may exist for all pairs of 3ntN coordinates (6tN lattice coordinates and (3n-6)tN internal coordinates for the crystal of non-linear molecules). The terms in the first parenthesis represent the potential which yields the lattice motion of rigid molecules. The terms in the second parenthesis are the sum of the potential for the internal motions of all of the individual molecules which are in the crystal field of the site symmetry. These terms also include the interaction among internal motions of the various molecules. In general, the amplitude of intramolecular motion is very much smaller then that of the lattice vibrations, therefore only the limit of small intramolecular vibrations will be considered below. The terms in the third parenthesis represent the interaction between lattice and internal vibrations.

In terms of these same coordinates, the kinetic energy is of the form

$$T = \sum_{j}^{tN}\left[\sum_{i}^{6} A_j^i \dot{S}_j^{i2} + \sum_{ii'}^{\substack{3n-6\\3n-6}} B_j^{ii'}\, \dot{R}_j^i\, \dot{R}_j^{i'} + \sum_{ii'}^{3n-6,6} C_j^{ii'}\, \dot{R}_j^i\, \dot{S}_j^{i'}\right] \qquad (20)$$

Where $\dot{S}_j^i$ and $\dot{R}_j^i$ are the velocities corresponding to S_j^i and R_j^i displacements. The coefficients A, B and C are functions of the coordinates chosen and masses of constituent atoms of the crystal. The first term is the translational and rotational energy of the molecules considered as rigid bodies. The second is the internal kinetic energy of the molecules and is analogous to that encountered in any molecular vibration problem. The third term does not vanish whenever R_j^i and S_j^i are not orthogonal.

If the cross terms between lattice coordinates and internal coordinates in both T and V are neglected, the problem would be separable into the problems of lattice vibrations and internal vibrations of the crystal. This is usually a satisfactory assumption since the large frequency separation between intramolecular vibration and lattice vibration prevents the two classes of motion from interacting appreciably. The lattice vibration will not be treated here, and the internal vibration will be treated by the theory of small vibrations. To this limit, we have the potential and kinetic energy of internal vibrational motion as

$$V_{\text{internal motion}} = \sum_{ii'jj'} M_{jj'}^{ii'}\, R_j^i\, R_{j'}^{i'} \qquad (21)$$

$$T_{\text{internal motion}} = \sum_{ii'j} B_j^{ii}\, \dot{R}_j^i\, \dot{R}_{j'}^{i'} \qquad (21A)$$

Following the procedure of vibrational analysis in molecular spectroscopy, one substitutes Eq. (21) and Eq. (21A) into Lagrange's equation:

$$\frac{d}{dt}\frac{\partial T}{\partial \dot{R}_j^i} + \frac{\partial V}{\partial R_j^i} = 0 \tag{22}$$

A set of (3n-6)tN equations is obtained. If we wish to determine whether there are any normal vibrations of the entire crystal, namely, motions in which all particles move with the same frequency of simple harmonic motion,

$$\begin{aligned} R_1^1 &= (R_1^1)^o \cos(2\pi\nu t + \theta_1^1) \\ &\vdots \\ R_j^i &= (R_j^i)^o \cos(2\pi\nu t + \theta_j^i) \\ &\vdots \\ R_{tN}^{3n-6} &= (R_{tN}^{3n-6})^o \cos(2\pi\nu t + \theta_{tN}^{3n-6}) \end{aligned} \tag{23}$$

One has to see whether the above condition expressed by Eq. (23) for simple harmonic motion can be fulfilled simultaneously for all internal coordinates with the same frequency. That is, one tries to substitute the R_j^i's of Eq. (23) and their derivative into the set of (3n-6)tN number of equations obtained above. In doing so, a system of linear and homogenous equations for $(R_1{}^1)^o, \cdots (R_j{}^i)^o, \cdots (R_{tN}{}^{3n-6})^o$ is obtained. In principle, from these equations, (3n-6)tN number of normal vibrational frequencies of the crystal could be obtained as functions of $M_{jj'}{}^{ii'}$ and $B_j{}^{ii'}$. They are exactly those internal frequencies of the crystal in Eq. (5). The relative values of $(R_1{}^1)^o, \cdots (R_j{}^i)^o, \cdots (R_{tN}{}^{3n-6})^o$ thus form the normal vibrations of the crystal, the Q_i of Eq. (2), could also be obtained in principle.

It is shown in Section B that only in-phase modes could be observed spectroscopically; that is, a maximum of (3n-6)t normal frequencies are observable. Therefore, the observable frequencies could never be sufficient for the evaluation of the $[(3n-6)tN]^2$ number of force constants, $M_{jj'}ii'$.

Since the molecular-normal-coordinates q^i and its frequency ν^i_o are usually known, one would like to express the normal frequency of the crystal ν^i as ν^i_o plus a crystal perturbation term. To clarify the effects of the crystalline force field, one may transform the internal coordinates in Eq. (21) into molecular-normal-coordinates, thus

$$V_{\text{internal motion}} = \sum_{ii'jj'} K^{ii'}_{jj'}\, q^i_j\, q^{i'}_{j'}$$

$$= \sum_{ij} K^i_j\, (q^i_j)^2 + \sum_{i,i'\neq i,j} K^{ii'}_j\, q^i_j\, q^{i'}_j + \sum_{i,i',j,j'\neq j} K^{ii'}_{jj'}\, q^i_j\, q^{i'}_{j'} \qquad (24)$$

In general, $K_j^{\,i,i'} \neq 0$, since $q_j^{\,i}$ are not normal coordinates of the molecule with site symmetry. $K_{j,j'\neq j}^{\,i,i'} \neq 0$, since $q_j^{\,i}$ are not normal coordinates of the entire crystal. $K_j^{\,i} \neq (\lambda_j^{\,i})_o$, $(\lambda_j^{\,i})_o$ is the force constant of an isolated molecule. The potential function for an isolated molecule is

$$V_j = \sum_i V^i_j = \sum_i (\lambda^i_j)_o\, (q^i_j)^2 \qquad (25)$$

Substituting Eq. (25) into Eq. (24), one has

$$V_{\text{internal motion}} = \sum_{j} V_j + \sum_{ij} \left[K_j^i - (\lambda_j^i)_o\right] (q_j^i)^2$$

$$+ \sum_{ii' \neq ij} K_j^{i\,i'} q_j^i q_j^{i'} + \sum_{ii'jj' \neq j} K_{jj'}^{ii'} q_j^i q_{j'}^{i'} \qquad (26)$$

In this equation, the existence of the 2nd, 3rd, and 4th terms is obviously due to the crystal field perturbation on the intramolecular vibrations. It is interesting to see (and will be shown below more explicitly) that Eq. (26) tells us: First--the lowering of the molecular symmetry to the site symmetry causes a frequency shift of $1/2\pi \sqrt{K_j^i - (\lambda_j^{\,i})_o}$ and is expressed by the second term. Second--the crystal field causes the coupling of the molecular normal modes within a molecule and among different molecules. Therefore, one should regard the molecular-normal-coordinates as a set of internal coordinates of the crystal. The coupling of a given molecular-normal-mode among tN molecules of the crystal splits the tN-fold degeneracy. Each of the resulting tN normal modes of the crystal is characterized by a certain phase relation among neighboring molecules. The sign and magnitude of the frequency shift and splitting are dependent on the crystal structure as well as the nature of the crystalline force fields. The crystalline forces are the repulsion forces, hydrogen bonding, London forces and Coulombic forces. In general all these forces exist at the same time. Nevertheless, one type of the force field may be dominant among all the others for a

small range of intermolecular distance.

We will proceed further toward the correlation of the molecular normal frequency with the normal frequency of the crystal, keeping in mind the previous assumption that the cross term between lattice motion and internal modes of the crystal is neglected. The total potential of the crystal, i.e., Eq. (19) may be rewritten to the limit of infinitesimal intramolecular vibration as

$$V = V_o + \left(\sum_{ii'jj'} L^{ii'}_{jj'}, S^i_j S^{i'}_{j'} + \sum_{ii'i''jj'j''} J^{ii'i''}_{jj'j''} S^i_j S^{i'}_{j'} S^{i''}_{j''} + \cdots \right)$$

$$+ \sum_j V_j + \sum_{ij} \left[K^i_j - (\lambda^i_j)_o \right] (q^i_j)^2 + \sum_{ii' \neq ij} K^{ii'}_j q^i_j q^{i'}_j$$

$$+ \sum_{ii'jj' \neq j} K^{ii'}_{jj'} q^i_j q^{i'}_{j'} \tag{27}$$

Therefore, the crystal potential energy is that of the isolated molecules plus a perturbation U. Namely,

$$V = \sum_j V_j + U \tag{27A}$$

$$U = U_o + \left[\sum_{ii'jj'} L^{ii'}_{jj'} S^i_j S^{i'}_{j'} + \sum_{ii'i''jj'j''} J^{ii'i''}_{jj'j''} S^i_j S^{i'}_{j'} S^{i''}_{j''} + \cdots \right]$$

$$+ \sum_{ij} \left[K^i_j - (\lambda^i_j)_o \right] (q^i_j)^2 + \sum_{ii' \neq ij} K^{ii'}_j q^i_j q^{i'}_j + \sum_{ii'jj' \neq j} K^{ii'}_{jj'} q^i_j q^{i'}_{j'}$$

(28)

U_o is the static lattice potential and is identical to that in the Mei Gruneisen equation of state. It is a function of crystal structure and unit cell dimension. If one divides the crystalline potential U into a static potential U_o plus dynamic potentials. Each of the other terms on the right hand side of Eq. (28) represent a dynamic potential.

C. Internal Vibrational Energy Levels (vibrational exciton levels) of Molecular Crystals

The vibrational energy levels of the ith normal mode of the jth isolated molecule is the eigen values of the Schredinger equation.

$$H_j^i \, \psi_j^i = \varepsilon_j^i \, \psi_j^i \tag{29}$$

where

$$H_j^i = T_j^i + V_j^i$$

$$= (\dot{q}_j^i)^2 + (\lambda_j^i)_o (q_j^i)^2$$

The solution for this equation is well known, namely:

$$\psi_{v_j i}(q_j^i) = \exp\left[-(\pi\omega^i{}_o/h)q_j^{i\,2}\right] \times H_{v_j i}\left[(2\pi\omega^i{}_o/h)^{1/2}\, q_j^i\right] \tag{29A}$$

$$\varepsilon_j^i = h\nu^i{}_o(1/2 + v_j{}^i) \tag{29B}$$

The internal vibrational energy levels of the crystal are the solution of a Schredinger equation of the form

$$\left[\sum_j H_j + T_{external} + U\right]\Phi = \left[\sum_j \varepsilon_j + E'\right]\Phi \qquad (30)$$

Where $T_{external}$ is the first term in Eq. (20). It is a constant here, i.e., it is not a function of internal coordinates of the crystal (molecular-normal-coordinates). U is defined in Eq. (28). In the following treatment, only the interaction of a molecular-normal mode among the tN molecules is to be considered. Thus, the superscript of q and ψ is to be omitted. The unperturbed wave function of the crystal ground state, $\Phi_{\sum_j v_j=0}$ is

$$\Phi^o = \prod_j \psi_j^{v_j} = 0 \qquad (30A)$$

The unperturbed first excited states $\Phi_{\Sigma v_j = 1}$ is the linear combination of the tN number of ϕ_p in which the pth molecule is excited and the others are in their ground state.

$$\phi_p = \psi_p^{v_p=1} \prod_j \psi_j^o \qquad (31)$$

The tN number of the unperturbed excited states $\Phi_{\Sigma v_j=1}$ are accidentally degenerate. Namely, they belong to various irreducible representation of the space group, and thus, the energy levels are expected to be split by the perturbation.

Since both H and Φ are the functions of intramolecular normal coordinates only, the bracket of Eq. (28) is a constant. U of Eq. (28) is reduced to

$$U(q_1, q_2 \ldots q_j \ldots q_{tN}) = \text{constant}$$

$$+ \sum_j [K_j - (\lambda_j)_o] q_j^2 + \sum_{jj'} K_{jj'} q_j q_{j'} \tag{32}$$

Assuming that the perturbation potential U can be expressed as a sum over pairs of molecules

$$U = \frac{1}{2} \sum_{jp} U_{jp} \tag{33}$$

It can be shown (2,3,5,6,9.15) by first order perturbation theory that the energy level of the excited states is split into t branches (to be designated by $\alpha, \beta, \gamma \ldots$). The energy difference between the spectrally excited state and the ground state is given by

$$E_\alpha - E^o = \varepsilon - \varepsilon^o + \frac{h}{8\pi^2 \nu_o c} \sum_j^{tN} \left(\frac{\partial^2 U_{jp}}{\partial q_p^2} \right)_o$$

$$+ \frac{ht}{8\pi^2 \nu_o c} \sum_{w, j_w}^{t,N} B^*_{\alpha a} B_{\alpha w} \left(\frac{\partial^2 U_{j_w p}}{\partial q_{j_w} \partial q_p} \right)_o \tag{34}$$

Where ε and ε^o are the energies of the states ψ^1 and ψ^o. $\varepsilon - \varepsilon^o = h\nu_o$. The partial differentials are evaluated at static equilibrium, namely, $\sum_{ij} |S_j^i| = 0$ and $\sum_{ij} |q_j^i| = 0$. Molecule p is on site a, and molecule j_w is on site w. w runs through a, b, . . . to t number of equivalent sites in a unit cell. B is the transformation matrix difined in, Eq. (16) and Eq. (18), for the case t=2.

For a crystal with two molecules per unit cell, there are two unit cell modes for each intramolecular vibration. They are

$$\nu_{\substack{\alpha\\\beta}} = \nu_o + \frac{1}{8\pi^2\nu_o c}\sum_{j}^{2N}\left(\frac{\partial^2 U_{jp}}{\partial q_p^2}\right)_o + \frac{1}{8\pi^2\nu_o c}\sum_{j_a}^{N}\left(\frac{\partial^2 U_{j_a p}}{\partial q_{j_a}\partial q_p}\right)_o$$

$$\pm \frac{1}{8\pi^2\nu_o c}\sum_{j_b}^{N}\left(\frac{\partial^2 U_{j_b p}}{\partial q_{j_b}\partial q_p}\right)_o \tag{35}$$

$$E_{\substack{\alpha\\\beta}} - E^o = h\nu_{\substack{\alpha\\\beta}} \tag{36}$$

The splitting of each gas state frequency into α and β factor group components is the so called factor group splitting and also called Davydov splitting. The frequency shift as gas condenses to the crystal is

$$\frac{1}{2}(\nu_\alpha + \nu_\beta) = \nu_o + \frac{1}{8\pi^2\nu_o c}\sum_{j}^{2N}\left(\frac{\partial^2 U_{jp}}{\partial q_p^2}\right)_o + \frac{1}{8\pi^2\nu_o c}\sum_{j_a}^{N}\left(\frac{\partial^2 U_{j_a p}}{\partial q_{j_a}\partial q_p}\right)_o \tag{37}$$

and the factor group splitting is

$$\nu_\alpha - \nu_\beta = \frac{1}{8\pi^2\nu_o c}\sum_{j_b}^{N}\left(\frac{\partial^2 U_{j_b p}}{\partial q_{j_b}\partial q_p}\right)_o \tag{38}$$

U_{jp} is a function of intermolecular distance as well as relative orientation of molecules in a crystal. The former is obviously varied with pressure and temperature. Therefore, both frequency shift

and factor group splitting are expected to be temperature and pressure dependent. Any discontinuity of relative orientation of the molecules and/or of intermolecular distances across the solid-solid phase transition may be detected from the expected discontinuity in the frequency-pressure plot. Thus, the frequency-pressure plot will offer us useful information about the existance as well as the nature of a phase transition.

It is possible, at this point, to develop a physical model to describe the mechanism which causes the frequency shift and Davydov splitting, when the gas becomes a crystal and the change when high pressure is applied on a solid, or when a solid-solid phase transition takes place. As was shown above, the perturbation potential U is the potential energy of the entire crystal minus that of the molecules in the gas state. U is thus the energy of interaction among the charge distributions of all molecules. U_{jp} is the intermolecular pair potential. It is important to realize that only the part of U_{jp} which is dependent on the intramolecular vibrational coordinates enters into Eq. (37) and Eq. (38). In these equation, $\left(\frac{\partial^2 U_{jp}}{\partial q_p^2}\right)_o$ and $\left(\frac{\partial^2 U_{jp}}{\partial q_j \partial q_p}\right)_o$ are force constants. The former is a pure number while the latter is a tensor. Namely, $\left(\frac{\partial^2 U_{jp}}{\partial q_p^{\,2}}\right)_o q_p$ is a restoring force along the unit vector $\hat{q}_p$, and is caused by an intramolecular displacement along $\hat{q}_p$. $\left(\frac{\partial^2 U_{jp}}{\partial q_j \partial q_p}\right)_o q_j$ is a restoring force along $\hat{q}_p$ and is caused by an intramolecular displacement along $\hat{q}_j$. In Fig. 2, a model is proposed to illustrate these force fields graphically. The numberical force constants are phase independent (because the displacement and the restoring force are always in phase) and contribute only to the frequency shift. The tensoral force constants are phase dependent and contribute to both

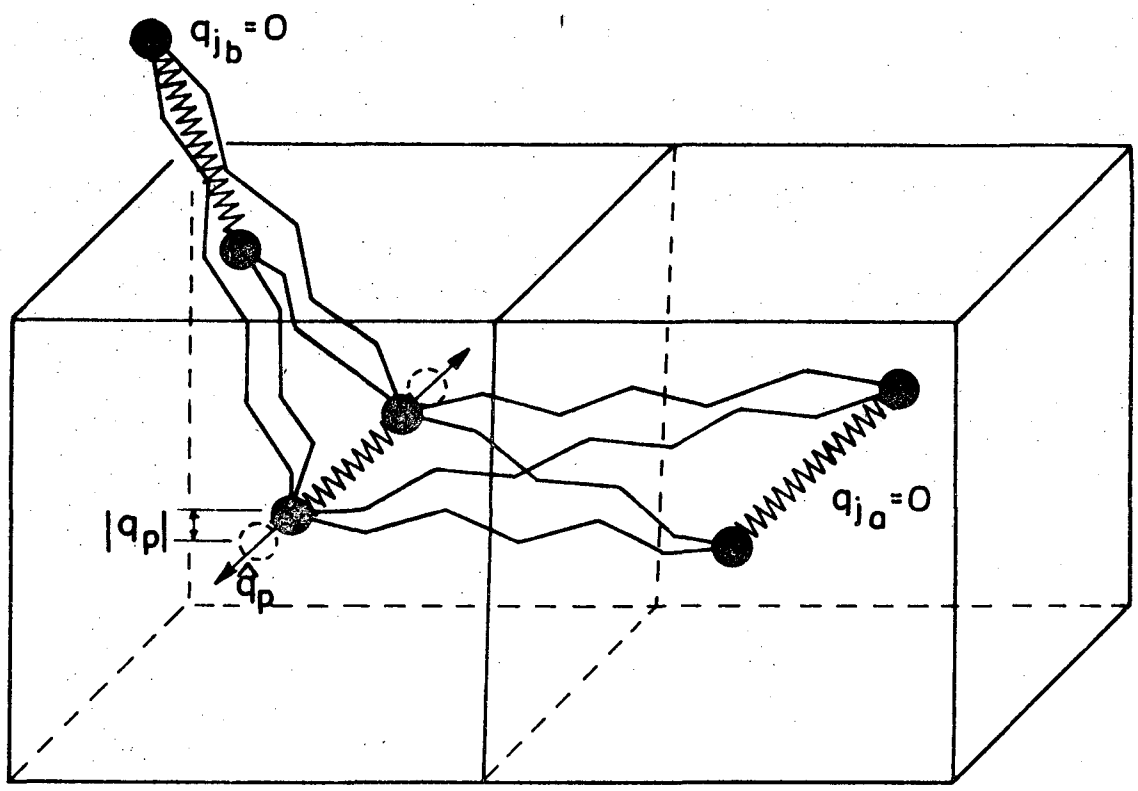

XBL 7110-7364

Fig. 2a $\left(\frac{\delta^2 U_{j_a p}}{\delta q_p^2}\right)_o q_p + \left(\frac{\delta^2 U_{j_b p}}{\delta q_p^2}\right)_o q_p$ is the $\hat{q}_p$ component of the force exerted by the eight loose springs, due to the intramolecular displacement q_p.

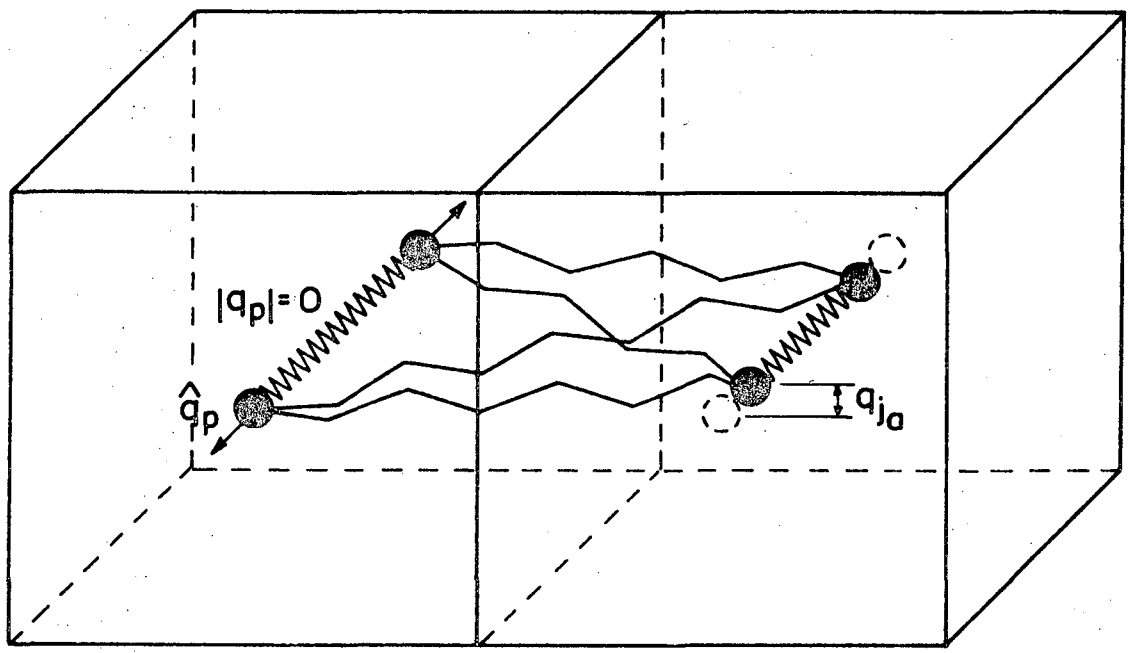

XBL7110-7365

Fig. 2b $\left(\frac{\delta^2 U_{j_a p}}{\delta q_p \delta q_{j_a}}\right)_o q_{j_a}$ is the $\hat{q}_p$ component of the force exerted by the four loose springs, due to the intramolecular displacement q_{j_a}.

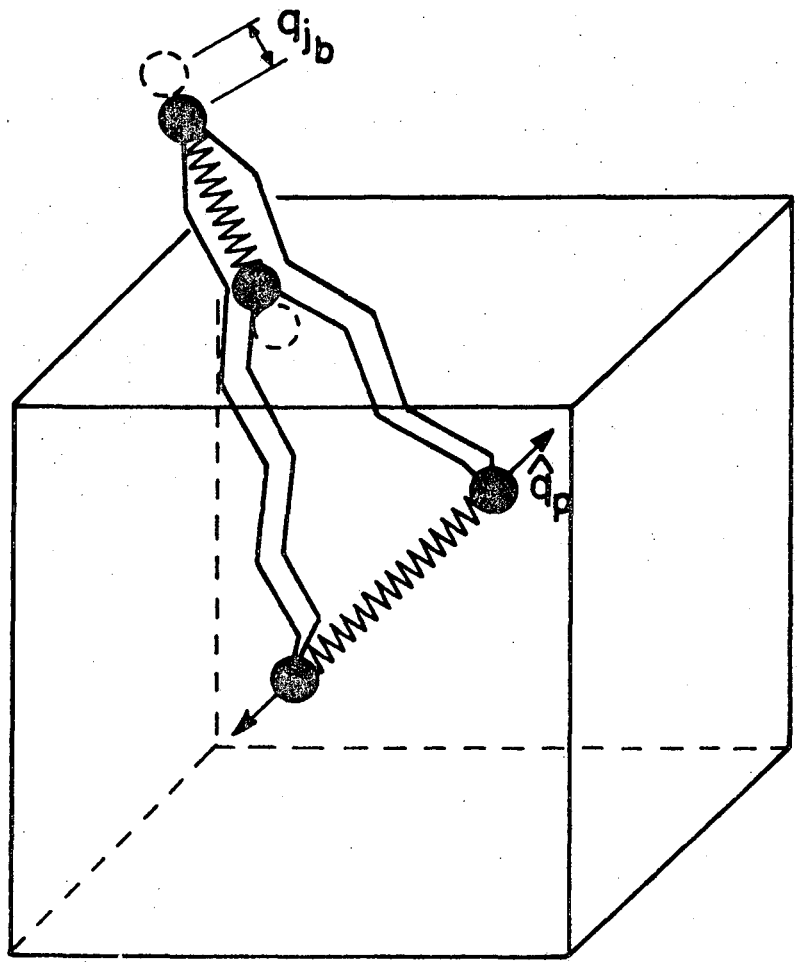

XBL 7110-7366

Fig. 2c $\left(\frac{\delta^2 U_{j_b\,p}}{\delta q_p \delta q_{j_b}}\right)_o q_{j_b}$ is the $\hat{q}_p$ component of the force exerted by the four loose springs, due to the intramolecular displacement q_{j_b}.

frequency shift and the splitting into t branches, of each of the gas state frequencies and are responsible for the exciton energy transfer mechanism.

Both scalar and tensoral force constants may cause site group splitting. (Site group splitting is predicted in the group theoretical consideration in Section A, namely, the degeneracy of molecular-normal-modes may be split due to the lower symmetry of the site.) This splitting may be visualized easily from the crystalline force field. As a simple model, assume that a linear triatomic molecule crystalizes in the naphthalene sites (see Fig. 1), one can then construct the crystalline forces, as in Fig. 2 for the doubly degenerate bending modes. The crystalline force fields so obtained are different for the two bending modes. That is, the two bending modes are no longer degenerate.

In the literature, the frequency shift and Davydov splitting are often described; the former, as due to a static crystalline force field and the latter as due to a dynamic crystalline force field (also called resonance interaction force field). From our definition of static and dynamic crystalline potentials in Eq. (28), both the frequency shift and Davydov splitting are obviously caused by the dynamic potentials. Two types of force constants, illustrated in Fig. 2, yields two kinds of dynamic forces. The frequency shift is caused by both types of dynamic forces while Davydov splitting is caused by the second type of the dynamic forces (tensor force constant). The dynamic interaction of the second type reaches a maximum value when all molecules vibrate with the same frequency and is the so called resonance interaction.

The possible force fields which could be involved in U_{jp} are the Coulumbic force which may be resolved into the summation of

monopole, dipole and all multipole interactions, London forces repulsion forces and hydrogen bonding. Certain intermolecular potentials (the latter three) may reasonably be broken up into central forces acting between pairs of atoms, one in each of the two molecules. That is

$$U_{jp} = \sum_{mn} U_{mn}(r_{mn}) \tag{39}$$

Where m is an atom of molecule j, n is an atom of molecule p, and r_{mn} is the interatomic distance.

The numerical and tensoral force constant in Eq. (37) and Eq. (38) can be written[41,55] as

$$\left(\frac{\partial^2 U_{jp}}{\partial q_p^2}\right)_o = \sum_{mn} \left(\frac{\partial^2 U_{mn}}{\partial r_{mn}^2}\right)_o \left(\frac{\partial r_{mn}}{\partial r_n} \cdot \frac{\partial r_n}{\partial q_p}\right)_o^2 \tag{40}$$

$$\left(\frac{\partial^2 U_{jp}}{\partial q_j \partial q_p}\right)_o = \sum_{mn} \left(\frac{\partial^2 U_{mn}}{\partial r_{mn}^2}\right)_o \left(\frac{\partial r_{mn}}{\partial r_m} \cdot \frac{\partial r_m}{\partial q_j}\right)_o \left(\frac{\partial r_{mn}}{\partial r_n} \cdot \frac{\partial r_n}{\partial q_p}\right)_o \tag{41}$$

Where r_m is a vector describing the position of atom m. $\left(\frac{\partial r_{mn}}{\partial r_n}\right)_o$ is the cosine of the angle between the molecular normal displacements of the atom n and the interatomic distance r_{mn}, and is calculable from the knowledge of the crystal structure and molecular normal coordinates. $\left(\frac{\partial r_n}{\partial q_p}\right)_o$ is a matrix element of the transformation from Cartesian coordinate to normal coordinates, and is usually

available in the literature for the gas state normal coordinate analysis.

Equation (38) there fore reduces to

$$\nu_\alpha - \nu_\beta = C \sum_{mn} \left(\frac{\partial^2 U_{mn}}{\partial r_{mn}^{\ 2}} \right)_o \tag{42}$$

Where C(which includes a structure factor) can be calculated, at least in principle. Atoms m and n are now those of two molecules in the same unit cell. Therefore, in this approximation, (with assumptions of Eq. (33) and Eq. (39)), the interatomic force constant may be obtained as a function of interatomic distance, when Davydov splitting is measurable as a function of unit cell dimensions. For a special case, when the interatomic forces are dominated by the nearest neighbor repulsion force, the summation and structural factor are reduced to a simply calculable constant. This will be shown in Chapter IV for n-paraffins.

D. Intensity

The intensity of an infrared absorption band is proportional to the square of the change in dipole moment during a normal motion of a crystal. The change in dipole moment of the crystal is the vector sum of the individual molecular dipole changes each weighted by the phase difference from a reference molecule. The weighting factors are exactly the coefficients of the linear combination of molecular normal coordinates in forming normal coordinates of the crystal. The change in the dipole moment of an individual molecule is proportional to the transition moment $M_j = \int \psi^{1^*}(q_j^i)\mu(q_j^i)\psi(q_j^i)dq_j^i$;

where $\psi^*(q_j^i)$, $\psi(q_j^i)$ and $\mu(q_j^i)$ are perturbed by the crystal field U. However, in the first order perturbation theory, both q_j^i and ψ's are of the zero order (unperturbed), and the transition dipole moment of a molecule in the crystal is identical with that of an isolated molecule. The intensity of the αth factor group transition (k = 0) is thus proportional to

$$I_\alpha \propto \left[N \sum_{w}^{t} B_{\alpha a} M_a \right]^2 \tag{43}$$

Where N is the number of unit cells, M_a is the transition dipole moment of a free molecule and is oriented in the direction of the change in dipole moment of the molecule at site a. $B_{\alpha a}/B_{\alpha b}$ is the phase difference of molecular motion between site b and site a. For a crystal with two molecules per unit cell using the B matrix in Eq. (18), we have

$$I_\alpha \propto N^2(M_a + M_b)^2 \tag{44}$$

$$I_\beta \propto N^2(M_a - M_b)^2 \tag{45}$$

For Naphthalene, each of the B_{2u} normal modes have a change of dipole moment along the x-axis. With the help of Fig. 1 and Table 1, it can be shown that $M_a + M_b$ is along the b-axis and $M_a - M_b$ is perpendicular to the b-axis. Namely, the α factor group component*

---

* The symmetry class and thus the spectroscopic activity of factor group components is usually deduced from the correlation table and group theoretical argument (see any book on exciton theory).

is IR active along the b-axis and β factor group component is IR active perpendicular to the b-axis. The intensity along the a and c axis is proportional to $|(m_a - m_b) \cdot \hat{a}|^2$ and $|(m_a - m_b) \cdot \hat{c}|^2$ respectively. Therefore, the intensity ratios which are readily observable are

$$\frac{I_a}{I_b} = \frac{|(M_a - M_b) \cdot \hat{a}|^2}{|M_a + M_b|^2} \tag{46}$$

$$\frac{I_c}{I_b} = \frac{|(M_a - M_b) \cdot \hat{c}|^2}{|M_a + M_b|^2} \tag{47}$$

The intensity ratios for B_{1u}, B_{2u}, and B_{3u} molecular normal modes of naphthalene are calculated by Person, Pimentel and Schnepp.[20] The intensity ratio are obviously dependent on the relative orientation of M_a and M_b.

The sum of the intensities of the two factor group components is obvious from Eq. (45) and Eq. (44) and is just equal to the intensity of the transition in the gas state. This conclusion is also true for crystals with more molecules per unit cell since B is a unitary matrix. In the beginning of this chapter, it was shown that some transitions that are IR inactive in the isolated molecule, e.g. A_u normal modes of Naphthalene, may become active in the crystal field with lower symmetry. Nevertheless the first order perturbation theory yields zero intensity. To discuss the intensity in the crystal field, it is necessary to correct the wave functions of the unit cell state to the first order. In other words, it is necessary to use the second-order perturbation theory.[5,19]

E. Selection Rules for Combinations and Overtones

Two kinds of combinations and overtones are possible. The combinations (or overtones) of the first kind may be called the intermolecular combinations (or overtones) and are the transitions from the ground state to the states in which two different molecules are each excited by one quantum. These transitions are a consequence of the anharmonic coupling of the various motions of different molecules; i.e. due to the higher order terms in the perturbation potential U of Eq. (32). For this type of combinations (or overtones), the more general selection rule (Eq. 11) requires that $k_1 = k_2$; where k_1 and k_2 are wave vectors of the two excitations. Since the combinations and overtones of this type has never been confirmed in the observed spectra, we shall not discuss it any further.

The combinations (or overtones) of the second kind may be called intramolecular combinations (or overtones) and are the transitions from the ground state to the states in which one molecule is excited by two quanta. These combinations and overtones are a consequence of the anharmonic coupling of various intramolecular motions; i.e., the consequence of the inclusion of the higher order terms in $H_j^{\,i}$ of Eq. (29).

Equation (8) is the selection rule for overtones. The restriction, that $\Delta v_i = \pm 1$, is removed, since Ψ_{v_i} and $\Psi_{v_i'}$ of Eq. (9) are no longer harmonic. In the case of combinations, the selection rule depends on the non-vanishing of the integrals:

$$\int \Psi_{v_i'}^{*} \Psi_{v_j'}^{*} \mu \Psi_{v_i} \Psi_{v_j} \, dQ_i dQ_j$$

Namely, a combination will be infrared active when at least one component of the dipole moment of the unit cell has the same species as the vibrational eigen function Ψ_{v_i}, Ψ_{v_j}, of the upper state. This type of overtones and combinations seems to be the ones most commonly observed, and as a result, the selection rules for the observed combinations and overtones usually follow the predictions of the unit cell group analysis.

It might be worthwhile to point out that the conventional terminologies "one molecule is excited by two quanta" or "two molecules each excited by one quantum" do not mean that a photon splits into two before it is absorbed. The physics for the overtone and combination transitions is illustrated in Appendix I.

F. Experimental Methods

It is known[21,22,23] that the transition energy and the corresponding oscillator strength are related to the observables: the refractive index, $n(\nu)$, and the extinction coefficient, $k(\nu)$. Namely, the transverse optical frequency is the peak frequency of the absorption band $n(\nu)k(\nu)$. The oscillator strength f is

$$f = \frac{m_e}{tN\pi^2 e^2} \int_{band} nk\nu d\nu \simeq \frac{m_e}{tN\pi^2 e^2} \bar{n} \int_{band} k\nu d\nu \tag{50}$$

Where m_e and e are the mass and charge of the electron respectively, tN is the number of molecules in the solid. The first integral is to be referred as the absolute intensity.

The experimental methods for obtaining crystal spectra at normal pressure are well established. A comparison of the use of infrared absorption, reflection and Raman scattering is presented in the following paragraphs.

The extinction coefficient as a function of ν, $k(\nu)$, may be measured by infrared absorption. For weak absorption bands, the peak frequency of the nk band may be taken as that of the k band within experimental error, since n is nearly constant. The absolute intensity may be approximated by the integrated area of the $k(\nu)$ band times $\bar{n}$. $\bar{n}$ is defined in Eq. (50). However, if one wishes to compute a more accurate value for the eigen frequency as well as the oscillator strength, one may calculate the refractive index from the $k(\nu)$ spectrum through the well-known Kramers-Kronig dispersion relationship,[24,25] which connects the real and imaginary parts of any complex optical indexes to the limit of linear optics. Infrared absorption measurement alone could in principle yield both eigen frequency as well as oscillator strength.

For intense absorption bands, the calculation of refractive index becomes essential. However, the absorption measurement becomes insufficient for quantitative study for the following three reasons: (1) An absorption band in a crystal is always accompanied by an anomaly in the dispersion of the index of refraction $n(\nu)$. The stronger the absorption, the greater the fluctuation in $n(\nu)$ through the band. The $n(\nu)$ anomaly is also accompanied by a maximum in the reflectance spectrum of the crystal. If reflection does occur to a measurable amount, the measured absorption spectrum $k(\nu)$ will include the effects of reflection as apparent absorption. Thus, the peak

position and the line shape as well as the absolute intensity can be in error. (2) The sample thickness required is of the order of 1 micron and below. Therefore, the sample is usually deposited in the form of a poly-crystal on a substrate. The sample thickness is usually uncertain and thus the absolute value of $k(\nu)$ can not be certain. (3) Disorder in the polycrystalline sample causes a broadening of the absorption band.

The reflection method is of importance in the study of intense bands. This method has been used to a great extent for ionic crystals where the oscillator strength is usually high. The processing of the normal incidence reflection data to obtain both extinction coefficient $k(\nu)$ and index of refraction $n(\nu)$ may again be accomplished by the use of the Kramers-Kronig dispersion relationship. However, the intensitiesof radiation reflected by a sample in the minimum-reflectance region are well below the instrumental noise level for very intense bands. The so obtained optical indicies have always been in doubt. Fortunately, with the so called partitioning technique of Wu and Andermann,[29,30] it is now possible to obtain reliable optical indices even for the most intense bands, e.g., the optical phonon band of LiF and MgO.[31]

Raman spectroscopy has different selection rules from those in the infrared. Beside being complimentary to the infrared, its additional advantages are that information can be obtained concerning the lattice modes without going to the far infrared and an occasional observation of longitudinal frequencies. Its disadvantages stem basically from the fact that Raman scattering is a second order process. They are: (a) the high background noise level precludes

very high resolution, and (b) a large (a few millimeters) clear single crystal is needed for the sample.

In this work, we are mainly interested in the frequency shift and splittings as a function of unit cell dimension. That is, only the relative values of the frequencies are needed. We feel that it is not yet necessary, at this stage, to calculate $n(\nu)$ for high pressure spectra.

III. INSTRUMENTATION

A. Pressure Devices

1. Selection of a High Pressure Sample Cell for Spectroscopic Measurements

For spectroscopic measurement under high pressure, the needs are cell windows which satisfies the following two requirements: (1) they are transparent in the interested frequency range, (2) they are able to stand high sheer stress. So far there is no material available which satisfies these two conditions simultaneously for infrared windows to the highest attainable pressures. H. G. Drickamer, et al. [26] used synthetic sapphire windows for the infrared transmission study of liquid solution to pressures of 12 kb. The sapphire window is transparent in the frequency range of 2000 cm^{-1} to 50,000 cm^{-1}. However, in this study, we are interested in the frequency range below 2000 cm^{-1}.

C. E. Weir, et al. [27] used a diamond squeezer for the infrared study of ionic and molecular crystals to pressures of 30 kb. Only two percent of all diamonds are relatively transparent for wave lengths longer than 6μ, and all diamonds have various absorbtion bands below 6 microns. It is noted that hydrostatic pressure is obtained in the sapphire cell, while a diamond squeezer exerts a uniaxial force to a specimen contained between two flat surfaces, and further has a very large pressure gradient.

For transmission purposes, the alkali halides are ideal, but they are mechanically weak. To overcome this weakness, Drickamer et al. [28] has invented a bomb design using sodium chloride simultaneously as the pressure transmission medium and pressure resisting window. Pressures up to 200 kb were obtained. However, the use of

this cell (to be called sodium chloride high pressure cell) is limited by the very small amount of radiation energy which can pass through the long windows. When black body radiation is used as a light source, the source intensity is much weaker in the infrared than in the UV and visible regions. Drickamer, et al. restricted their study to the latter frequency regions. In this study, we have extended the usage of this cell into the infrared.

A sodium chloride cell is made available to us by Nicol, who modified the sodium chloride cell for Raman measurements.[68] The references cited above give detailed information on the construction of the cell as well as the preparation of the cell windows.

2. Press

A force of 7120 lbs. is sufficient for generating a 40 kb in a sample chamber of 0.125 inch diameter. An easily portable press sketched in Fig. 3, is thus constructed to suit optical alignments.

In a compression process, the pressure transmission fluid is forced to enter above a Bridgeman seal, into the cylinder of the press. In order to remove an optical cell immediately after decompression, the Bridgeman seal is lifted up by compressed air.

When compressed air is introduced, one has to be sure to keep fingers away from the sample cell position, since the compressed air which lifts the Bridgeman seal also presses the piston downward.

B. Optics

A Perkin-Elmer Model 21 IR spectrophotometer was reconstructed with its optics modified for high pressure measurements. The optics used and presented below make a quantitative study of high pressure

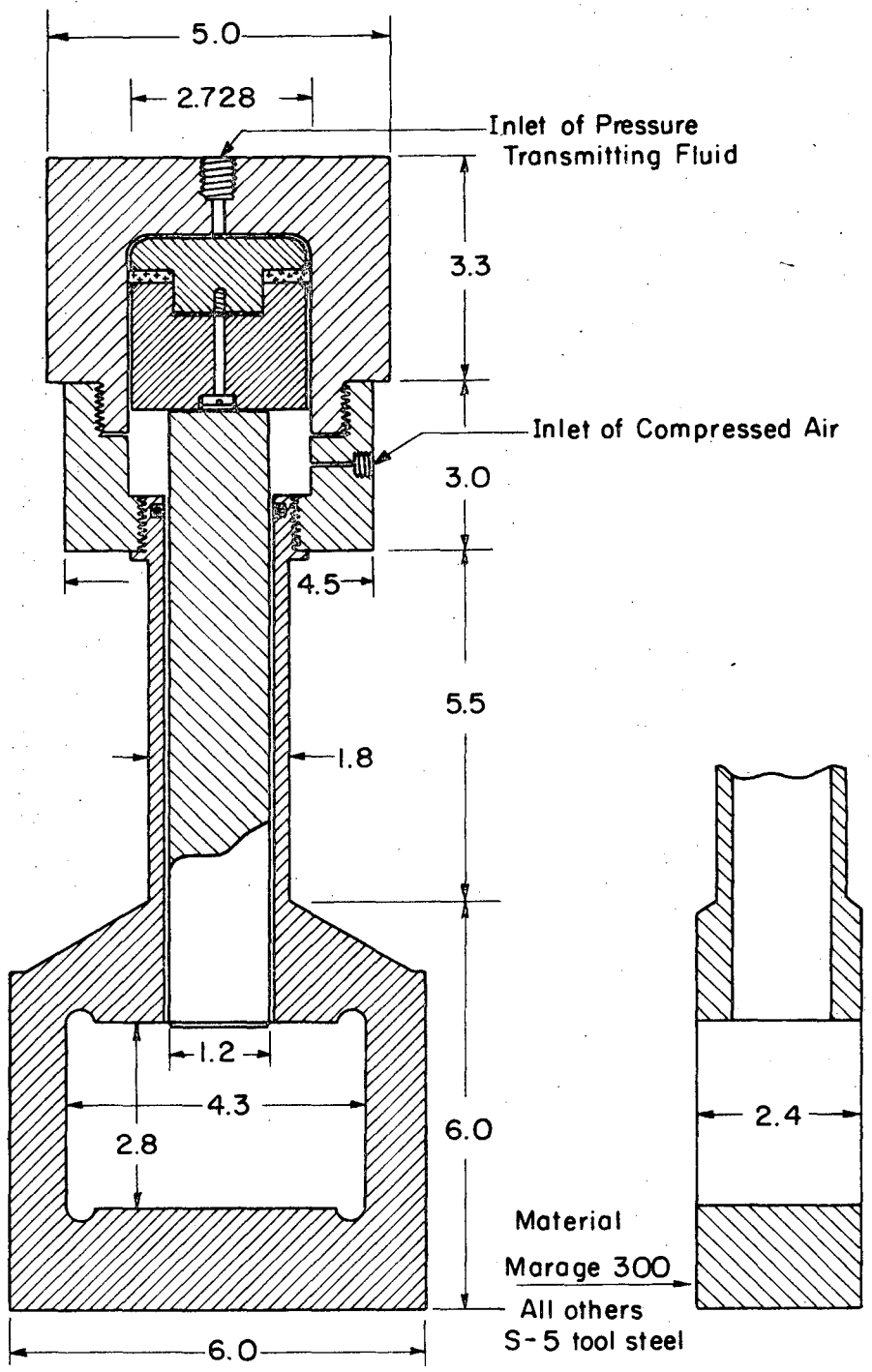

XBL 7110-7367

Fig. 3 Sketch of a press constructed for this study. All numbers indicated are in inches.

IR spectra, 650 to 2000 cm^{-1}, possible for the first time.

The optical system which precedes the monochromator is shown in Fig. 4. In the transmittance measurements, the first light source (S_1) is used. The passage of radiation follows the order of M_1, M_2, Sample, M_3, M_4 and the monochromator. For reflectance measurements, the second light source (S_2) is employed. The light passage follows the order of M_5, M_6, Sample, M_3, M_4 and the monochromator, and it is necessary that M_3 is shifted along the mirror plane, in the direction shown in Fig. 4, such that only half of the M_3 mirror surface is in the light beam. The operational mode is to focus the source radiation on the center of a sample cell and then refocus on the entrance slit of the monochrometer.

The ideal amount of energy which can be passed through the NaCl cell is that which is emitted from the cell when an imaginary light source is located at the center of the sample cell. Since the aperature of the sample cell and the cross-section of the light passage at the cell center is fixed, i.e. constant for a given cell, the energy that passes through the cell is simply proportional to the product of the intensity of light source $I(\nu)$ and the cross-sectional area for the passage of radiation at the cell center. The Sylvania concentrated Zr arc lamp, water jacketed, with a NaCl window, is used as the light source for the sample beam for the following reasons: (1) $I(\nu)$ is at least 2.25 times more intensive than a globar in the entire infrared frequency range, (2) it is relatively cheap and easy to operate, and (3) output intensity is very steady.

Although the aperture of the sample cell is smaller than the maximum aperture of the radiation which can be accepted by the

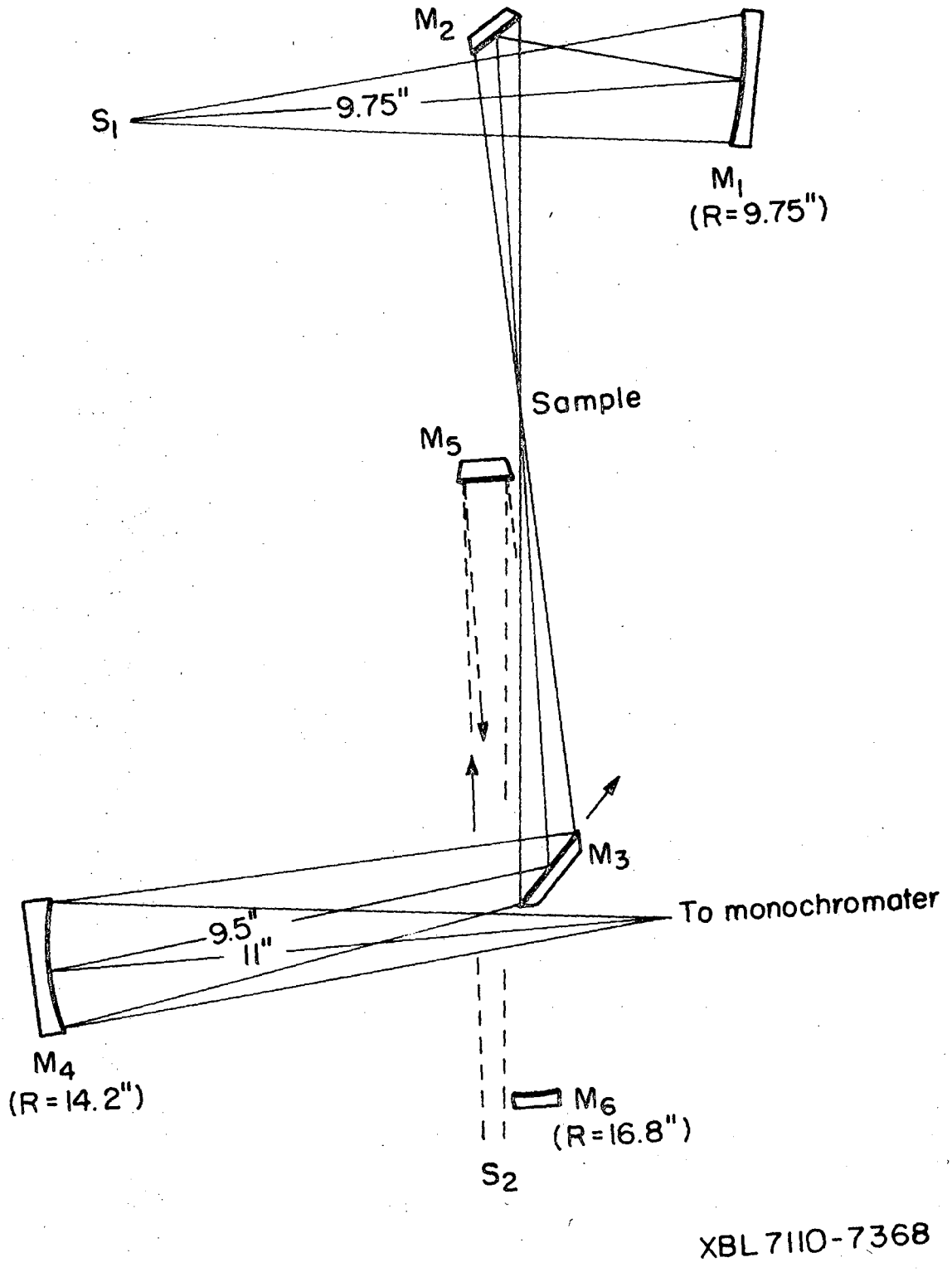

Fig. 4 Optical system of sample beam.

thermocouple, the optics is aligned such that the maximum aperture of radiation is seen by the thermocouple, i.e., the entire surface of all the mirrors in the monochrometer is enveloped with radiation. Energy is gained, since the focus of the light source at the cell center is larger than the slit width used.

The theoretical intensity is obtained by minimizing spherical aberration and astigmatism.

C. Pressure Scale and Precision of the Measured Frequencies

A recent calibration of the pressure scale for samples of ionic crystals by Fong and Nicol[67] shows an approximately linear relationship between the pressure within the NaCl cell and the applied load at pressures up to 25 kb. However, the compressibility of the substances in this study is nearly twice that of the NaCl window and the ionic crystals used in their calibration. Therefore, Fong and Nicol's calibration is not necessarily applicable to the system in this study. Furthermore, it is obvious that pressure within the cell might be dependent on the fit of the pistons with the sample chamber, and on the compression process; i.e., how fast the load is increased.

Before a suitable calibration of an absolute pressure scale for this system is obtained, a reference pressure scale is defined in Fig. 29 (Which is the P-ν relation of the 730 cm^{-1} absorption band of polyethylene). In this P-ν plot, pressure of the sample is simply defined as the applied load divided by the area of piston. The choice of this particular band is based on the following reasons: (1) a 1 mil. polyethylene sheet (Marlex 6009) supplied by Phillips Petroleum Company, can readily be used as a test sample. (2) reproducible and large frequency shifts of this absorption band. (3) the

position of the peak maximum can be determined with certainty, since this absorption band is fairly narrow and symmetric, and its intensity as well as band width are independent of pressure.

Throughout this study, the pressure-scale is checked with Fig. 29. It is found that the pressure-load relation remains for an old cell just as when it was new. However, the upper pressure limit is dropped as the cell is used repeatedly (order of 50 runs). This is probably due to the slight enlargement of the sample chamber.

The observed frequencies for the 730 cm^{-1} absorption band of polyethylene at various pressures are tabulated in Table 3 for two runs of different samples. For pressures above 15 kb, the frequencies of different runs agree within the experimental precision of a single run; the data presented is the adverage values of five to ten runs. For pressures below 10 kb, and especially below 5 kb, the agreement between two runs is not as good. This is due to a poor reproducibility of the compression process at low pressures.

From Table 3, it is seen that the reproducibility for the frequency of a given sample at each pressure is below $\pm$ 0.125 cm^{-1}. This is the reproducibility of our spectrophotometer. However, the precision of the frequencies to be presented in Chapter 4 ranges from $\pm$ 0.25 to $\pm$ 1.0 cm^{-1}, owing to additional uncertainties. For example: (1) the intensity of the sample beam is increased with pressure (may be 20 to 30% from zero to 40 kb) owing to the increase in transparency of the contact surfaces between the sample and windows. (2) uncertainty in the determination of peak maximum for asymmetric bands and very broad bands. (3) uncertainty in the reproducibility of compression process.

Table 3. The average frequencies (before calibration) for the 730 cm^{-1} absorption band of polyethylene.

Sample I		Sample II	
P(kbar)	freq.	P(kbar)	freq.
0	728.31 ± 0.06	decompressed 0	729.73 ± 0.07
5	733.61 ± 0.06	0.755	730.72 ± 0.05
		1.35	730.71 ± 0.09
7.5	733.98 ± 0.15	2.1	730.82 ± 0.08
		2.76	730.76 ± 0.10
10	735.50 ± 0.125	3.4	731.50
		4.04	731.90 ± 0.14
12.5	736.63 ± 0.1	4.72	732.36 ± 0.11
		5.4	732.59 ± 0.08
15.0	737.796 ± 0.1	6.075	732.75 ± 0.03
		6.67	733.06 ± 0.10
17.5	739.09 ± 0.09	7.45	733.56 ± 0.04
20	740.34 ± 0.09	10.08	734.95 ± 0.08
		12.5	736.38 ± 0.01
22.5	741.47 ± 0.05	15.0	737.62 ± 0.1
		20.0	740.31 ± 0.01
25	742.856 ± 0.14		
27.5	744.0 ± 0.05		
30.0	745.31 ± 0.11		
32.5	746.98 ± 0.106		
35.0	748.22 ± 0.10		
37.5	749.51 ± 0.075		
40.0	750.38 ± 0.20		

Since high resolution is not essential for this study, the resolution of our high pressure spectrophotometer is limited by the usage of a sodium chloride prism alone for the dispersion system. Nevertheless, a good reproducibility of the instrument is essential and is obtained in this study.

While no reflectance spectra are measure for this study, over one hundred absorption bands are studied as a function of pressure.* Among them, the frequency shifts range from a few wave-numbers of red shifts to 40 cm^{-1} blue shifts. Intensities for most of the bands are nearly independent of pressure, although some bands show increased intensities with pressure and others decrease with pressure, (See Fig. 8(a), 8(b), and 25). Most of the bands with constant intensities have band widths that are also independent of pressure. However, there are bands with increasing band widths and bands with decreasing band widths.

We tend to believe that pressure exerted on the sample is fairly uniform throughout the area of light passage, since no pressure gradient over the sample surface is observed.** It is especially convincing from the fact that most of the absorption bands have a constant band width, and that some bands, for example, the B_{3u} band (gas state frequency 1214 cm^{-1}) of naphthalene as shown in Fig. 5, have a decreased band width, while the frequency is shifted considerably with pressure.

---

* In order to assure a consistant pressure scale, only first compression data are recorded. (Recompression and decompression data are studied for special purposes.)

** Large pressure gradients are observed in a diamond cell by C. E. Weir.[70] As a result, all absorption bands are greatly broadened at high pressures.

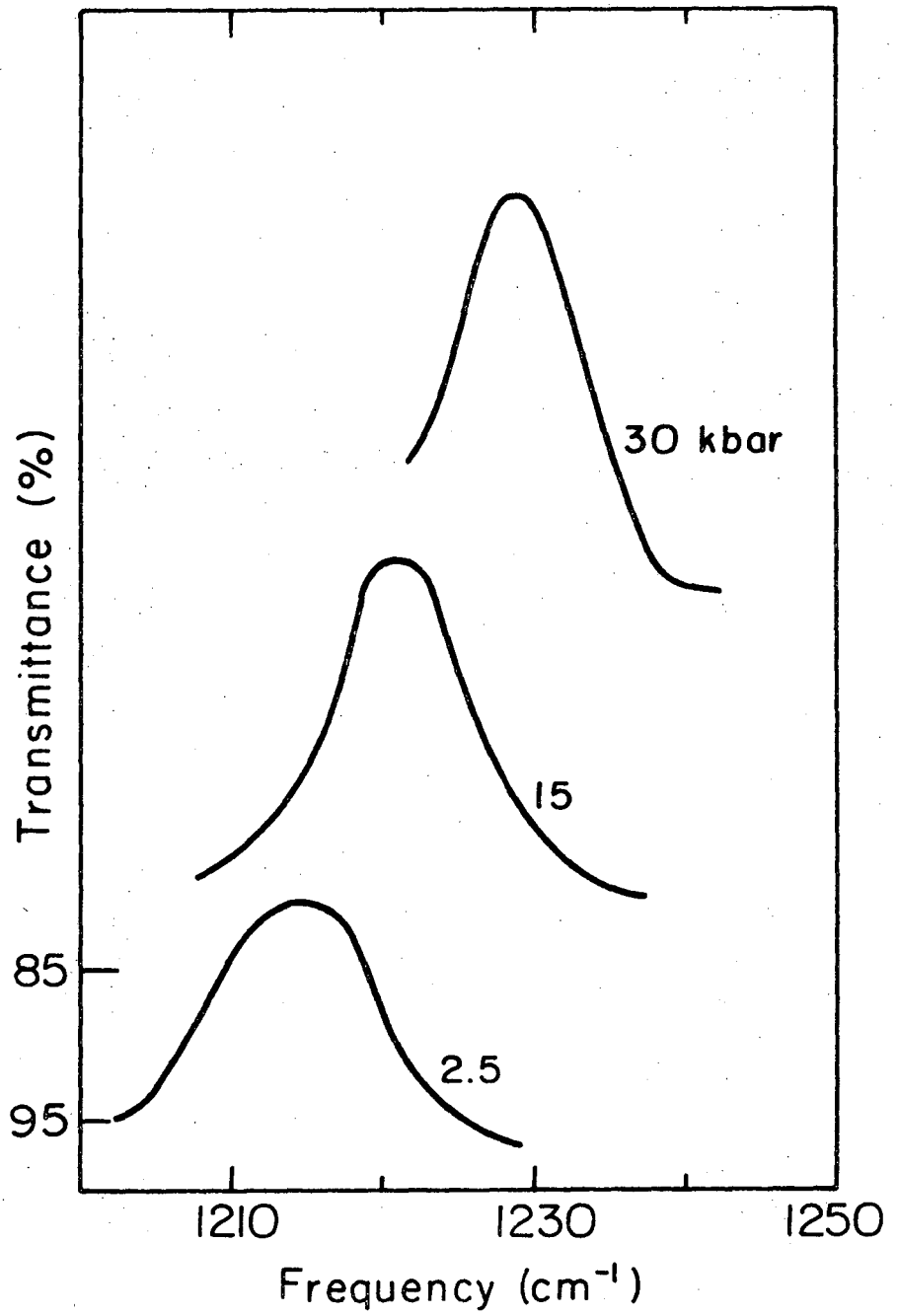

XBL 7110-7369

Fig. 5. Observed B_{3u} (1214 cm^{-1}) band at various pressures.

IV. EXPERIMENTAL RESULTS, CALCULATIONS AND DISCUSSIONS

PART I. Naphthalene

A. Blue and Red Shifts

Clear single crystals in a plate form are prepared by evaporation from reagent grade naphthalene. The transmission spectra (700 cm^{-1} to 2000 cm^{-1}) of naphthalene single crystals were measured with the light beam perpendicular to the ab crystal plane to a pressure (defined in Chapter III) of 40 kilobar. All of the absorption peaks in this frequency range observed at room temperature and pressure are resolved in our high pressure spectra. The observed peak frequencies at pressures of 5 kilobar intervals are tabulated in Table 4. To compare the pressure induced frequency shift with the frequency shifts of gas to solid, the gaseous as well as the solid state frequencies at 1 atm. as reported by Pimentel[34] are included in the table. The average frequency shift of gas to solid ($\nu_{solid} - \nu_{gas}$) is +3 cm^{-1}. All but three are blue shifts. At high pressure, the three exceptions show evidence of interaction with neighboring states. This phenomenon will be discussed later. The pressure induced frequency shifts for bands which appear throughout the entire pressure range studied, are to be found in Table 4 under $\Delta\nu_{(40\ kb)}$. $\Delta\nu_{(40\ kb)}$ ranges from +5.7 to 37.3 cm^{-1} with an average value of 23 cm^{-1}. For naphthalene, 40 kb corresponds to a 21% change in volume, i.e. 7% change in the intermolecular distance from that of the crystal at 1 atm. Even though the volume change of a solid to an ideal gas is essentially infinite, the frequency shift of naphthalene from gas state to solid state is an order smaller than the pressure induced shift, $\Delta\nu_{(40\ kb)}$. Does this indicate that the intermolecular force reaches only to the range of

Table 4. The peak frequencies in the vibrational spectra (700 to 2000 cm^{-1}) of crystalline naphthalene at various pressures.

Assignment*	$\Gamma_4 + \omega_5$				$\gamma_4(783)$
Symmetry Class	B_{1u}	B_{1u}	B_{1u}	B_{1u}	B_{1u}
Gas State Freq.**	698		747		779
Solid State Freq.**	699	726	749	766	787
I_a/I_b***	1.7/0.7	7/5	7/5	6.5/2	10/10
P(kb)\ freq.					
1	695.5‡	722‡	745‡	767‡	788.5
2.5	696.5	724	744	767	788.5
5			745	771.5	790
10	700			773	792
15	703.5(?)				794.2
20					795.5
25					797.5
27.5	707.7				799.3
30	708.7				799
35	711			774.5	801
40	712.8	734.8		774.5	802.5
$\Delta\nu^{\ddagger}_{(40\ kb)}$	17.75	12.3			15.7
$\nu_{solid}-\nu_{gas}$	1		2		3.5
$\Delta\nu/\nu_0$	0.0254	0.0169			0.019

*Fundamental: after N. Claverie.[33] Their gas state frequencies are shown in parenthesis. Combination: after S. S. Mitra and H. J. Bernstein.[39]

**After Pimentel, et al.[34]

***Intensity ratio of a- and b- two factor group components from Pimentel's measurement with polarized light.[20,34]

‡The ν-p plot is nearly a straight line for most of the absorption bands. Therefore, a least square fit of the experimental data to a straight line is carried out to calculate $\Delta\nu_{40kb}$.

‡Owing to the presence of the very intense band, these side bands are not resolved at each pressure.

Table 4 continued

Assignment		$\gamma_2^{(843)}$		$\gamma_3^{(955)}$	
Symmetry Class	B_{1u}	A_u		B_{1u}	
Gas State Freq.	821			949	
Solid State Freq.	819	841		953	
I_a/I_b	7.5/7	8/6		9/9	
P(kb)\ freq.					
1	818	843.7		961.5	**
2.5	817.0	844		961.5	
5	817.5	846		962.0	976.75
10	817.5	847.0		963.5	979.25
15	816.2	848.8*		965.0	982.0
17.5					
20		851.1		965.7	983.4
25		854.0		967.0	984.5
27.5		855.5		967.8	986.0
27.5 (overnight)				968.0	986.5
30		856.5		968.5	987.5
32.5				969.7	989.5
35		859.5	867	970.0	990.0
37.5				970.9	992.0
40		861.5	870	971.0	993.0
$\Delta\nu_{(40kb)}$		18.9		10.4	18.8
$\nu_{solid}-\nu_{gas}$	-2			4	3
$\Delta\nu/\nu_o$	0.0225			0.011	0.0194

*Evidence of splitting start to develop

**Zero intensity at atmospheric pressure, gain intensity through Fermi resonance with $\gamma_1^{(965)}$; see also Fig. 8(b).

Table 4 continued

Assignment	$\gamma_1(965)$	$\delta_8(1008)$		$\delta_5(1126)$ or δ_7	
Symmetry Class	A_u	B_{3u}		B_{2u} or B_{3u}	
Gas State Freq.		1012		1130	
Solid State Freq.	970	1014		1133	
I_a/I_b	9/4	9.5/9.5		15	1
P(kb)\ freq.					
1	978	1010.1		1127.0	
2.5	982	1009.9		1126.5	
5	983.5	1010.5		1127.0	
10	985.5	1011.8		1127.5	
15	988.0	1013.0	1024.5*	1128.7	
17.5				1129.2	
20	990.0	1013.0	1028.0	1129.0	
25	992.5	1013.5	1030.2	1129.5	
27.5	(993.5)***	1014.0	1033.0	1129.8	
27.5 (overnight)	(993.5)	1014.2		1130.0	
30	(994.5)	1014.7		1130.1	
32.5	(996.5)	1016.4	1038.6	1131.2	
35	(997.0)	1016.8	1042	1131.0	1146.0**
37.5	(998.5)	1018.0		1131.7	
40		1018.5	1042	1131.9	1147.2
$\Delta\nu_{(40kb)}$	21.5	8.75		5.7	
$\nu_{solid}-\nu_{gas}$		2		3	
$\Delta\nu/\nu_o$		0.00865		0.0057	

*Pressure induced peak; the resonance partner is unidentified if the intensity is obtained through Fermi resonance.

**A factor group component of (1126) band.

***The frequencies in parenthesis are from shoulder bands and have poorer precision.

Table 4 continued

Assignment	δ_5 or δ_7(1136)		$\Gamma_6+\Gamma_3$	δ_6(1266)
Symmetry Class	B_{3u} or B_{2u}	B_{3u}	B_{2u}*	B_{2u}
Gas State Freq.	1146	1214	1238	1266
Solid State Freq.		1217	1244	1271
I_a/I_b		7/8	9/9.5	9/9.5
P(kb)\ freq.				
1	1144.8	1214.0	1249.7	1277.0
2.5	1144.6	1214.5	1250.0	1277.0
5	1146.4	1215.5	1252.0	1278.25
10	1148.0	1218.5	1255.5	1280.0
15	1151.0	1221.0	1259.0	1283.3
17.5	1152.0			
20	1152.2	1223.2	1261.5	1285.2
25	1154.8	1226.0	1265.0	1288.0
27.5	1156.0	1227.4	1267.5	1290.0
27.5 (overnight)	1156.5	1228.0	1268.0	1290.4
30	1157.3	1229.0	1269.0	1292.5
32.5	1159.0	1231.2	1272.0	1295.0
35	1159.7	1232.5	1273.0	1298.0
37.5	1160.7	1234.2	1275.3	
40	1161.2	1234.6	1275.6	
$\Delta\nu_{(40kb)}$	18.2	21.8	28.1	20.3
$\nu_{solid}-\nu_{gas}$		3	6	5
$\Delta\nu/\nu_o$	0.016	0.0179	0.0226	0.016

*Exchange intensity (in Fermi resonance) with δ_6(1266). See also Fig. 8(a).

Table 4 continued

Assignment		$\omega_{14}(1360)$*	$\omega_{11}(1389)$*		$\omega_{15}(1509)$
Symmetry Class	B_{3u}	B_{3u}	B_{2u}		B_{3u}
Gas State Freq.		1366			
Solid State Freq.	1307	1362	1385		1506
I_a/I_b	5/3	8/9	9/9.4		
P(kb)\ freq.					
1	1308.0	1367.75	1393.1		1513.0
2.5	1308.5	1368.8	1393.1		1513.5
5	1312.0	1369.8	1394.5	1528	1513.6
10		1372.0	1394.5	1532.5	1515.0
15	1315.0		1395.7		1517.0
20	1318.0			1537.0	1518.0
25					1519.3
27.5	1324.6	1370.0			1520.6
30	1324.25	1370.5		1544.5	1521.0
35	1329	1372.0	1395		1523.2
40	1331.5	1374.0	1395.5		1525
$\Delta\nu_{(40kb)}$	24.5				12.1
$\nu_{solid}-\nu_{gas}$		-4			
$\Delta\nu/\nu_0$					0.00803

*Evidence of interaction between ω_{14} and ω_{11} is observed. See also Fig. 11.

Table 4 continued

Assignment		ω_{10}(1596)		
Symmetry Class	B_{2u}	B_{2u}	B_{2u}	B_{3u}
Gas State Freq.		1596	1661	1720
Solid State Freq.	1563	1594	1673	1337
I_a/I_b	8/9		7/8.5	
P(kb)\ freq.				
1	1572.0	1598.5	1673.0	1735.5
2.5	1573.0	1598.5	1675.0	1736.0
5	1576.5	1599.7	1676.0	1740.0
10	1578.0	1600.5	1680.0	
15	1582.5	1602.5	1683.0	1745.0
20	1585.0	1602.8	1684.7	
25	1586.5	1603.4	1686.0	1756*
27.5	1589.0	1605.0		1756.0*
30	1590.0	1605.2		1757.5*
35	1593.0	1606.5	1690	
40	1597	1608		
$\Delta\nu_{(40kb)}$		9.9		31.9
$\nu_{solid}-\nu_{gas}$		-2	2	17
$\Delta\nu/\nu_o$		0.0062		0.00185

*A pressure induced peak at 1738 is resolved.

Table 4 continued

Assignment	$\delta_6+\omega_5$		$\omega_5+\omega_{11}$	
Symmetry Class	B_{2u}	B_{3u}	B_{2u}	B_{2u} or B_{3u}(?)
Gas State Freq.	1763	1835	1896	1938
Solid State Freq.	1786	1845	1919	1944
I_a/I_b				
P(kb)\ freq.				
1	1787.0	1846.0	1932	1966.5
2.5	1788.25	1848.5	1933.5	
5	1789.0	1849.0	1935.5	1968.5
10	1792.0	1851.5	1938.5	1970.0
15	1799.5	1856.5	1945.8	1976.5
20	1800.5	1858.5	1947.8	1982.5
25	1803.2	1862.0	1950.0	1986.5
27.5	1808.8	1864.0	1954.5*	1988.5
30	1809.5	1865.5	1954.0	1990.0
35	1816	1868.5	1964.2	1996.2
40	1819.5	1870.3	1968.2	1998.5
$\Delta\nu_{(40kb)}$	33.6	25.2	37.3	33.3
$\nu_{solid}-\nu_{gas}$	23	10	23	6
$\Delta\nu/\nu_o$	0.019	0.01375	0.0197	0.0172

*Evidence of exchange in intensity between B_{2u}(1896) and (1938) is observed above 27.5 kb.

unit cell dimension? This question as well as its relation to the blue and red shift will be discussed in the following paragraphs.

For a qualitative discussion of the frequency shift, only the numerical force constant* of Eq. (37) will be considered. The tensor force constant is probably much smaller than that of the numerical constant for naphthalene, since the pressure induced change in Davydov splitting is much smaller than the corresponding frequency shift for all bands except one in the naphthalene spectra. From Eq. (40), it is obvious that each attractive term (e.g. $-ar^{-b}$ where a and b are positive numbers) in U_{mn} contributes a red shift to $\Delta\nu$(gas to solid) as well as to $\Delta\nu(P_2-P_1)$. Although multipole-coulombic forces can contribute either red or blue shifts depending on the relative orientation of the molecules, the fact that the condensed phase could be formed from the gas state indicates that the net long range forces must be attractive. The short range repulsion potential always causes a blue shift. If one hypothetically decreases the density of a crystal continuously to that of a gas, there should be a red shift in a range of density below a certain value and a blue shift above this value. This qualitative consideration agrees with the experimental observation of Wiederkehr and Drickamer[35] in their measurement utilizing a sulfide cell. Figure 6 shows their results of the measurement of the C-N stretching frequency in various solvents to 10 kb. The change from red to blue shifts implies a chance in the dominant force field from attractive to repulsive. It is thus concluded that the small frequency shift of gas to solid is probably a result of the cancellation of a large red and a larger blue shift.

---

*Only the first term in Eq. (37) is left if one studies molecules or ions in a matrix or in liquid solutions.

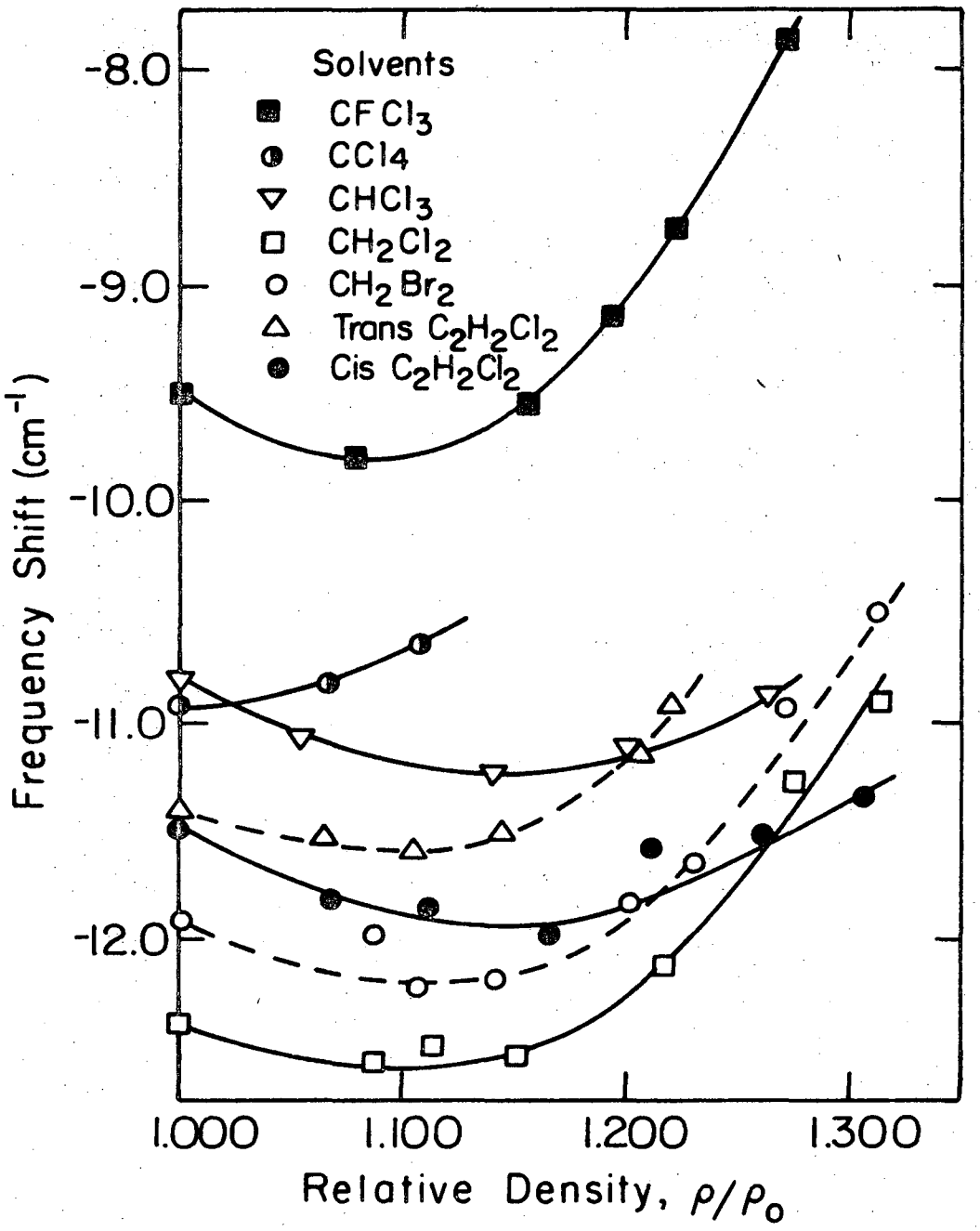

XBL 7110-7370

Fig. 6 CN vibration of CH_3CN in various solvents. ρ_o is the density of a solution of 1 atm and ρ is that at 1 atm to 10 kbar. (after R. R. Wiederkehr and H. G. Drickamer (35))

The observed pressure induced frequency shifts $\Delta\nu_{(40kb)}$ for the fundamentals range from 5.7 cm^{-1} to 21.3 cm^{-1}. There is no obvious evidence of any correlation* between the frequency shifts of the normal modes and their symmetry classes, nor correlation among the normal modes of the same type of motions, e.g. ω_{12}, ω_{16}, and ω_{17}. This may be understood from Eq. (40) and Eq. (41).

In Eqs. (40) and (41), only the factor $(\partial r_n | \partial q_p^i)_o$ is dependent on the molecular normal coordinate q^i. One may re-write the second term in the parenthesis of Eq. (40) as $(\partial r_{mn}/\partial q^i)_o^2$. It is then obvious that the normal motions which connect with larger changes in the non-bonded interatomic distances are expected to show greater frequency shifts. One can define the hard collision as that due to the short range repulsion force and the soft collision as that due to the long range forces. (Similar definitions have been used in the transport theory of the liquid phase.) It may be concluded that the frequency shift as well as the Davydov splitting are caused by collisions (both hard and soft collisions are involved in this mechanism) of non-bonded atoms, and that the pressure induced blue shifts of the naphthalene normal modes are due to the dominance of hard collisions between non-bonded atoms during their normal motions. It can be understood from Fig. 2 that only the $\hat{q}^i$ component of the restoring force of the non-bonded atomic collisions is responsible for the frequency shift and the Davydov splitting of the q^i normal mode.

---

*To correlate the frequency shift among different normal modes, it is proper to compare the values of $\Delta\nu_{40kb}/\nu_{gas}$ instead of $\Delta\nu_{40kb}$. The former is listed in Table 4 under $\Delta\nu/\nu_o$.

B. Discussion of Non-Bonded Interatomic Potential

One may assume a functional form for U_{mn} with unknown parameters: e.g.

$$U_{mn} = Ar_{mn}^{-c} - Br_{mn}^{-d} \tag{51}$$

Three sets of each of the parameters A, B, c and d are necessary to account for H-H, H-C, and C-C non-bonded atomic potentials. Using these potential functions, one may be able to calculate both the tensoral and numerical force constants of Eq. (40) and Eq. (41). $(\nu_{p_1} - \nu_{p_2})$ of the fundamentals can thus be obtained as a function of the twelve unknown parameters. These unknown parameters and thus the interatomic potential functions could then be evaluated from the observed $(\nu_{p_1} - \nu_{p_2})$ of Table 4. However, the numerical calculation can not be carried out until high pressure x-ray data are available.

The interatomic potential could also be calculated from the pressure dependence of Davydov splitting. This will be illustrated with n-paraffins, since only one pair of factor group components are resolved for naphthalene in this study and the assignment of this doublet (at 1126 cm^{-1}) is still uncertain. The resolved doublet has a separation of 5 and 15.3 cm^{-1} respectively at 1 atm and 40 kb. The factor group components are identified through the comparison of the intensity ratio with that observed by Pimentel, et al.[20] in their measurements with polarized radiation at 1 atm.

C. A Direct Observation of Resonance Phenomenon and Calculation of Unperturbed Levels as well as Coefficients of Mixing

In the frequency range, 690 cm^{-1} to 1600 cm^{-1}, Naphthalene shows 18 bands in its gas state spectrum and 37 bands in its solid state spectrum. There are 28 bands in the spectrum of solutions[34] of Naphthalene in carbon disulfide, methyl cyclopentane and carbon tetrachloride. The additional bands in the condensed phases are believed to be overtone and combination bands, although the assignment is still far from complete.

The appearance of overtone and combination bands is, naturally due to the effect of anharmonicity or higher terms in electric dipole expansion. The former is usually more important and is assumed to be the cause. In first order perturbation theory, the consequence of considering the anharmonic terms is that the perturbed energy level is shifted, and the amount of shifting is equal to the diagonal matrix element of the perturbation function $\langle \psi_v^o | H' | \psi_v^o \rangle$. As the result of this shift, the overtone frequencies are not exactly integral multiples of the fundamental frequencies. The combination frequencies are not exactly equal to the sums of the fundamental frequencies making up the combination. In second order perturbation theory, the perturbation causes a mutual interaction of the energy levels. This is represented by the off diagonal matrix perturbation function $H'_{vv'}$, $(= \langle \psi_v^o | H' | \psi_{v'}^o \rangle)$. As a result of this second order effect, each level ε_v^o produces a shift of any other $\varepsilon_{v'}^o$ and at the same time contributes to the eigen function of the others; both effects increase with decreasing separation of unperturbed levels and the larger the perturbation function H' the larger will be this effect.

In a molecule or crystal, should there exist two levels of nearly the same energy and all the others are far apart, the perturbed energy levels ε are the solution of the secular determinant.[36]

$$\begin{vmatrix} \varepsilon_v^o - \varepsilon & H'_{vv'} \\ H'_{v'v} & \varepsilon_{v'}^o - \varepsilon \end{vmatrix} = 0 \tag{52}$$

The solution of which may be written as

$$\varepsilon = \frac{\varepsilon_v^o + \varepsilon_{v'}^o}{2} \pm \frac{1}{2}\delta \tag{53}$$

Where

$$\delta = \left[\delta_o^2 + 4|H'_{vv'}|^2\right]^{\frac{1}{2}} \tag{54}$$

δ is the observed separation and $\delta_o (= \varepsilon_v^o - \varepsilon_{v'}^o)$ is the separation of the unpertrubed levels. The eigen functions of the reaulting states are[36]

$$\psi_v = a\psi_v^o - b\psi_{v'}^o \tag{55A}$$

$$\psi_{v'} = b\psi_v^o + a\psi_{v'}^o \tag{55B}$$

Where

$$a = \left[\frac{\delta + \delta_o}{2\delta}\right]^{\frac{1}{2}}; \qquad b = \left[\frac{\delta - \delta_o}{2\delta}\right]^{\frac{1}{2}} \tag{56}$$

H' have the full symmetry of the system and is totally symmetric. Therefore ψ_v^o and $\psi_{v'}^o$ must have the same symmetry in order for this resonance interaction to exist, i.e. $H'_{vv'} \neq 0$. An interesting case is $\delta_o = 0$; both perturbed states are fifty-fifty mixtures of the unperturbed states, i.e. $a=b= \frac{1}{\sqrt{2}}$.

We define the unperturbed states of a resonance pair $\psi_{v'}^o$ and ψ_v^o as follows. $\psi_{v'}^o$ is the upper state of an overtone or combination. ψ_v^o is the upper state of an IR active fundamental. A situation where the energy level of $\psi_{v'}^o$ is below that of ψ_v^o at 1 atm. and $\psi_{v'}^o$ is above ψ_v^o at high pressure, may exist when a larger blue shift of $\psi_{v'}^o$ is induced by pressure. The resonance pair is thus described by a positive δ_o value at 1 atm., by $\delta_o = 0$ at a cross-over pressure, and by negative δ_o values at higher pressures. The resonance interaction between the overtone (or combination) and the fundamental reaches a maximum at the cross-over pressure. The extent of interaction is decreased by either increasing or decreasing pressure from the cross-over pressure. The expected frequency vs. pressure plot of the perturbed and unperturbed levels is depicted in Fig. 7. In this figure, $\psi_{v'}$ and ψ_v are perturbed states. The ψ_v states (marked as stars) contain more than 50% of the states ψ_v^o and may be observed with a higher intensity than the $\psi_{v'}$ states (marked as darkened circles) which have less than a 50% content of ψ_v^o. At the cross-over pressure ($\delta_o = 0$) the observed separation δ is minimum. The two perturbed states marked with Δ in Fig. 7 have the same intensity, if the intensity of the fundamental is much greater than that of the overtone or combination.*

---

* Private communication with Proffessor G. Pimentel.

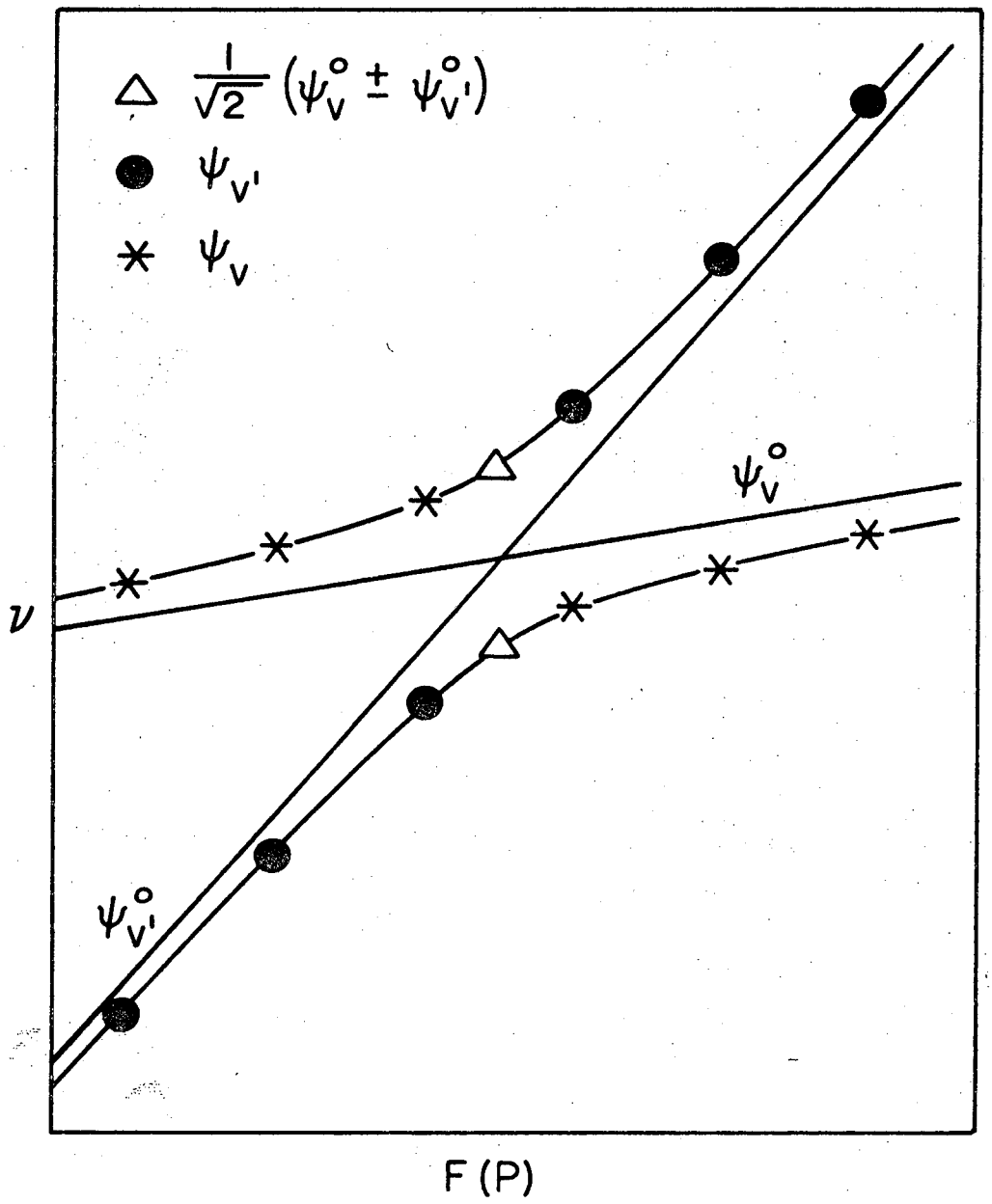

XBL7110-7371

Fig. 7 The expected frequency vs pressure plot for the perturbed as well as the unperturbed states of a resonance pair. F(p) is defined such that the energy levels of the unperturbed states are approximately linear functions of F(p).

Two pairs of this type of resonance phenomenon are observed in the high pressure spectra of crystalline naphthalene. The intensity transfer phenomenon is obvious in the observed spectra, as shown in Figs. 8(a) and 8(b). In Fig. 8(a), the resonance pair is δ_6(1266 cm^{-1}) fundamental and $\Gamma_6 + \Gamma_3$ (1238 cm^{-1}) combination band. The symmetry classes of both partners are well established[20,34,33,39] and are both B_{2u}. In Fig. 8(b), γ_1(965 cm^{-1}) belongs to the A_u[40] symmetry class. Its resonance partner is not resolved in the atmospheric spectra, and has not been assigned. The observed energy level separations of these resonance pairs at various pressure are shown in Figs. 9(a) and 9(b). At the cross-over pressure, the observed energy level separation is equal to $2|H'_{vv'}|$. The cross-over pressures are 24 kb and 17.5 kb respectively for the B_{2u} and A_u resonance pairs. The off diagonal matrix elements of anharmonic perturbation functions are 11.4 cm^{-1} and 2.6 cm^{-1} respectively for the B_{2u} and A_u resonance pairs. Assuming H' as independent of pressure, the δ_o values as well as the coefficients of mixing, a and b can be calculated from Eqs. (54) and (56) by utilizing the obtained $H'_{vv'}$ and δ values. The calculated unperturbed energy level separation and the coefficients of mixing at various pressures are shown in Table 5(a) and 5(b). In Figs. 10(a) and 10(b), the predicted unperturbed, as well as the perturbed energy levels, are plotted as a function of pressure.

The anharmonic potential of a crystal includes the higher order terms in Eqs. (29) and (32). As mentioned in Chapter II, the observed overtones and combinations of molecular crystals usually originates from the anharmonic coupling of intramolecular motions. Thus, in principle, one should apply the perturbation treatment of this section

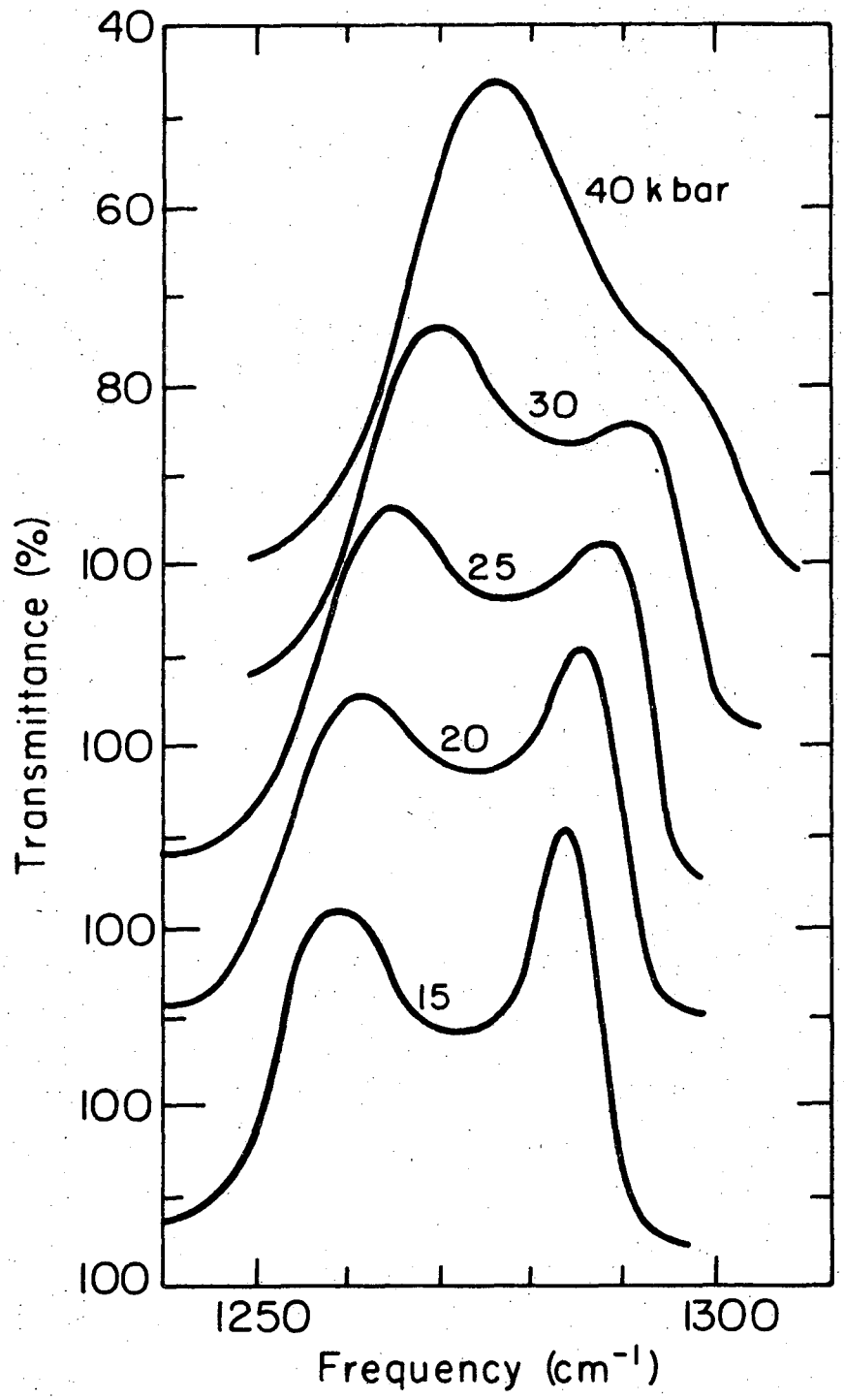

XBL7110-7372

Fig. 8a The high pressure spectra of the B_{2u} resonance pair; δ_6(1266 cm^{-1}) and $\Gamma_3 + \Gamma_6$(1238 cm^{-1}) of crystalline naphthalene.

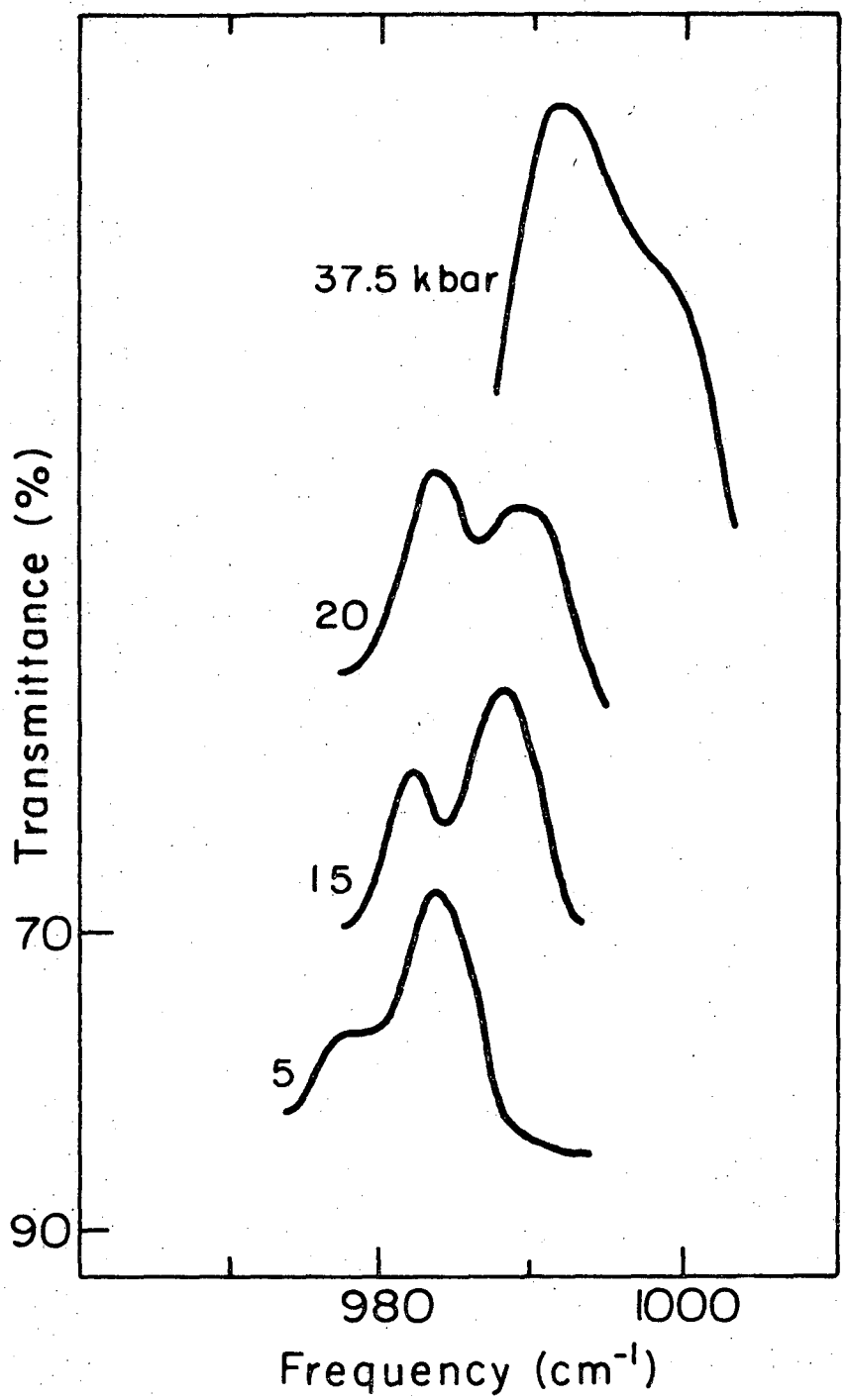

XBL7110-7373

Fig. 8 b . The high pressure spectra of the A_u resonance pair of crystalline Naphthalene.

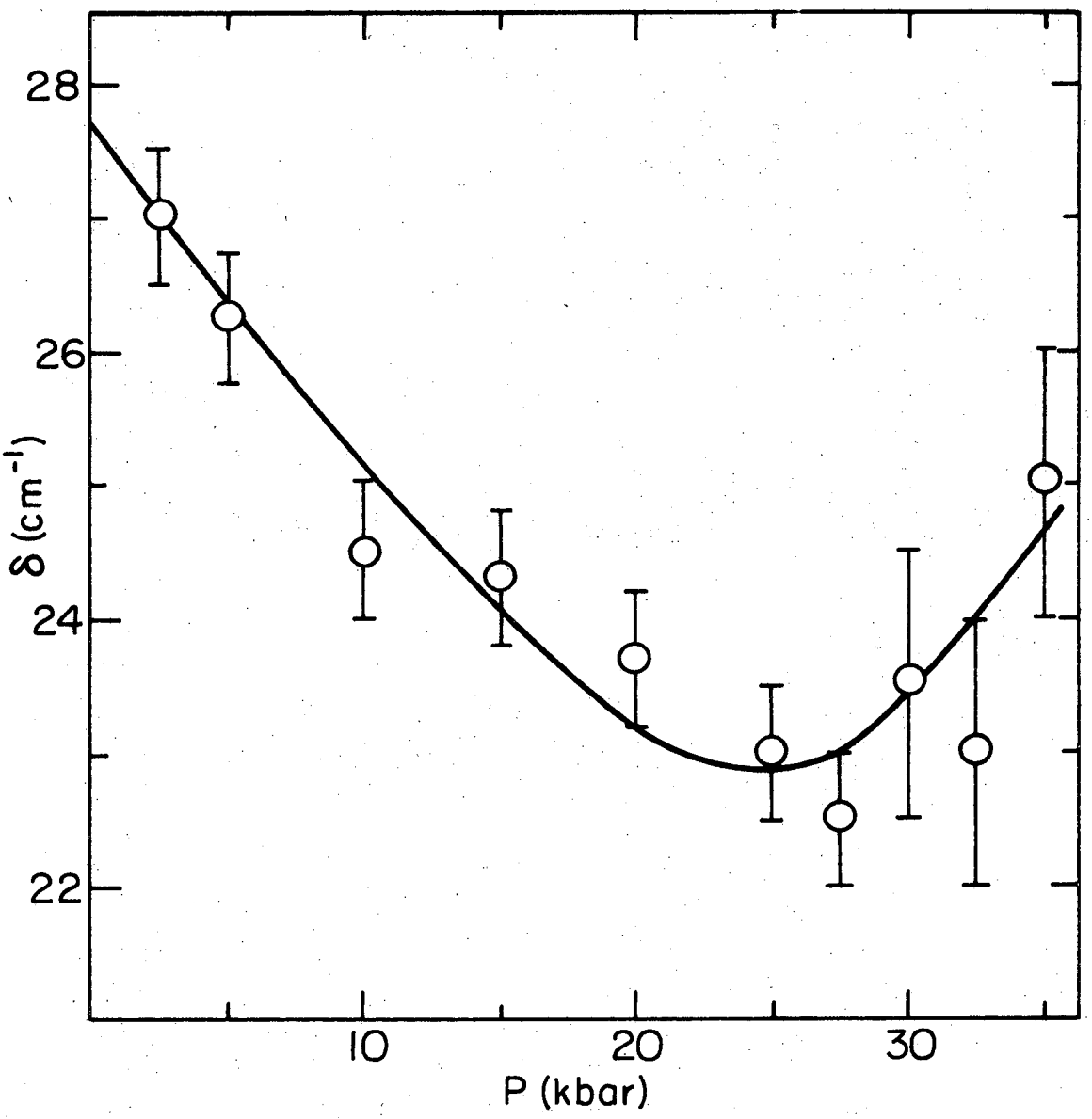

XBL 7110-7374

Fig. 9a The observed energy level separation at various pressures for the B_{2u} resonance pair of crystalline naphthalene.

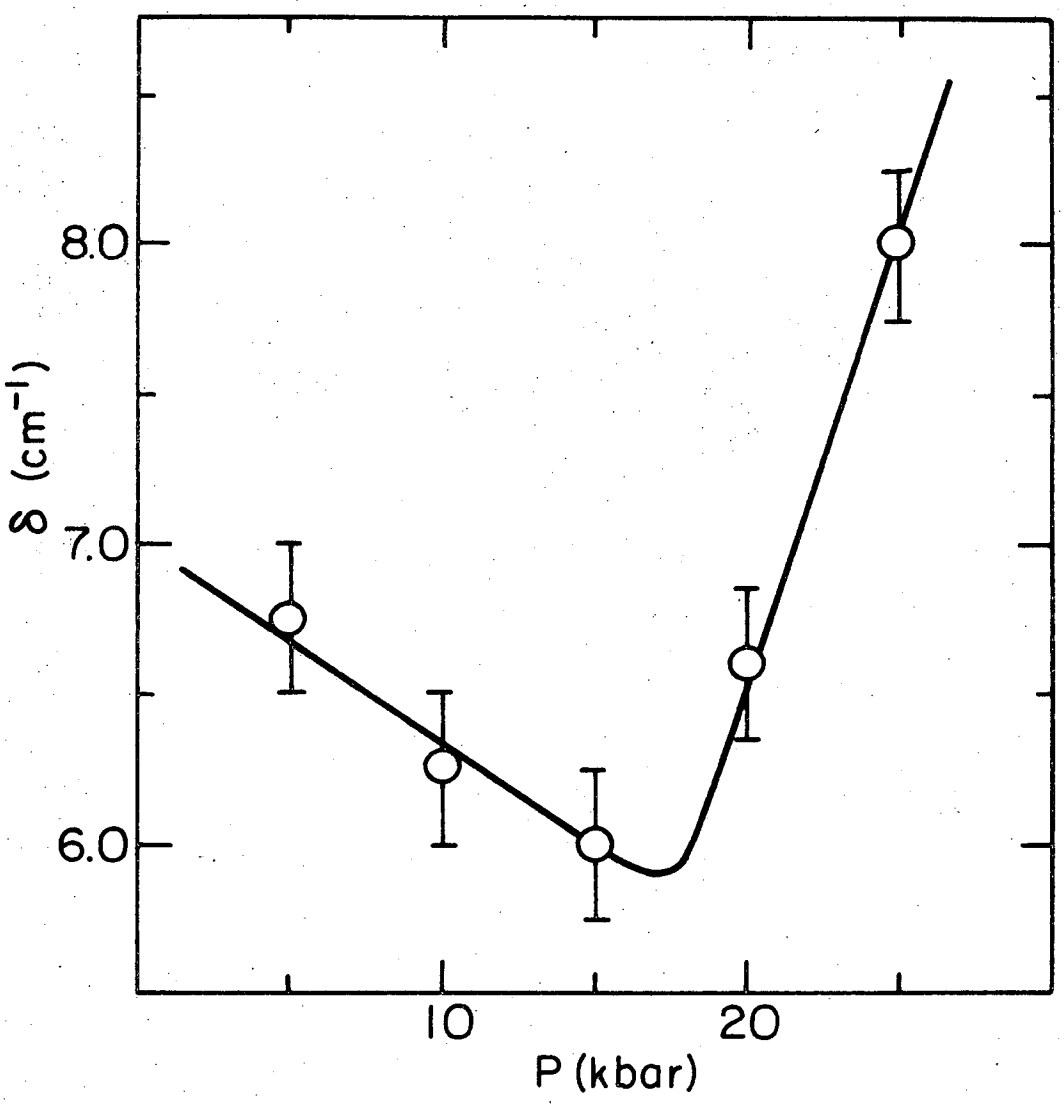

XBL7110-7375

Fig. 9b The observed energy level separation at various pressures for the A_u resonance pair of crystalline naphthalene.

Table 5(a). The unperturbed frequency separations and the coefficients of mixing at various pressures for the B_{2u} resonance pair of crystalline Naphthalene.

P(kbar)	0	5	10	15	20	24	30	35
$\delta_o(cm^{-1})$	15.7	13.1	10.5	7.5	4.0	0	5.3	9.35
a	0.88	0.87	0.84	0.81	0.76	0.706	0.78	0.83
b	0.47	0.50	0.54	0.59	0.65	0.706	0.62	0.56

Table 5(b). The unperturbed energy level separations and coefficients of mixing at various pressures for the A_u resonance pair of crystalline Naphthalene.

P(kbar)	0	5	10	15	17.5	20	25
δ_o (cm^{-1})	3.8	3.3	2.3	1.3	0	2.8	5.5
a	0.88	0.86	0.83	0.79	0.706	0.85	0.92
b	0.48	0.50	0.56	0.62	0.706	0.53	0.39

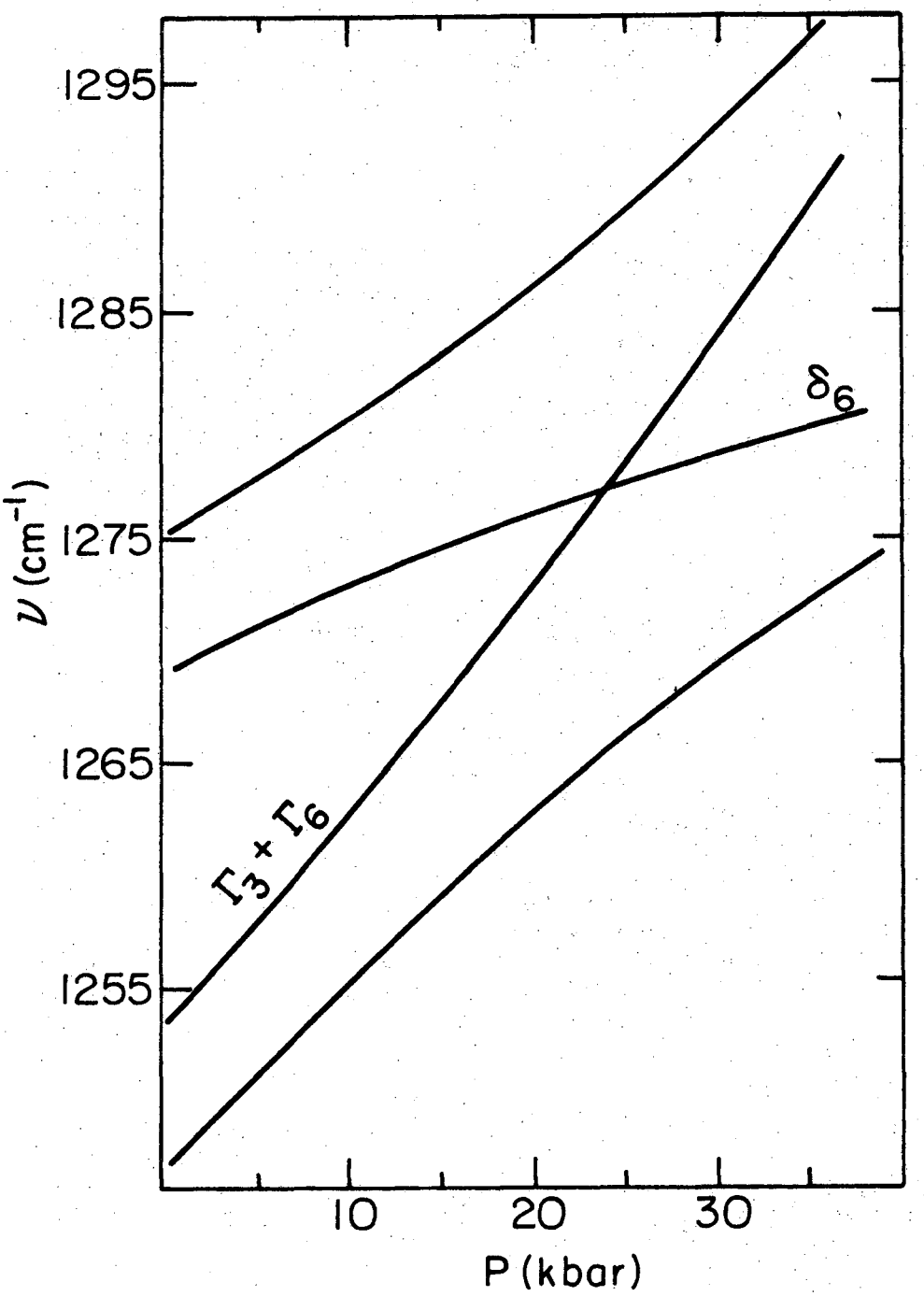

XBL 7110-7376

Fig. 10a The predicted unperturbed and perturbed energy levels (corresponding to the curve of Fig. 9a) for the B_{2u} resonance pair of crystalline naphthalene at various pressures.

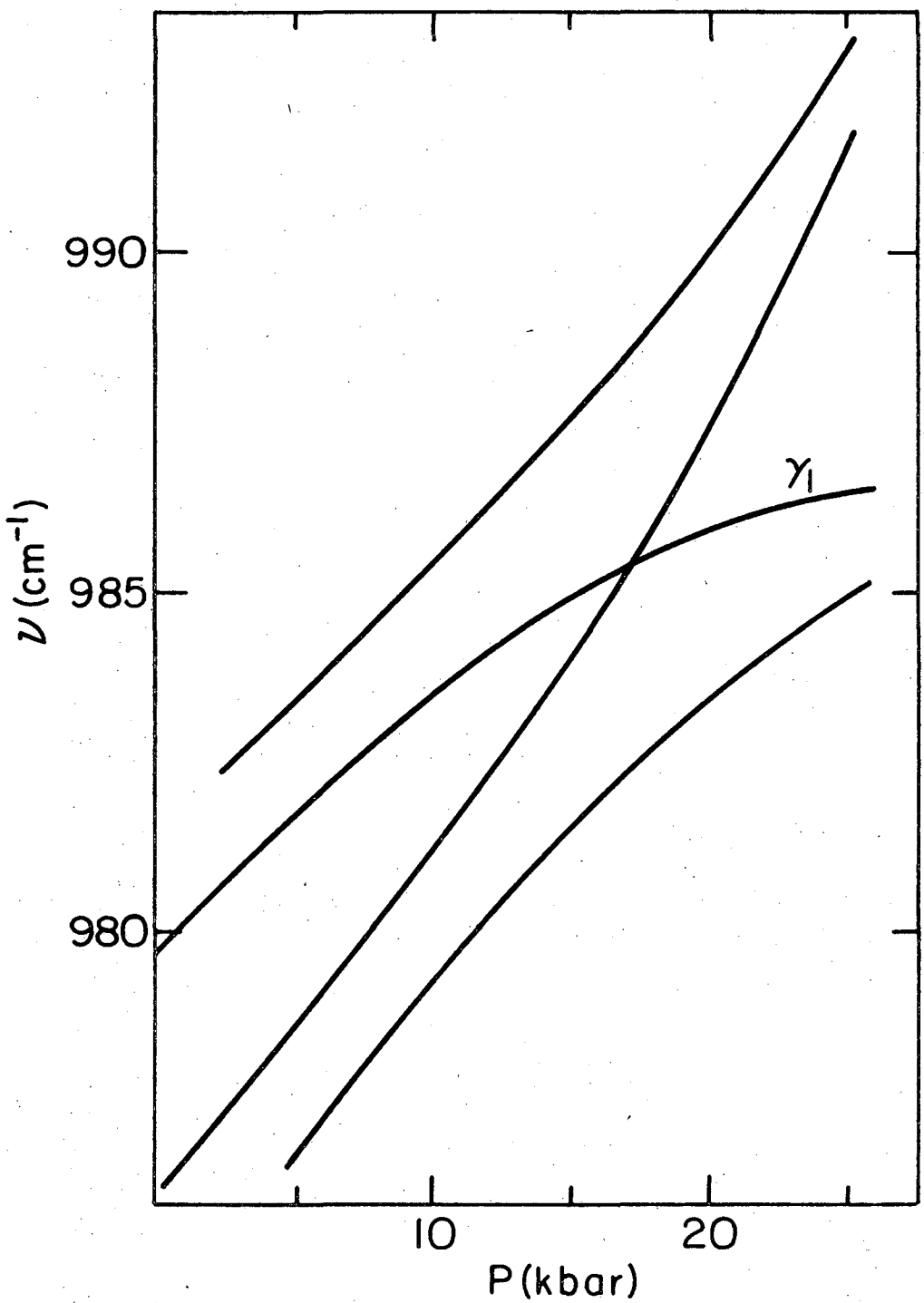

XBL7110-7377

Fig. 10b The predicted unperturbed and perturbed energy levels (corresponding to the curve of Fig. 9b) at various pressures for the A_u resonance pair of crystalline naphthalene.

to the solution of Eq. (29) before attempting to solve Eq. (30). H' is thus the total Hamiltonian of a molecule minus that of the harmonic approximation. It may be concluded that the observed resonance phenomenon is exactly that which was first recognized by Fermi[37] in the vibrational spectra of CO_2.

If the resonance partner of a fundamental is not an overtone or combination, but a vibrational level of a different electronic state, the above treatment holds exactly, except that $H'_{vv'}$ is now the perturbation due to the interaction of vibration and electronic motion.[38] The vibrational assignment of the B_{2u} resonance partners are reasonably certain. Therefore, the latter resonance mechanism is probably eliminated, at least, for this resonance pair.

To the limit of the second order perturbation theory, there could be no interaction among normal modes of different symmetry classes. Nevertheless, normal modes $\omega_{14}(B_{3u})$ and $\omega_{11}(B_{2u})$ are observed to exchange intensities as depicted in Fig. 11. At atmospheric pressure, the intensity of the $\omega_{14}(B_{3u})$ band is approximately half of that of the $\omega_{11}(B_{2u})$ band. The B_{3u} band loses its intensity to the B_{2u} band with increasing pressure. The $\omega_{14}(B_{3u})$ band is nearly diminished at 25 kb. When the pressure is further increased, the B_{3u} band regains part of its intensity from the B_{2u} band. This interaction phenomenon is different from that of Fermi resonance, through which one band is continuously increasing intensity at the expense of the other.

The interaction among normal modes of different symmetry classes is probably a result of higher order perturbation effects. Further study on this interaction phenomenon, both experimentally and

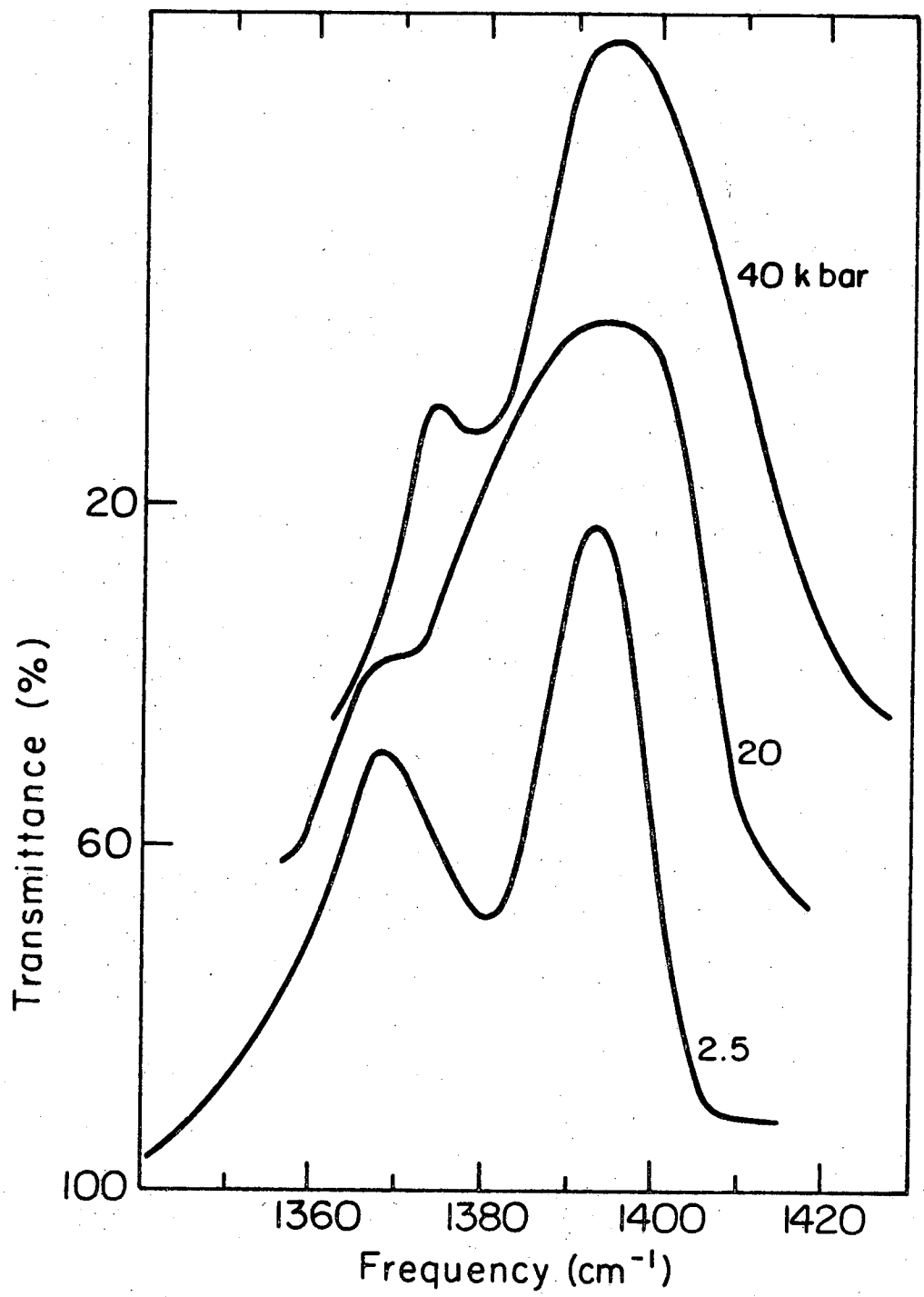

XBL7110-7378

Fig. 11. The high pressure spectra of $\omega_{11}(B_{2u})$ and $\omega_{14}(B_{3u})$ of crystalline Naphthalene.

theoretically could be fruitful.

Among the 34 bands studied, most keep a constant intensity to 40 kb. However, aside from the three resonance pairs, the bands at 818 cm^{-1} and 1572 cm^{-1} are diminished with increasing pressure. The pressure induced peaks, 867 cm^{-1} and 1024.5 cm^{-1} are apparent at 35 kb and 15 kb respectively. Their intensities are increased with pressure. The intensity changes of these bands might also be associated with resonance interaction. However, their resonance partners (one may have to consider the resonance among several levels) are not the nearest neighboring bands. The resonance partners cannot be found without a quantitative analysis of absolute band intensities. The same resonance mechanisms may also be responsible for the change of the absolute band intensity from gas to solid phase.

The vibrational analysis of the molecular spectra is exceedingly complicated as a consequence of the anharmonicity, owing to both the first and second order effects mentioned in the beginning of this section. The direct observation of the Fermi resonance for any substance will certainly be helpful for the vibrational analysis of its molecular spectra.

Other aspects of the usefulness of the solid state spectra and high pressure study for vibrational analysis will be discussed in the next section.

D. Application of High Pressure Crystalline Data on Molecular Vibrational Assignment

A Naphthalene molecule has 48 vibrational degrees of freedom. Among them, 20 ungerade normal modes are IR active and 24 gerade normal modes are Raman active. The solid state IR spectra of

Naphthalene was first studied for the purpose of the vibrational assignment of gas state spectra. As shown in Chapter II, the 4 A_u normal modes which are inactive in the gas state become active in its crystal site. The gas phase infrared active modes remain active in the solid state. Two factor group components were observed for each of the solid-state-active-molecular-normal-modes in the polarized infrared measurement.[34] It was demonstrated by Pimentel[34,20] that the observed intensity-ratio of these two components could be employed to divide the observed bands of Naphthalene into the appropriate symmetry classes to allow the selection of the fundamentals from just the restricted number of frequencies in the proper class; As a consequence one may identify a B_{1u} absorption band of Naphthalene from the expected intensity relationship: $I_a > I_b$ and $I_c < I_b$. B_{2u} from the relationship: $I_a < I_b$ and $I_c < I_b$. B_{3u} from $I_a > I_b$.and $I_c > I_b$.

The vibrational analysis has been improved a great deal in the past few years with the extensive application of computers and least square refinements. However, it is still very difficult to analyze the vibrational spectra of molecules as large as Naphthalene. With the help of the symmetry assignment from the intensity ratio of the factor group components, the vibrational spectra of Naphthalene are best understood among molecules of this size. However, the assignment of its fundamental frequencies is still uncertain for at least two normal modes, δ_5 and δ_7. Not many overtones and combinations are assigned unambiguously.

The direct observation of resonance pairs, together with the calculation of the unperturbed levels might be able to alleviate the

difficult situation in the vibrational analysis. The high pressure study can further offer us the following rules for verifying an assignment and for knowing the quality of the assignment.

If one defines $\Delta\nu$ as the frequency shift from 1 atm to 40 kb, it immediately follows that

$$\Delta\nu_{o \to v'} - \Delta\nu_{o \to v} = \Delta\nu_{v \to v'} \tag{57}$$

The subscripts represent a set of quantum numbers specifying a vibrational state. To the harmonic approximation,

$$\Delta\nu_{o \to v} + \Delta\nu_{o \to v'} = \Delta\nu_{o \to v + v'} \tag{58}$$

To verify the applicability of the above two rules, it is necessary to obtain high pressure Raman spectra as well, and to anticipate a more complete assignment of the overtone and combination bands of Naphthalene.

PART II. N-Paraffins and Polyethylene

A. Pressure Effects on the Spectra of N-Paraffins

The IR spectra of n-paraffins at 1 atm. have been measured by many authors. The most recent studies are those by Primas and Gunthard,[45,46] Brown, et al.,[47,48] Snyder[49,50] and Tasumi, et al.[51,52,53,54] The assignment of the frequency regions to specific types of vibrations are well established. They are summarized in Table 6. Also included in this table are the vibrational assignment which give rise to the IR activity of the normal modes.

In their normal coordinate analysis of an infinite chain, (namely, solving the 18 × 18 GF matrix of two CH_2 groups for various phase differences), Tasumi and Shimanouchi obtained normal coordinates of an infinite chain as a function of phase differences kc. Where k is a wave vector, and c is the distance along the chain axis between two adjacent methylene groups. The constituent symmetry coordinates for each class of normal modes are also included in Table 6.

For an isolated n-paraffin, the vibrational frequencies of a specific type of vibrations are cosine functions of kc.[49] Normal modes of a n-paraffin molecule are characterized by various values of phase differences. They are

$$kc = \frac{m\pi}{N-1} \quad \text{where} \quad m = 1,2,3 \ . \ . \ . \ N-2 \tag{59}$$

Where N is the number of carbon atoms in a n-paraffin molecule. Normal modes of a given type of vibrations are thus specified by m and N values. In order to facilitate our presentation of the observed frequencies, notations for molecular normal modes are defined in Table 6.

Table 6. Character of n-paraffin normal modes

Tasumi and Shimanouchi's Vibrational Assignment	Composite Symmetry Coordinates	Symmetry Coordinates Which Contribute IR Activity	Our Notation For These Normal Modes	Frequency Region of the Corresponding Spectra
ν_8	CH_2 rocking and CH_2 twisting modes	CH_2 rocking modes	$\nu(R_m^N)$	720-1050
ν_4	c-c stretching modes, CH_2 wagging modes and c-c-c bending modes	CH_2 wagging modes		970-1140
ν_7	CH_2 twisting modes and CH_2 rocking modes	CH_2 rocking modes	$\nu(T_m^N)$	1168-1295
ν_3	CH_2 wagging, c-c stretching and c-c-c bending modes	CH_2 wagging modes	$\nu(W_m^N)$	1176-1415
ν_2	CH_2 bending modes	CH_2 bending modes	$\nu(B_m^N)$	~ 1470

Very pure n-$C_{23}H_{48}$, n-$C_{24}H_{50}$, n-$C_{28}H_{58}$ and n-$C_{29}H_{60}$ were made available to us by A. E. Smith.* IR spectra of melt grown polycrystallines are measured at various pressures to 35 kb in the frequency range 700 to 1600 cm^{-1}. Polyethylene film (Marlex 6009) supplied by Phillips Petroleum Company in the form of 1 mil. sheets was also measured.

Among the progressions of absorption bands in Table 6, only that of wagging modes and rocking modes are properly assigned.[49] The high pressure frequencies of these two types of vibrations together with that of the in-phase bending mode are presented in Table 7,8 and 9.** In these tables, a factor group component is specified by a subscript of ν. When both factor group components for a chain mode are measured, $\bar{\nu}$ and $\Delta\nu$ defined in Eqs. (37) and (38) are tabulated.

There are three different crystal structures among the four n-paraffins measured. The high pressure spectra of n-paraffins which crystallizes in orthorhombic structure are to be discussed first. Following this discussion, a comparison of crystalline effects among various crystal structures, orthorhombic (n-$C_{23}H_{48}$, n-$C_{29}H_{60}$ and polyethylene), monoclinic (n-$C_{28}H_{58}$) and triclinic (n-$C_{24}H_{50}$) are presented.

---

* N-paraffins from Smith are those studied by Smith[65] in his x-ray measurements and by Snyder[49] in his IR measurements.

** Phase differences were defined for each of the nine classes of chain modes somewhat independently and arbitrarily by Tasumi and other authors, in their normal coordinate analysis of molecular polyethylene and n-paraffins. Snyder defined all the ungerade modes as in-phase modes and gerade modes as 180° out-of-phase modes. This definition yields different vibrational assignments from that of Tasumi, et al. However, it is noted that by defining kc as the phase difference of transition dipole moments between two adjacent methylene groups, the assignment of kc values for the absorption bands in a progression is consistent with that of Snyder.

Table 7. Frequencies of Rocking Modes

Pressure (Kbar) normal modes	$\bar{\nu}(R_1^{23})$	$\Delta\nu(R_1^{23})$	$\bar{\nu}(R_9^{23})$	$\Delta\nu(R_9^{23})$	$\bar{\nu}(R_{11}^{23})$	$\Delta\nu(R_{11}^{23})$*	$\bar{\nu}(R_{13}^{23})$
5	724.25 725.0	14.5 16.0	752.0	8	784.5	3	832.0
10	726.0 726.8	17.0 18.6	752.5	9	785.0	3	832.2
15	727.75 728.75	19.5 20.5	753.5	11	785.6	4.8	832.7
20	729.75 729.75	21.5 23.5	754.0	12	786.4	4.8	833.3
25	731.25 731.75	24.5 25.5	754.75	13.5	786.8	5.7	833.6
30	732.5 732.75	27.0 27.5			787.5	4.8	834.2
35	733.0	28.0			788.0	5.7	834.4

* Unresolved Davydov splittings $\Delta\nu(R_{11}^{23})$ and $\Delta\nu(R_{13}^{23})$ are evaluated from the change in band width as described in Appendix I.

Table 7, continued

Pressure (Kbar) Normal modes	$\Delta\nu(R_{13}^{23})$*	$\bar{\nu}(R_{17}^{23})$	$\Delta\nu(R_{17}^{23})$	$\bar{\nu}(R_{19}^{23})$	$\Delta\nu(R_{19}^{23})$	$\nu(R_1^{24})$	$\nu(R_9^{24})$
5	0	942.25	6.5	933.5	7	716.0 716.5	744.0 744.0
10	0.45	942.75	7.5	995.875	8.25	717.0 717.5	744.0 744.0
15	0.45	943.5	9.0	996.0	7	718.0 718.8	744.5 745.0
20	0.45	944.5	9.0	996.15	7.7	719.0 720.0	
25	1.0	945.0	10.0	996.25	8.5	720.5 720.5	
30	1.5	945.25	10.5	996.65	9.3	721.0 721.0	
35	1.8	946.0	11.0	997.375	10.75	722.0	
				997.5	11.0		

Table 7, continued

Pressure (Kbar) normal modes	$\nu(R_{11}{}^{24})$	$\nu(R_{13}{}^{24})$	$\nu(R_{15}{}^{24})$	$\nu(R_{17}{}^{24})$	$\nu(R_{19}{}^{24})$	$\bar{\nu}(R_1{}^{28})$	$\Delta\nu(R_1{}^{28})$
5	772.5	814.5	866.0	920.4	974.0	723.85 724.75	14.7 15.5
10	772.5	814.3	866.0	921.0	975.0	725.6 726.5	16.8 17.0
15	772.5	814.0	866.0	921.5	976.0	727.5 728.25	18.1 18.5
20	772.5	813.5	865.5	921.8	976.5	729.0 729.75	19.6 20.5
25	722.0	813.2	865.0	922.0	977.5	730.5 731.25	22.0 23.5
30	722.0	813.0	864.5	922.0	978.0	732.0 733.0	24.0 26.0
35	771.5	812.5	864.0	992.0	978.0	733.5	27.0

Table 7, continued

Pressure (Kbar) normal modes	$\bar{\nu}(R_{13}{}^{28})$	$\bar{\nu}(R_{15}{}^{28})$	$\bar{\nu}(R_{17}{}^{28})$	$\bar{\nu}(R_{21}{}^{28})$	$\Delta\nu(R_{21}{}^{28})$	$\bar{\nu}(R_{23}{}^{28})$	$\Delta\nu(R_{23}{}^{28})$
5	774.0	811.5	853.5	946.5		911.0	
10	744.0	811.5	854.0	947.0		992.0	
15	774.5	812.0	854.3	948.0		993.0	
20	744.8	812.3	854.7	949.0		994.0	
25	775.0	813.0	855.4	950.0	5.5	996.0	7.0
30	775.0	813.0	855.5	950.0	6.0	997.0	9.0
35	775.0	813.0	856.0	950.0	6.0	998.0	11.0

Table 7, continued

Pressure (Kbar) normal modes	$\bar{\nu}(R_1^{29})$	$\Delta\nu(R_1^{29})$	$\bar{\nu}(R_{11}^{29})$	$\Delta\nu(R_{11}^{29})$	$\bar{\nu}(R_{13}^{29})$	$\Delta\nu(R_{13}^{29})$	$\bar{\nu}(R_{15}^{29})$
3	724.1	13.0	748.7	6.5	770.5	4.0	803.5
7.5	725.4	15.8	748.7	7.5	770.0	4.5	803.5
10	726.25 727.3	16.5 17.7	749.0	8.0	770.5	4.5	803.9
15	728.3 729.25	18.6 19.5	749.7	9.5	770.7	5.3	804.25
20	729.85 730.25	20.7 21.5	751.0	12.0	771.6	6.6	804.7
25	731.1 732.0	23.1 23.4	751.5	13.0	773.0	6.5	805.6
30	731.85 732.75	25.0 26.0			772.5	6.5	806.0
35	733.5	27.7					

Table 7, continued

Pressure (Kbar) normal modes	$\bar{\nu}(R_{17}{}^{29})$	$\bar{\nu}(R_{21}{}^{29})$	$\Delta\nu(R_{21}{}^{29})$	$\bar{\nu}(R_{23}{}^{29})$	$\Delta\nu(R_{23}{}^{29})$	$\bar{\nu}(R_{25}{}^{29})$	$\Delta\nu(R_{25}{}^{29})$
3	843.5	932.5	5.3	976.5	6.0		
7.5	843.5	933.3	6.0	977.0	8.0		
10	843.5	933.0	8.0	977.0	7.4		
15	844.0	933.5	8.0	977.0	8.1		
20	845.0	933.5	9.0	976.5	9.0		
25	845.5	934.0	9.0	977.25	8.5	1017.25	17.5
30	846.0	934.75	9.5	977.5	10.0	1018.7	18.5

Table 8. Frequencies of CH_2 Bending Modes

Pressure (Kbar)	$\nu(B_1^{24})$ normal modes	$\bar{\nu}(B_1^{28})$	$\Delta\nu(B_1^{28})$	$\bar{\nu}(B_1^{29})$	$\Delta\nu(B_1^{29})$	$\bar{\nu}(B_1^{\infty})$	$\Delta\nu(B_1^{\infty})$
5.0	1478.0	1472.7	10.7	1473.0	10.9	1472.1	12.2
7.5		1472.8	11.5	1472.9	11.3	1472.2	12.5
10.0	1478.5	1473.1	11.5	1473.0	12.0	1472.4	12.8
12.5		1473.0	13.0	1472.75	12.5	1472.7	13.2
15.0	1478.5	1473.3	12.5	1473.25	12.5	1473.0	13.8
17.5		1473.6	13.1	1473.2	13.3	1472.7	14.4
20.0	1478.5	1473.8	13.5	1473.6	13.5	1473.2	14.5
22.5		1474.0	14.0	1474.1	14.2	1473.8	14.7
25.0	1479.0	1474.2	14.4	1474.25	14.5	1475.0	14.9
27.5		1474.4	15.7	1474.5	15.0	1474.8	15.7
30.0	1480.0	1474.5	15.0	1474.8	15.5	1474.7	15.8
32.5		1474.8	15.5	1475.0	16.0	1475.0	16.1
35.0	1481.0	1474.9	15.8	1475.5	17.0	1475.2	16.5
37.5				1475.4	17.3	1475.5	17.0
40.0	1481.5					1475.2	17.5

Table 9. Frequencies of Wagging Modes

Pressure (Kbar) / normal modes	$\nu(W_1^{23})$	$\nu(W_2^{23})$	$\nu(W_3^{23})$	$\nu(W_4^{23})$	$\nu(W_5^{23})$	$\nu(W_6^{23})$	$\nu(W_7^{23})$
5		1202.6	1219.3	1236.5	1249.5		1278.7
10	1188.0	1202.8	1219.8		1250.3	1263.0	1277.6
15	1187.0		1219.6	1235.9	1248.5	1264.5	
20	1186.5		1220.5	1234.6	1249.2		1278.3
25	1186.6		1219.0	1233.3	1248.0	1264.0	1276.6
30	1185.7	1198.1	1219.7	1233.7	1247.8		1275.3
35	1185.5	1198.0	1219.2	1233.3	1247.6		

Table 9, continued

Pressure (Kbar) normal modes	$\nu(W_9^{23})$	$\nu(W_{11}^{23})$	$\nu(W_1^{24})$	$\nu(W_3^{24})$	$\nu(W_5^{24})$	$\nu(W_7^{24})$	$\nu(W_9^{24})$
5		1332.5		1217.0	1247.0	1275.5	1302.0
10	1306.5	1331.5		1217.0	1247.0	1274.5	1303.0
15	1306.5		1183.0	1215.5	1244.0	1273.5	1303.0
20	1306.7		1183.5		1247.0	1273.5	1304.5
25	1305.0		1184.0		1245.0	1273.0	1305.0
30	1304.6		1184.0		1244.5	1273.5	1306.5
35	1306.4						

1. Odd-Numbered N-Paraffins--n-$C_{23}H_{48}$ and n-$C_{29}H_{60}$

N-Paraffins with an odd-number of carbon atoms have orthorhombic structure. As shown in Fig. 12, four molecules are arranged in an orthorhombic unit cell. Crystal axis a, b, and c are defined in the figure. Molecules are arranged in layers with the chain axis perpendicular to the ab plane. A sub-cell defined as the repeating unit of a single layer is enclosed by solid lines in the figure.

Each layer of the crystal may be considered as a two dimensional crystal. The two adjacent layers are identical crystals with a different orientation. The vibrational selection rules may thus be derived from the symmetry of the sub-cell.

Molecular axes x, y, and z are defined such that all the carbon atoms of a n-paraffin molecule are in the xz plane. z is the chain axis. Since $\hat{z} \parallel \hat{c}$, x and y are in the ab plane. Let μ'_I and μ'_{II} be the transition dipole moments of the two molecules in a sub-cell. Wagging modes have $\mu'_I \parallel \mu'_{II} \parallel \hat{z}$. $(\mu'_I + \mu'_{II})$ is thus parallel to the z axis, and $(\mu'_I - \mu'_{II})$ vanishes. Therefore, only one factor group component is IR active.

Rocking modes and bending modes have $\mu'_I \parallel \mu'_{II} \perp \hat{z}$. ($CH_2$-bending modes with $\mu' \parallel \hat{x}$, CH_2 rocking modes, $\mu' \parallel \hat{y}$). Both $(\mu'_I + \mu'_{II})$ and $(\mu'_I - \mu'_{II})$ do not vanish as long as the setting angle θ, which is defined as the angle between the skeletal plane of a n-paraffin molecule and the a-axis of the unit cell, is not zero. Therefore, both a and b factor group components of the crystal are IR active.

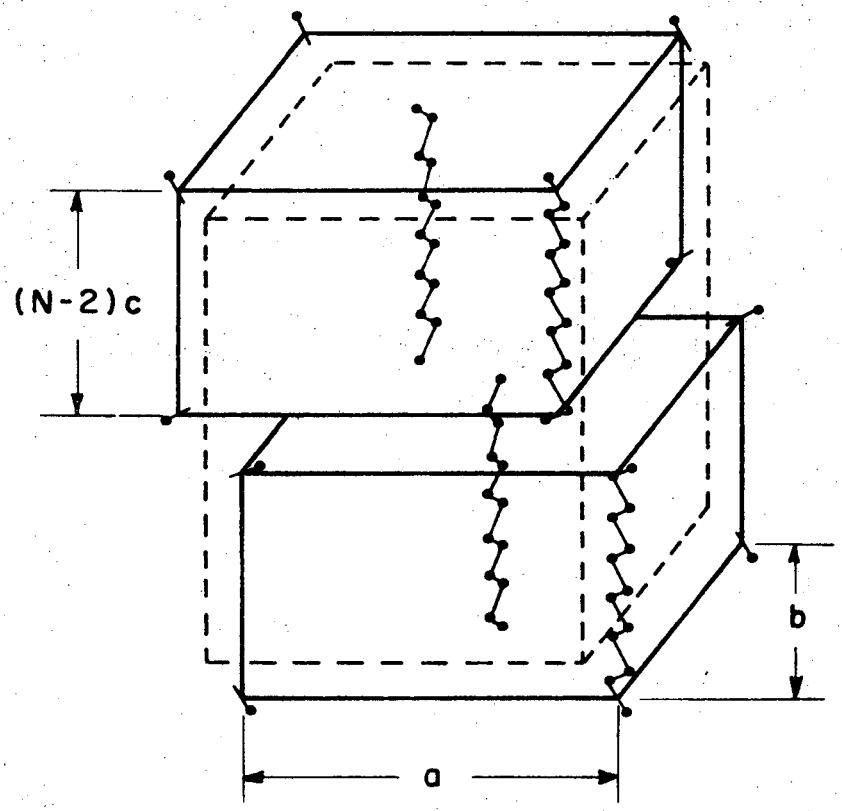

XBL 7110-7379

Fig. 12 A unit cell of odd-numbered n-paraffins. (After A. E. Smith (65) and Snyder (50))

These three classes of normal frequencies, rocking, wagging, and bending modes will be discussed separately in the following paragraphs.

(a) Rocking Modes

A progression of absorption bands in the frequency range 720 cm^{-1} to 1050 cm^{-1} results from the fundamentals of the normal modes $\nu(R_m^N)$ which are composed of CH_2 rocking and twisting motions. It is the rocking motion which contributes the IR activity. We refer to these normal modes as rocking modes, although only $\nu(R_1^\infty)$ is a purely rocking motion for an infinite chain.[51]

The dispersion curves of $\bar{\nu}(R_m^{23})$ and $\bar{\nu}(R_m^{29})$ are shown in Fig. 13. In this figure, the circles represent $\bar{\nu}(R_m^{29})$ and the triangles represent $\bar{\nu}(R_m^{23})$. The fact that both circles and triangles lie along the same smooth curve for any given pressure implies that the normal frequencies of rocking modes in the orthorhombic structure are functions of kc only, i.e. independent of chain length N for any given unit cell dimensions. $\bar{\nu}(R_m^N)$ vs. pressure plot for each of the N and m values is approximated by a straight line. The slopes so obtained for various phase differences are to be found in Fig. 13 as well. The pressure induced change in the entire dispersion curve may be visualized by imposing the two curves in Fig. 13. Namely, as pressure is increased, the entire dispersion curve is shifted upward and the energy band is narrowed.

The dispersion curve at each pressure may be represented by Eq. (37), where ν_o is now a function of kc. In the first order perturbation treatment of Chapter II, ν_o is assumed to be independent of pressure. The change of the dispersion curve with pressure is entirely due to the change of intermolecular potential.

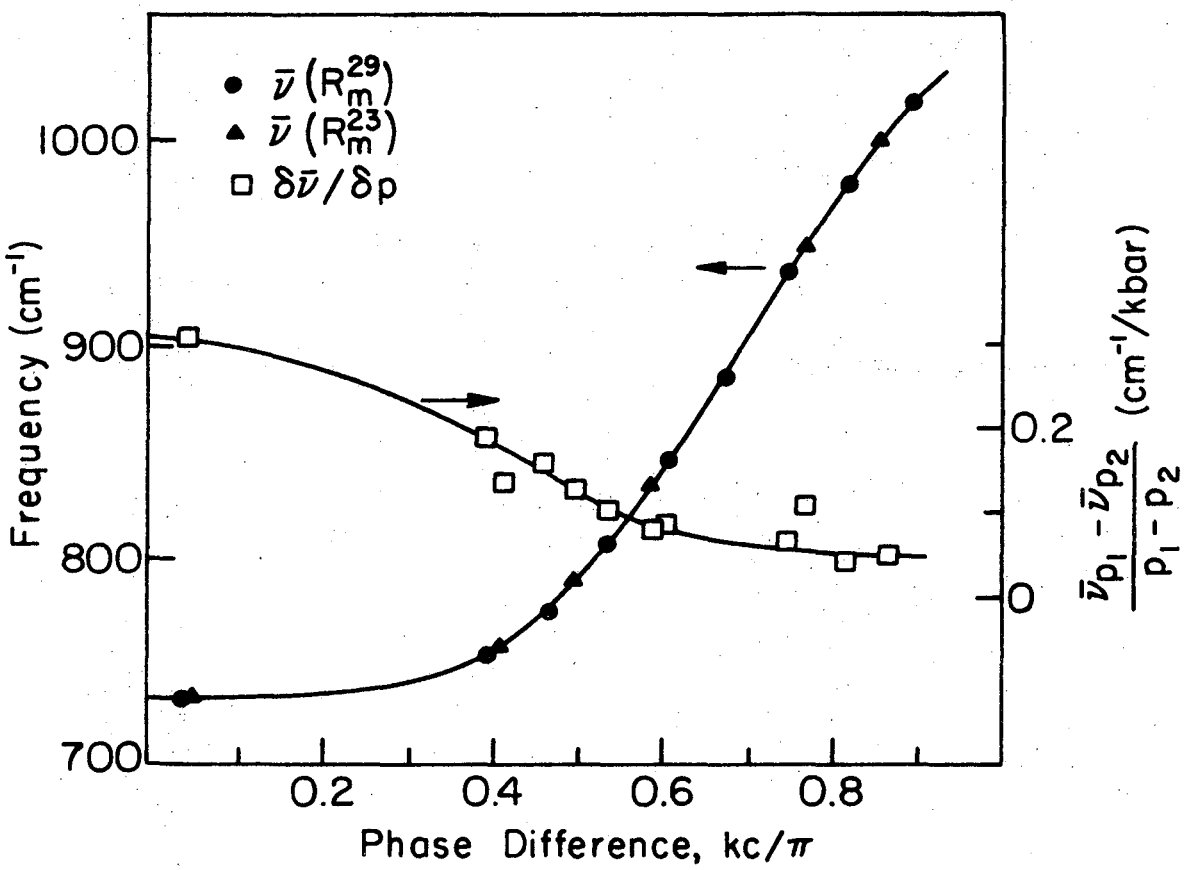

XBL 7110-7380

Fig. 13 Observed dispersion relation for rocking frequencies of odd-numbered n-paraffins $\bar{\nu}(R_m{}^N)$ at 25 kb. The pressure induced frequency shift is also plotted as a function of the phase difference, kc.

It is obvious from Fig. 13 that there is a decided convergence of energy levels to the limiting mode (m=1). This results in several absorption bands being unresolved, and is responsible for the absence of $\nu(R_3)$, $\nu(R_5)$ and $\nu(R_7)$ in Table 7. At the other end of the dispersion curve, a proper assignment of the last mode in this series is obstructed by the presence of several unrelated absorption bands.

At room temperature and pre-sure, the majority of the doublets (factor group components) can not be resolved, because the bands overlap. When the temperature of the sample is lowered, the bands are narrowed considerably and the factor group splitting is increased slightly. Snyder was able to resolve most of the doublets at -180°C. In our measurements, as shown in Figs. 14 and 15 when pressure on the sample is increased, the splitting of the doublet is increased considerably. Some bands unresolved at 1 atm. are resolved at high pressures. For the rocking modes of N-$C_{23}H_{48}$, the factor group splittings as a function of pressure are presented in Fig. 16. The phase difference kc is a parameter in this figure.

(b) Wagging Modes

A progression of observed absorption bands in the frequency range 1180 to 1300 cm^{-1} is the result of the fundamentals of the normal modes $\nu(W^N_m)$. These normal modes are composed of CH_2 wagging, C-C stretching and C-C-C bending motions, as shown in Table 6. One band for each of the normal modes (m = 1,2,3,4, . . .) is observed at all pressures. Wagging modes with $m > 11$ are not observed owing to the presence of much stronger absorption bands, i.e. symmetric methyl bending mode at approximately 1375 cm^{-1}.

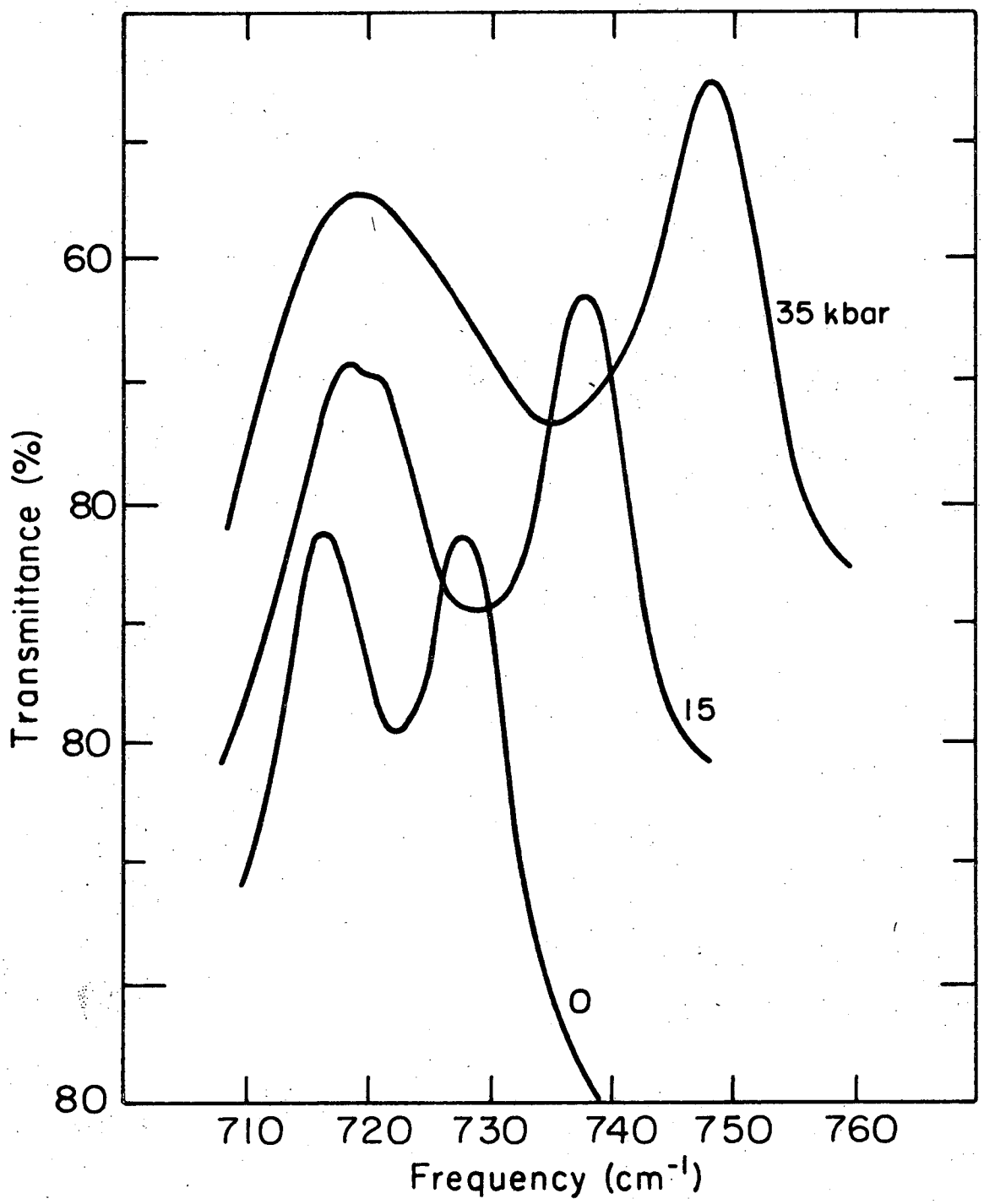

XBL 7110-7381

Fig. 14 Spectra of ν_a and $\nu_b(R_1^{\infty})$ at three pressures. The broadening of the lower frequency peak (b factor group component) is due to the presence of an unrelated band which is not resolved.

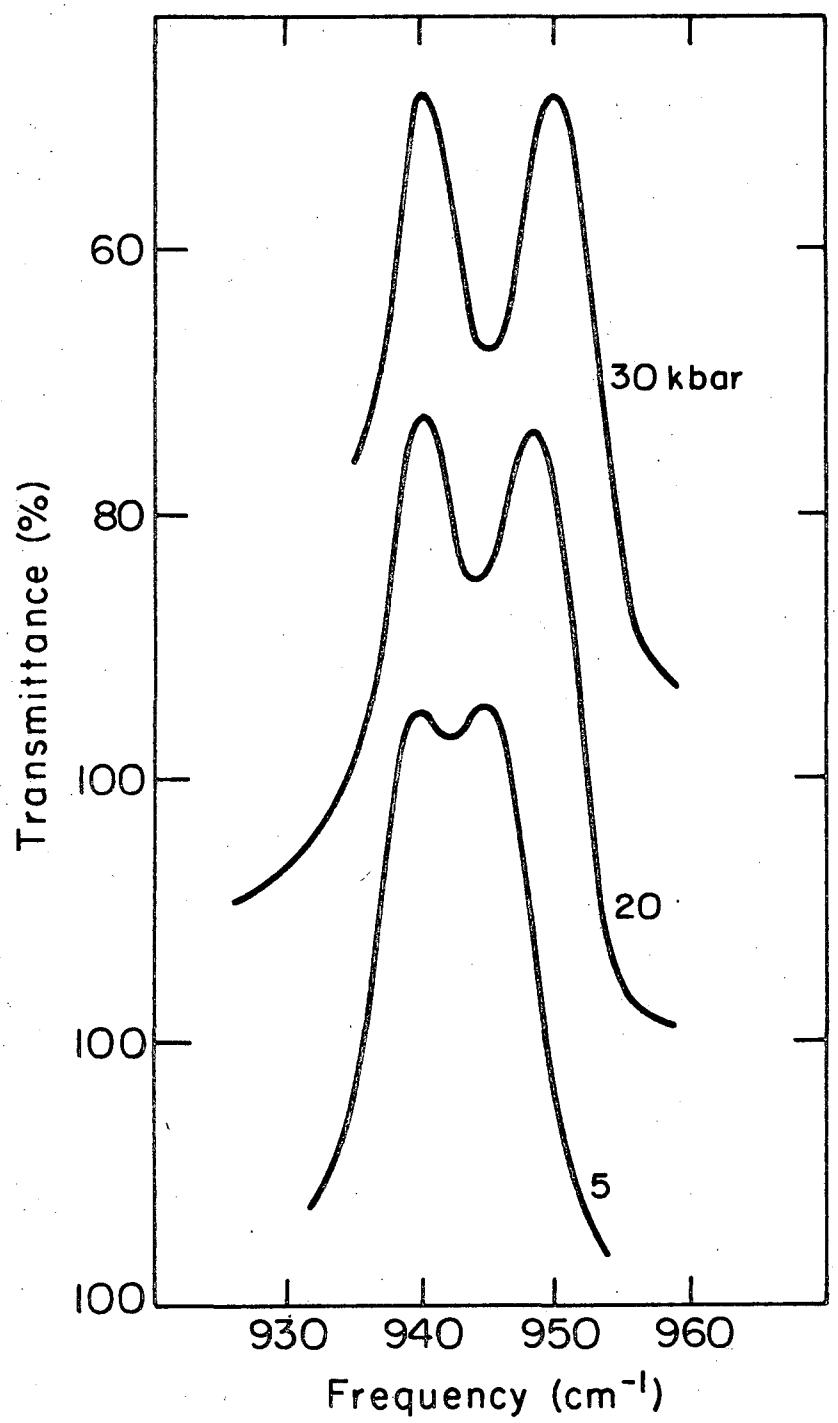

XBL7110-7382

Fig. 15 Spectra of $\nu_{\substack{a\\b}}(R_{17}{}^{23})$ at three pressures.

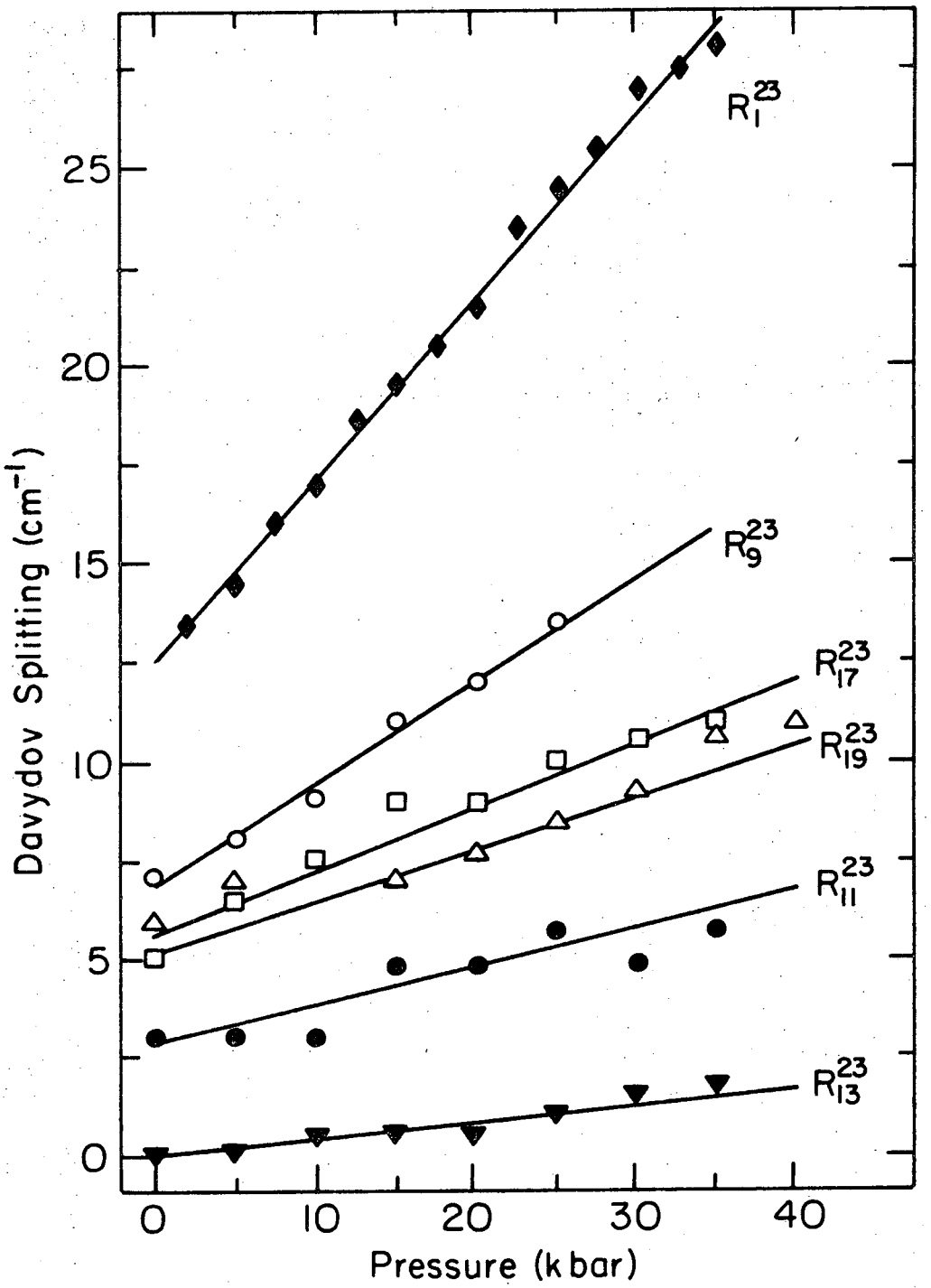

XBL7110-7383

Fig. 16 Observed Davydov splittings of rocking modes $\Delta\nu(R_m{}^{23})$ at various pressures. The phase difference, kc(= (mπ/22) is a parameter.

(c) Bending Modes

As shown in Fig. 17, two factor group components are observed at various pressures. The pressure dependence of $\bar{\nu}(B_1^N)$ and $\Delta\nu(B_1^N)$ will be discussed later in comparison with that of different crystal structures.

The relative intensity (I_a/I_b) of two factor group components (the one with a lower frequency is the b-component) is changed from unity at 5 kb to approximately 2 at 35 kb. This phenomenon may be interpreted with the oriented gas model for either of the following two reasons: (1) the relative orientation of two molecules in a unit cell is changed, e.g. the setting angle θ is changed with pressure. (2) the polycrystallites randomly oriented at 1 atm. to 5 kb are partially oriented at higher pressures. However, there is no similar change in the relative intensities of the two factor group components of the rocking modes. The first reason is thus excluded. The second one is still possibly valid, since different samples are needed for taking the spectra of rocking modes and bending modes. The sample thickness is of the order of 2.5 microns for measuring bending modes, 25 microns for in-phase rocking modes and 25 mils for out-of-phase rocking modes.

It was shown[47] that an oriented polycrystalline film can be obtained by slowly cooling and pressing a melt of paraffin between two potassium chloride windows. The polycrystallites of the odd-numbered n-paraffins are then oriented such that the direction of the chains is perpendicular to the faces of the windows.

For a polycrystalline sample of either completely ordered or completely random orientations, $I_b/I_a = \tan\theta = 1.1$ to the oriented gas

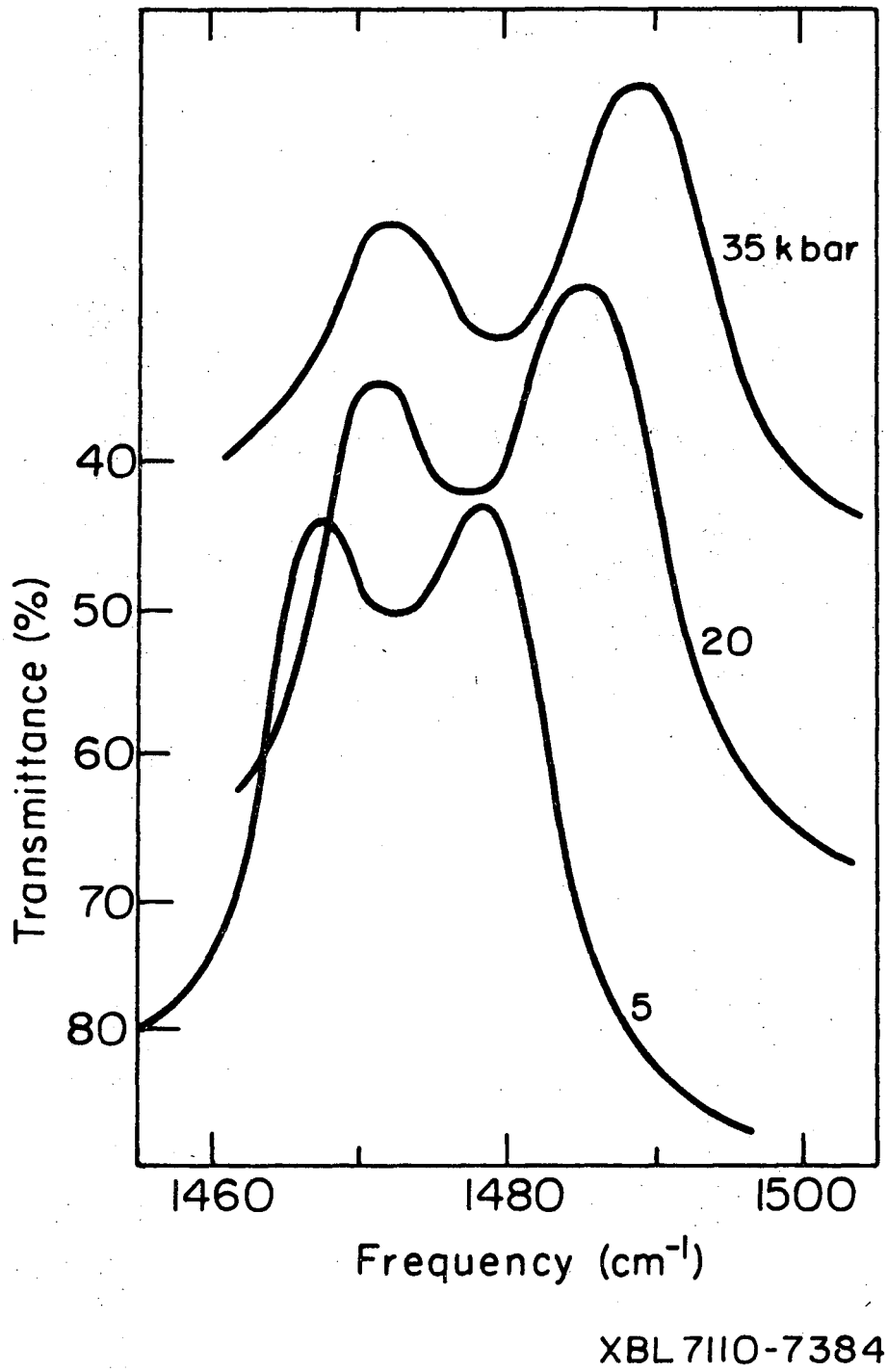

Fig. 17. Spectra of $\nu_{\substack{a\\b}}(B_1^{29})$ at three pressures.

model approximation. The relative intensity of the two factor group components may deviate from 1.1 when the polycrystalline sample is partially oriented in certain ways. The sample thickness for measuring bending modes is of the right order as that of the melt between two potassium chloride windows. Therefore, the polycrystallites under high pressure ($P > 5$ kb) may be in a transition state from random to orderly. The observed phenomenon may thus be accounted for.

This phenomenon may also be a result of second or higher order perturbation effect; namely, the vibrational wave function is perturbed by the crystalline potential.

2. A Comparison of Pressure Effects among Various Crystal Structures

In order to compare the spectra and its pressure dependence among various crystal structures, vibrational spectra of polyethylene, n-$C_{28}H_{58}$ (monoclinic) and n-$C_{24}H_{50}$ (triclinic) are also measured at various pressures.

Polyethylene has an orthorhombic structure with two molecules per unit cell. The unit cell is identical with the sub-cell of odd numbered n-paraffins. For an infinitely long zig-zag polyethylene, only the transition of an in-phase mode (i.e., kc = 0) is observable for each type of vibrations.

N-$C_{28}H_{58}$ has a monoclinic structure, and a space group symmetry of P_{2_1}/a. Two molecules in a unit cell lie parallel to the c-axis and are thus tilted with respect to the normal of the ab plane. Since there are two molecules per unit cell, two factor group components are observed for rocking modes and bending mode.

N-$C_{24}H_{50}$ has a triclinic structure with one molecule per unit cell. Its space group is not known. Nevertheless, one would not

expect any factor group splitting, since there is only one molecule per unit cell.

The substantial phase dependence of rocking frequencies for all crystalline n-paraffins (See Fig. 13 for example) is mainly due to the phase dependence of the intramolecular potential, e.g., the combination coefficients of rocking and twisting symmetry coordinates are functions of the phase difference kc. The phase dependence of Davydov splitting (e.g., see Fig. 16) originates from the variation of intermolecular coupling forces with the phase difference kc (vibration modes of different kc are different normal modes). The pressure induced frequency shifts and the pressure induced change in Davydov splittings originate from the variation of intermolecular forces with the contraction of unit cell dimensions. The variation of intermolecular coupling forces as well as its effects on vibrational frequences can be understood from a similar force diagram as depicted in Fig. 2 of Chapter II.

In Fig. 16, factor group splittings of rocking modes are approximated as linear functions of pressure. The slopes so obtained are expressed as $(\Delta\nu_{p + 30kb} - \Delta\nu_p)$, for various phase differences. This is shown in Fig. 18. Also shown in this figure is the factor group splitting at 1 atm. for n-paraffins with the orthorhombic structure (Snyder's atmospheric data on odd-numbered n-paraffins are included in the latter plot).

From this figure, the phase dependence of both Davydov splitting and its pressure induced change can be evaluated for an orthorhombic structure. If n-$C_{28}H_{58}$ belonged to the orthorhombic structure as $C_{29}H_{60}$ does, the expected difference in Davydov splitting at 1 atm.

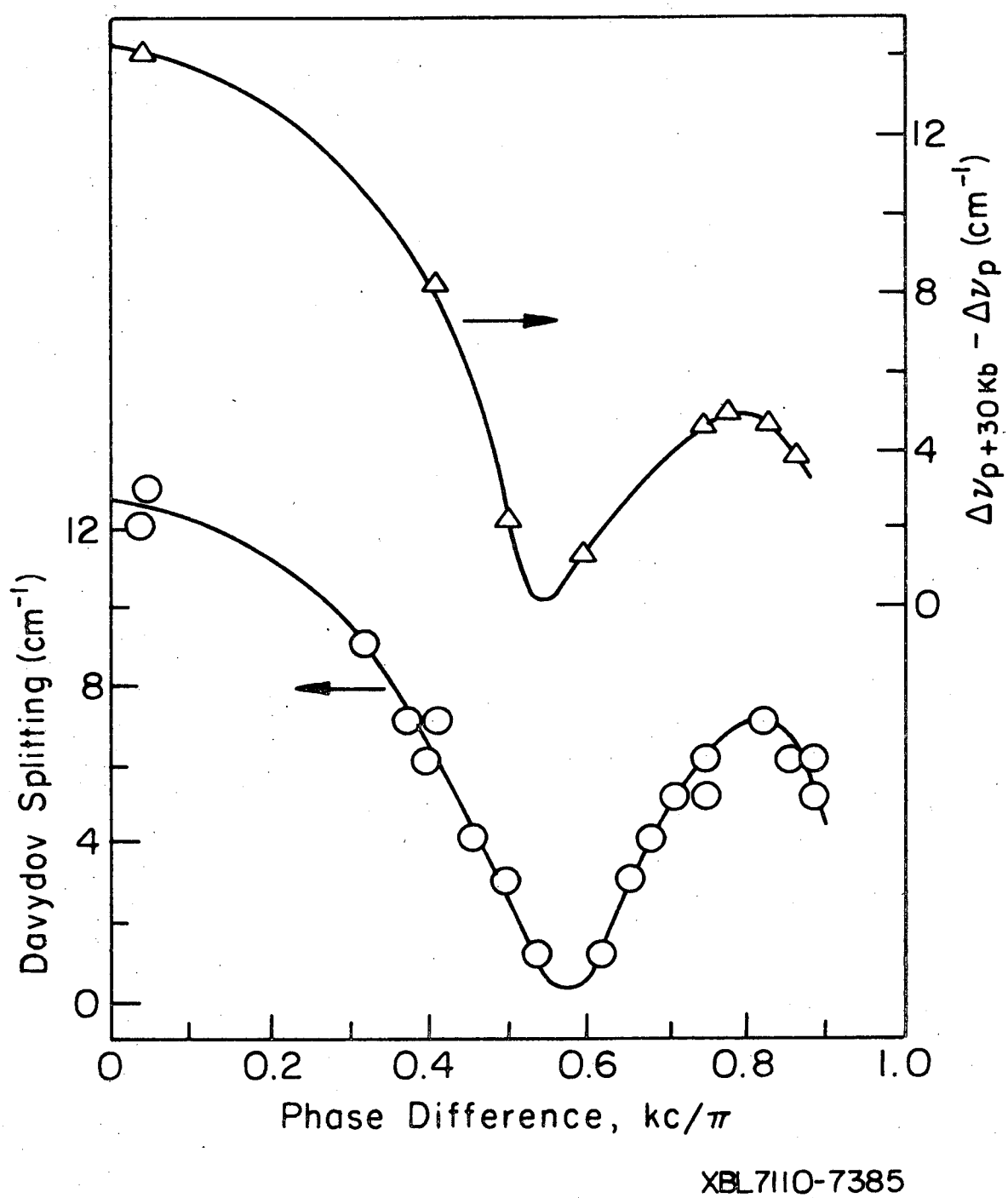

Fig. 18 Observed phase dependence of Davydov splittings of odd-numbered n-paraffins $\Delta\nu(R_m{}^N)$ at 1 atm. The pressure induced change of $\Delta\nu(R_m{}^{23})$ is also plotted as a function of phase difference kc.

between normal modes R_1^{28} and R_1^{29} is of the order of 0.1 cm^{-1}. Also from Fig. 18, the corresponding difference in the pressure induced change of Davydov splitting is of the order of 0.1 cm^{-1}/30 kb. These values are within experimental errors of a single $\Delta\nu$ vs. pressure plot. Therefore, the observable difference, if any, in the value as well as the pressure induced change of Davydov splittings between R_1^{28} and R_1^{29} is not due to their discrepancy in kc (i.e. different normal motions, since a chain mode is defined such that the phase difference kc is specified) and is due to the distinction of the crystal structures. As shown in Fig. 19, $\Delta\nu$ vs. p plots for R_1^{28} and R_1^{29} are identical within experimental errors. The corresponding plot for the bending mode is shown in Fig. 20. A simple explanation for the coincidence in the values as well as the pressure induced changes, of $\Delta\nu(R_1^{28})$ with $\Delta\nu(R_1^{29})$, and $\Delta\nu(B_1^{28})$ with $\Delta\nu(B_1^{29})$ is possible. Namely, in the monoclinic structure, although the chain axis is tilted from the normal of the ab plane, the non-bonded hydrogen distances remain the same as that in the orthorhombic structure.

Since a unit cell of n-$C_{24}H_{50}$ (triclinic structure) has only one molecule, there is no Davydov splitting. In order to compare its crystalline potential with that of other structures, the observed frequencies are to be compared with the average frequencies of the corresponding factor group components for the orthorhombic and monoclinic structures.

The phase dependence of the vibrational frequencies of rocking modes and their pressure induced shifts for an orthorhombic structure can be evaluated from the curves of Fig. 13. If n-$C_{24}H_{50}$ and n-$C_{23}H_{48}$ had the same crystal structure, the expected difference in the

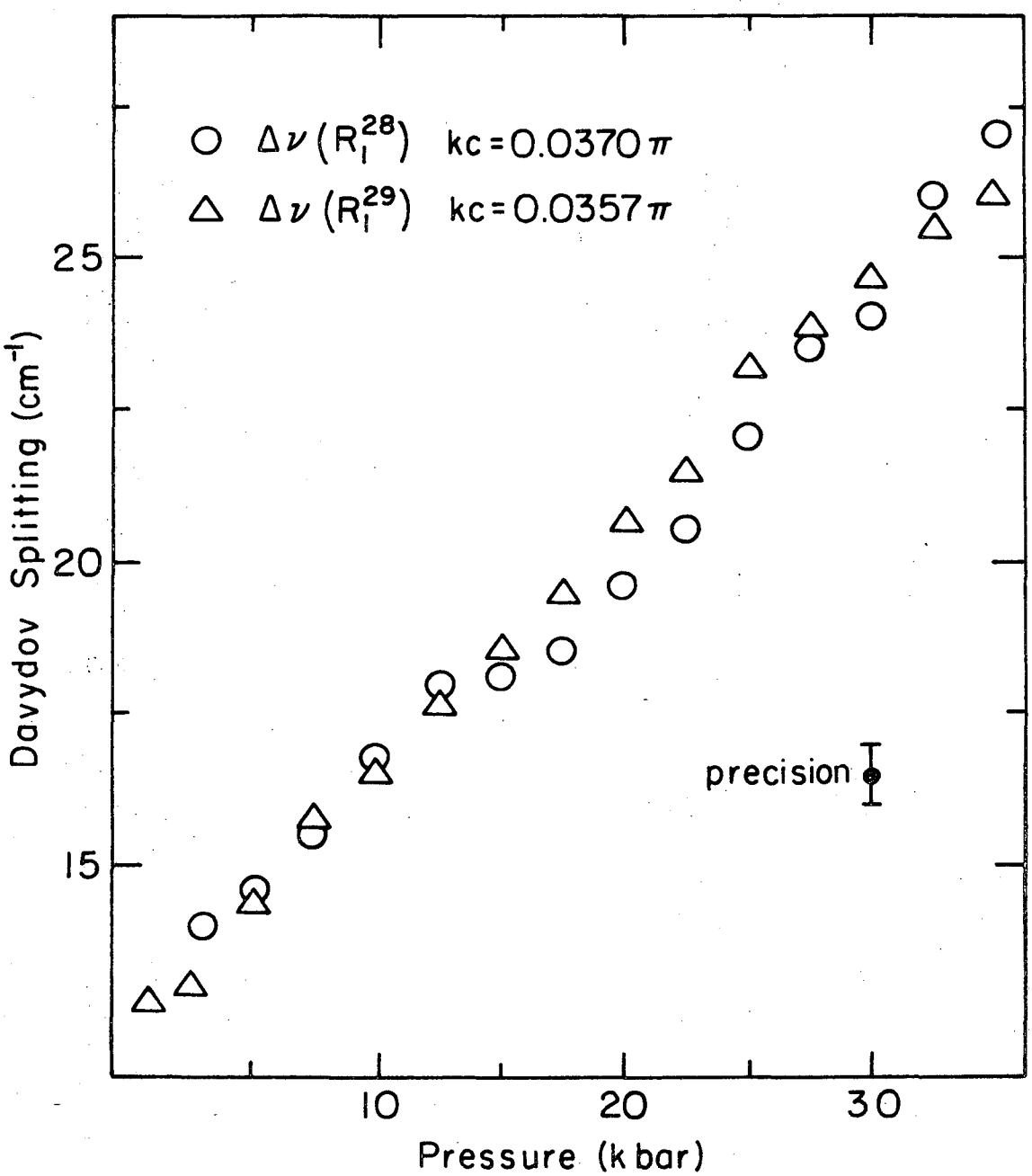

XBL 7110-7386

Fig. 19 Davydov splittings in orthorhombic and monoclinic structures vs pressure, for nearly in-phase rocking modes.

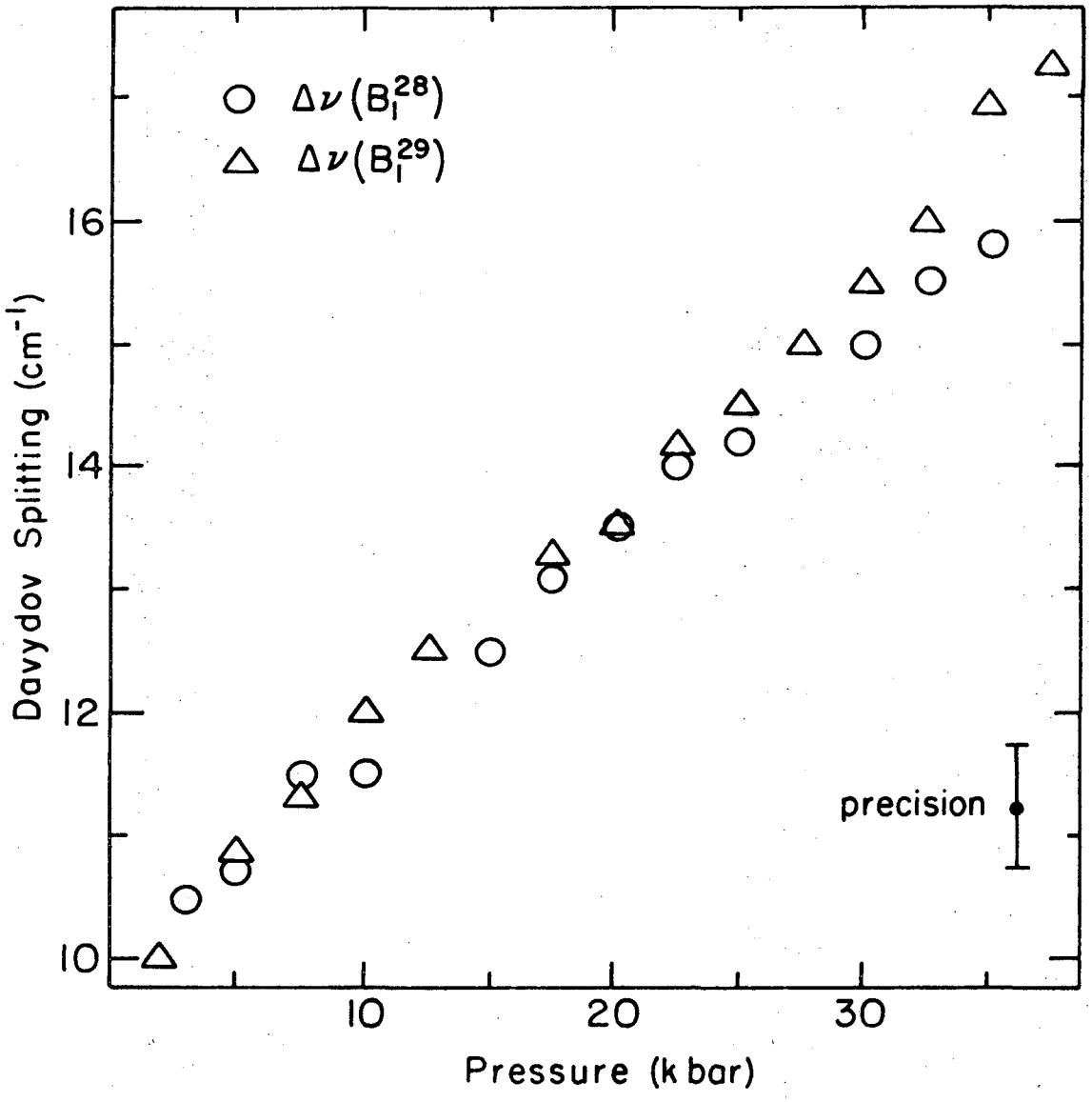

Fig. 20 Davydov splittings in orthorhombic and monoclinic structures vs pressure, for a nearly in-phase bending mode.

frequencies of R_1^{23} and R_1^{24} is 0.000 cm^{-1}. The corresponding difference for the pressure induced shift is of the order of 0.01 cm^{-1}/kbar. These values are again within experimental error for a single $\bar{\nu}$ vs. p plot. Therefore, any difference in $\bar{\nu}$ and its pressure dependence between normal modes R_1^{23} and R_1^{24} is not due to their discrepancy in kc and is due solely to the distinction in the crystal structures. In Fig. 21 $\bar{\nu}$ vs. p for R_1^{23}, R_1^{24} and R_1^{28} are presented. The corresponding plots for bending modes are shown in Fig. 22. It is seen that the vibrational frequency as well as the pressure induced frequency shifts of n-$C_{24}H_{50}$ differ considerably from that of n-$C_{23}H_{48}$ and n-$C_{28}H_{58}$. At all pressures the nearly in-phase rocking mode of a triclinic structure has a lower frequency than that of the orthorhombic and monoclinic structures. However, the bending mode for the triclinic structure has a higher frequency than that for the orthorhombic and monoclinic structures.

While there is no obvious change in intensity (there may be a slight increase with pressure, beyond experimental uncertainties) for absorption bands of rocking modes in the n-$C_{23}H_{48}$ and n-$C_{29}H_{60}$ spectra at various pressures, one pressure induced peak is observed at roughly 15 cm^{-1} below each of the average frequencies of factor group components. As shown in Fig. 23, the location of their appearance seems to be more precisely described by $\frac{1}{4}$ $[\bar{\nu}(R_{m+2})-\bar{\nu}(R_m)]$ below $\bar{\nu}(R_{m+2})$. These pressure induced peaks become apparent at 15 kb. The intensity of each peak is increased up to 10 to 15% of that of an adjacent band.

In the high pressure spectra of n-$C_{24}H_{50}$, pressure induced peaks are observed above rocking frequencies in contrast to what is observed in the spectra of odd numbered n-paraffins. This is shown in Fig. 24.

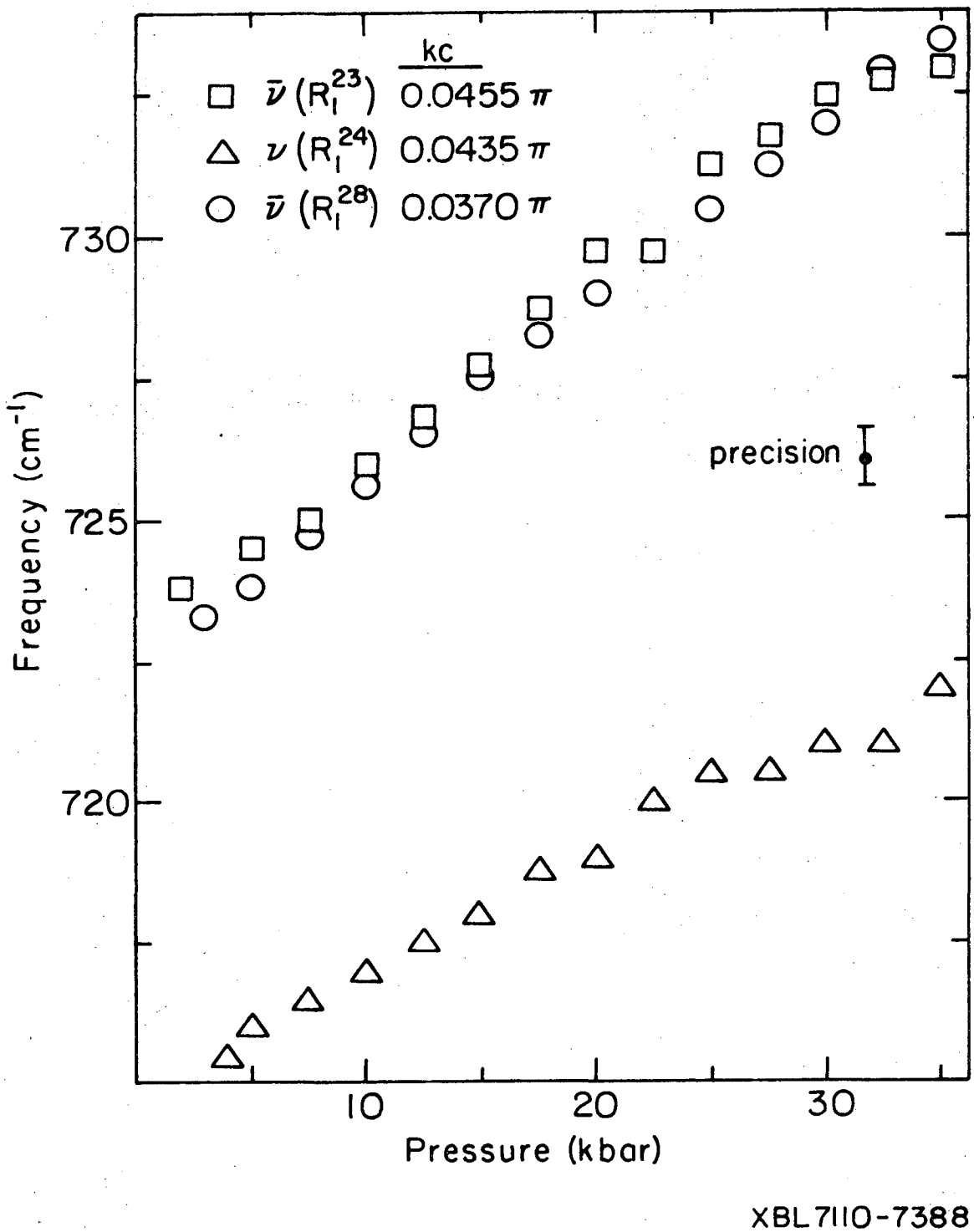

Fig. 21 Frequencies of nearly in-phase rocking modes in three crystal structures vs pressure.

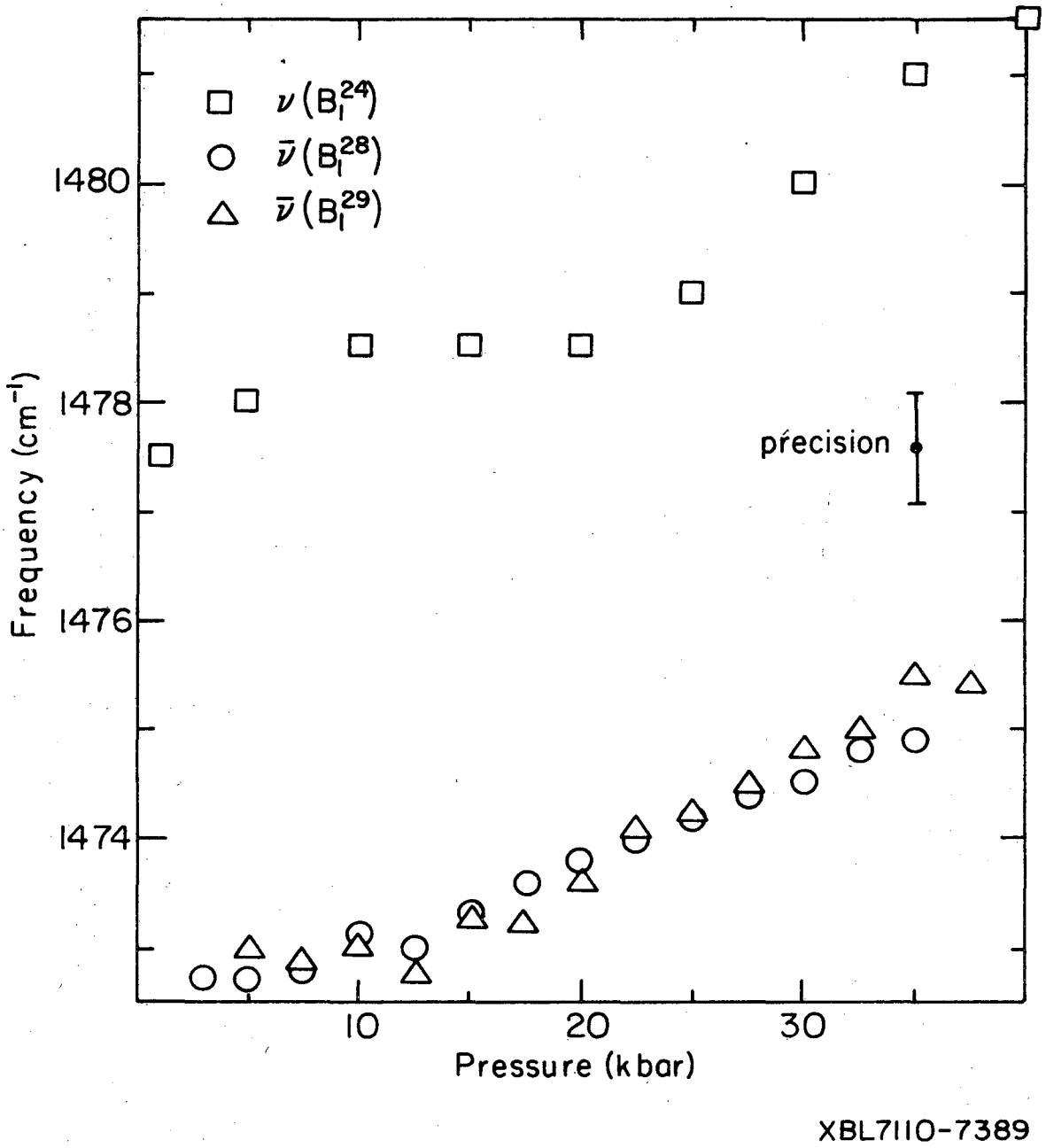

Fig. 22 Frequencies of bending modes in three crystal structures vs pressure.

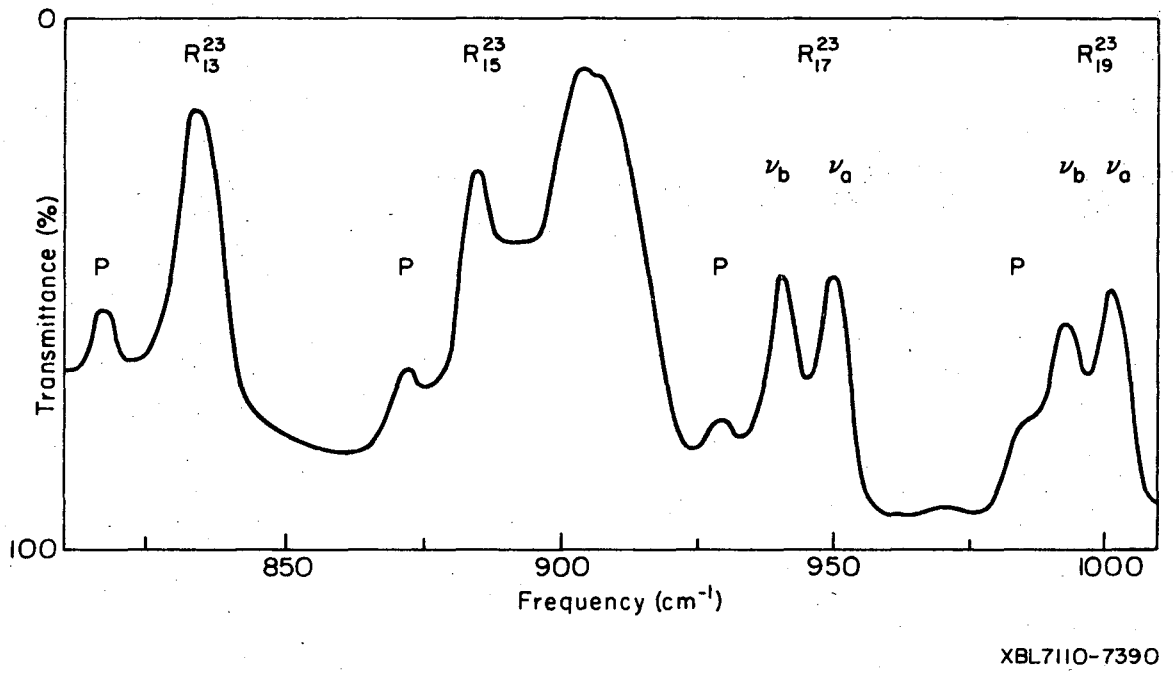

Fig. 23. Part of the observed progression of rocking modes in the absorption spectrum of n-$C_{23}H_{48}$ at 30 kb. P represents a pressure induced peak.

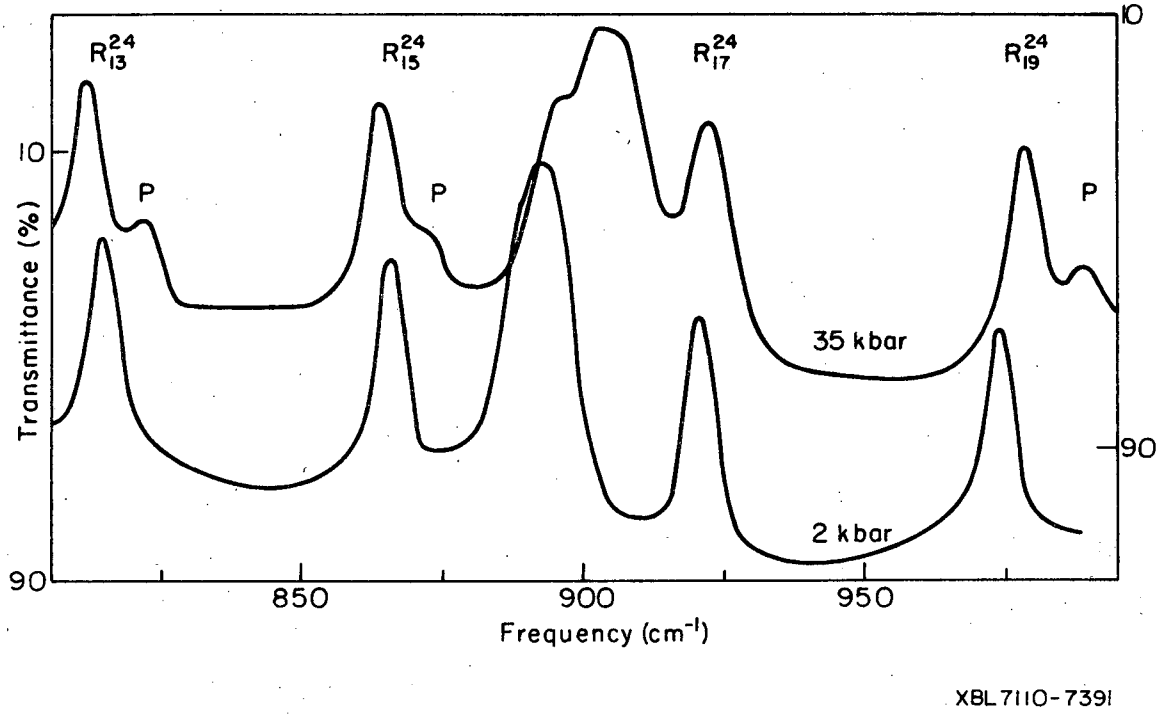

XBL 7110-7391

Fig. 24. Part of the observed progression of rocking modes in the absorption spectra of n-$C_{24}H_{50}$ at two pressures.

However, no similar pressure induced bands are observed in the high pressure spectra of n-$C_{28}H_{58}$. (The crystal structures are monoclinic, triclinic and orthorhombic for n-$C_{28}H_{58}$, n-$C_{24}H_{50}$ and odd numbered n-paraffins respectively).

The observed pressure induced peaks seem too far away from the center of $\nu(R_m)$ and $\nu(R_{m+2})$ to be identified as even-m-numbered rocking modes. These peaks are also unlikely to be a result of Fermi resonance for the following two reasons: First, it is certain that the intensities of the odd-m-numbered rocking modes are not decreased with pressure. Second, statistically, it is very unlikely to have overtone or combination energy levels at equal distance from every one of the rocking modes.

A strange phenomenon is observed consistantly among wagging modes of all n-paraffins studied. The observed intensities for the series of wagging modes at 1 atm. is nearly opposite to what we would expect for a progression of purely wagging modes. (One expects the intensity to decrease along a progression of increasing m values). Moreover, as shown in Fig. 25, the expected intensity ratio for the progression of bands is attained in the high pressure spectra. $\nu(W_1)$ is hardly observed at 1 atm. owing to its very low intensity. At 35 kb, its intensity is increased to roughly the intensity of out of phase ($m \geqslant 9$) rocking modes.

B. Applications

From the observed pressure dependence of Davydov splitting, the repulsion potential between non-bonded hydrogens is calculated. The calculated repulsion potential as well as the Gruneisen parameters which are readily obtained from the change in vibrational frequencies

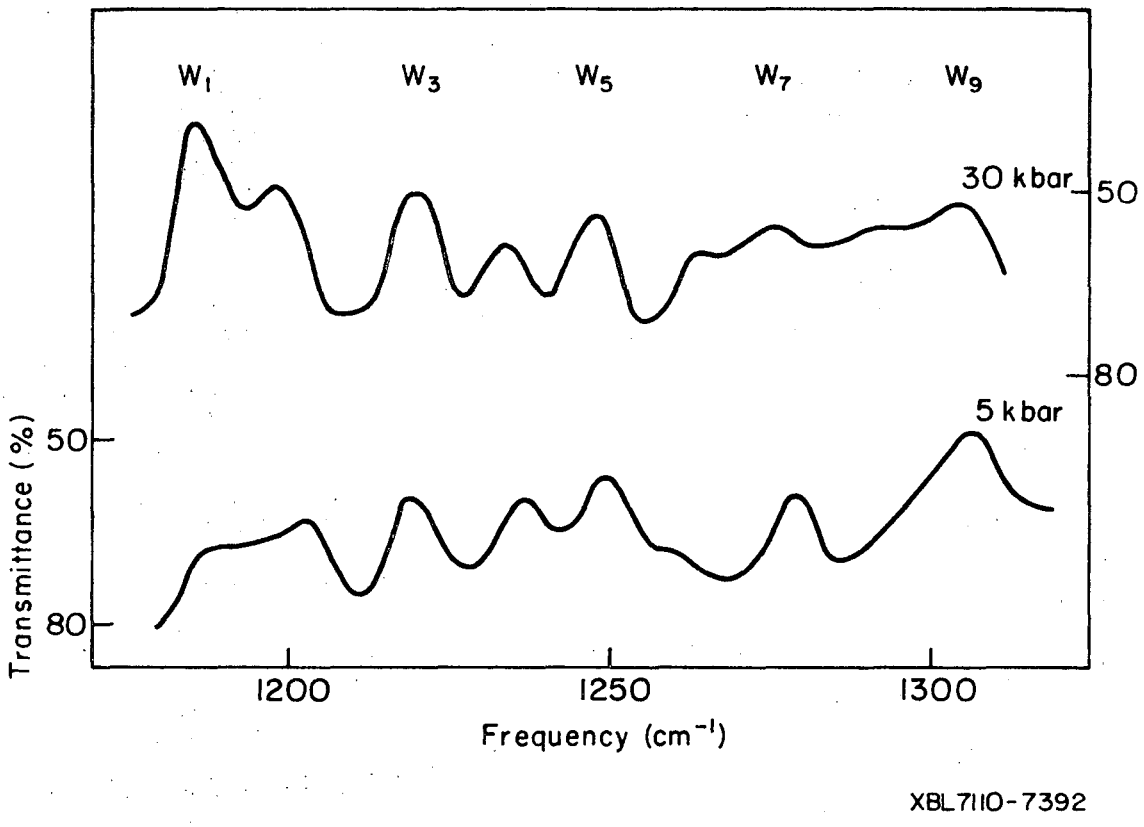

Fig. 25. The observed progression of wagging modes in the absorption spectra of n-$C_{23}H_{48}$.

with unit cell dimension are important roles in the Mei-Gruneisen equation of state. These two aspects of applications for high pressure study will be elaborated in the following sections. Applications mentioned in Part I for Naphthalene will not be repeated here for n-paraffins.

1. Non-bonded Hydrogen Repulsion Potential

As derived in Eq. (38), Davydov splitting is expressed as a sum of the interaction force constants between q_p (normal coordinate of reference molecule p at site a) and q_{j_b} (normal coordinate of each molecule in b sub-lattice). For the following consideration, q_p is a rocking coordinate of the reference C_2H_4 group, and q_{j_b} is a rocking coordinate of j_b^{th} C_2H_4 group in b sub-lattice. It was shown[55] that Davydov splitting of rocking modes is primarily due to the repulsion potential between non-bonded hydrogens. The summation in Eq. (38), running through j_b is reduced to include only eight C_2H_4 groups surrounding the reference group p as indicated in Fig. 26. Shown in this figure is a cross-section (perpendicular to the chain axis and bisecting a C-C bond) of the orthorhombic unit cell. Employing Eq. (41), factor group splittings of rocking modes are simply as follows;

$$\Delta\nu = \frac{1}{4\pi^2\nu_o c}\left[8\left(\frac{\delta^2 U_{23}}{\delta r_{23}{}^2}\right)\left(\frac{\delta^r 23}{\delta^r 2}\cdot\frac{\delta^r 2}{\delta q_{j_b}}\right)\left(\frac{\delta^r 23}{\delta^r 3}\cdot\frac{\delta^r 3}{\delta^q p}\right)\right.$$

$$+\ 8\left(\frac{\delta^2 U_{13}}{\delta r_{13}{}^2}\right)\left(\frac{\delta^r 13}{\delta^r 1}\cdot\frac{\delta^r 1}{\delta q_{j_b}}\right)\left(\frac{\delta^r 13}{\delta^r 3}\cdot\frac{\delta^r 3}{\delta q_p}\right)$$

$$\left.+\ 4\left(\frac{\delta^2 U_{24}}{\delta r_{24}{}^2}\right)\left(\frac{\delta^r 24}{\delta^r 2}\cdot\frac{\delta^r 2}{\delta q_{j_b}}\right)\left(\frac{\delta^r 24}{\delta^r 4}\cdot\frac{\delta^r 4}{\delta q_p}\right)\right]_o \qquad (60)$$

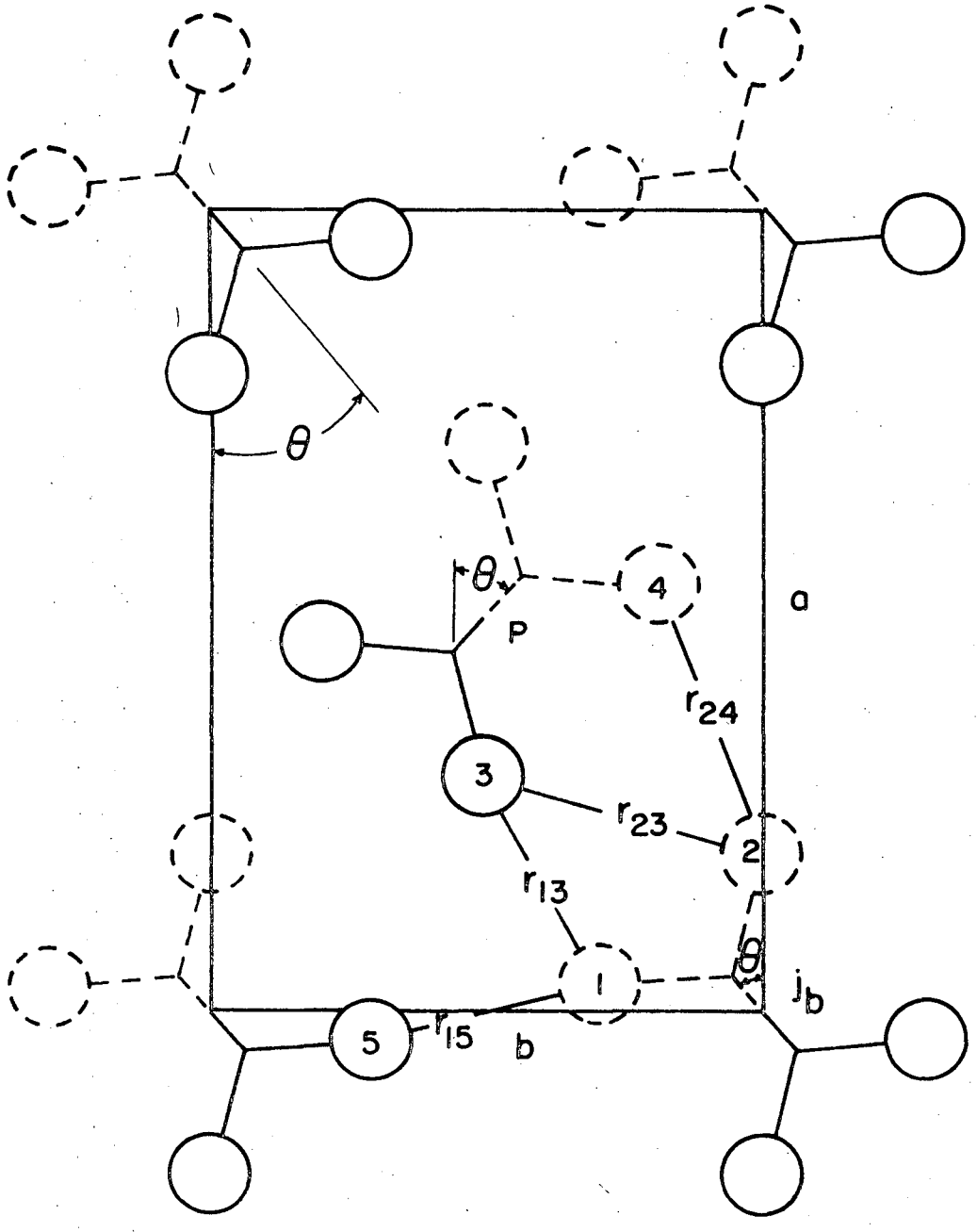

XBL 7110-7393

Fig. 26 A cross section (perpendicular to chain axis) of the orthorhombic n-paraffin unit cell.

Where U_{mn} is the interaction potential between non-bonded hydrogens of different chains. $r_{2,3}$, $r_{1,2}$, and $r_{2,4}$, defined in Fig. 26, are 2.954Å, 2.925Å and 2.586Å respectively at static equilibrium and 1 atm. These figures are calculated from the values of unit cell dimensions reported by Swan,[56,54] i.e. a = 7.414Å, b = 4.942Å, 2C = 2.5473Å and the setting angle $\theta = 48°$. The next nearest pair of hydrogen separation is 3.7 A. This pair and all the other pairs at greater separations are considered as non-interacting.

As mentioned previously, Davydov splitting of rocking modes is primarily due to the repulsion potential between non-bonded hydrogens.[55] One may assume a functional form for the interaction potential between non-bonded hydrogens as

$$U_{mn} = Ar_{mn}^{-B} \tag{61}$$

Where A and B are parameters to be determined. The force constant β is

$$\beta = \left(\frac{\delta^2 U_{mn}}{\delta r_{mn}^2}\right)_o = B(B+1)A\left[r_{mn}^{-(B+2)}\right]_o \tag{62}$$

Upon substituting Eq. (62) into Eq. (60), one gets

$$\Delta\nu = c\left[r_{mn}^{-(B+2)}\right]_o = F[(r_{mn})_o] = F(P) \tag{63}$$

Where c includes the directional cosines and coordinate transformation matrix elements in Eq. (60). If the ab planes of n-paraffins contract isotropically and if c remains constant at various pressures (this is

already implied in Eq. (38)), it was revealed[57] that $dV_p \propto d[(r_{mn})_o]^2$. Where V_p is the unit cell volume for odd numbered n-paraffins or polyethylene at P kbar. We obtain from Eq. (63)

$$B + 2 = -\frac{d\ \mathrm{Log}\ \Delta\nu}{d\ \mathrm{Log}(r_{mn})_o} = 2\frac{d\mathrm{Log}\Delta\nu}{(-\ d\mathrm{Log}\ V_p)} \tag{64}$$

$\frac{1}{2}(B + 2)$ is the slope of log $\Delta\nu$ vs. $\log(V_p)^{-1}$ plot, which is readily available from our high pressure measurements. As shown in Fig. 27, the slopes obtained for three rocking modes, R_1^{∞}, R_1^{29} and R_{17}^{23} are identical within experimental error. The deviation of the dashed curve from the upper straight line may be a consequence of the volume dependence of the parameters A and B, if not due to experimental errors. Assuming that A and B are constants for $2.33 < (r_{mn})_o < 2.954$Å, B is obtained from Fig. 27 to be 6.4 ± 0.4. This is in excellent agreement with Amdur's result,[58] $B = 6.18$, $2.09 < r_{H.H} < 2.77$ A, from molecular beam scattering experiments.

The directional cosines as well as the coordinate transformation matrix elements included in the constant C of Eq. (63) may be calculated from the result of the normal coordinate analysis by Tasumi and Shimanouchi.[53,54] Nevertheless, in their normal coordinate analysis of infinitly extended polyethylene crystals,[54] three β values at $(r_{13})_o$, $(r_{23})_o$ and $(r_{24})_o$ were selected to obtain a good fit to the observed Davydov splittings at 1 atm. By imposing $\beta = 0.0165$ m dyne/Å for $r_{H,H} = 2.586$ A (The value used is an average value for their two sets of calculations) on Eq. (63), and $B = 6.4$. We obtain

$$\beta = 48.6r^{-8.4}\ \text{m dyne/Å} \tag{65}$$

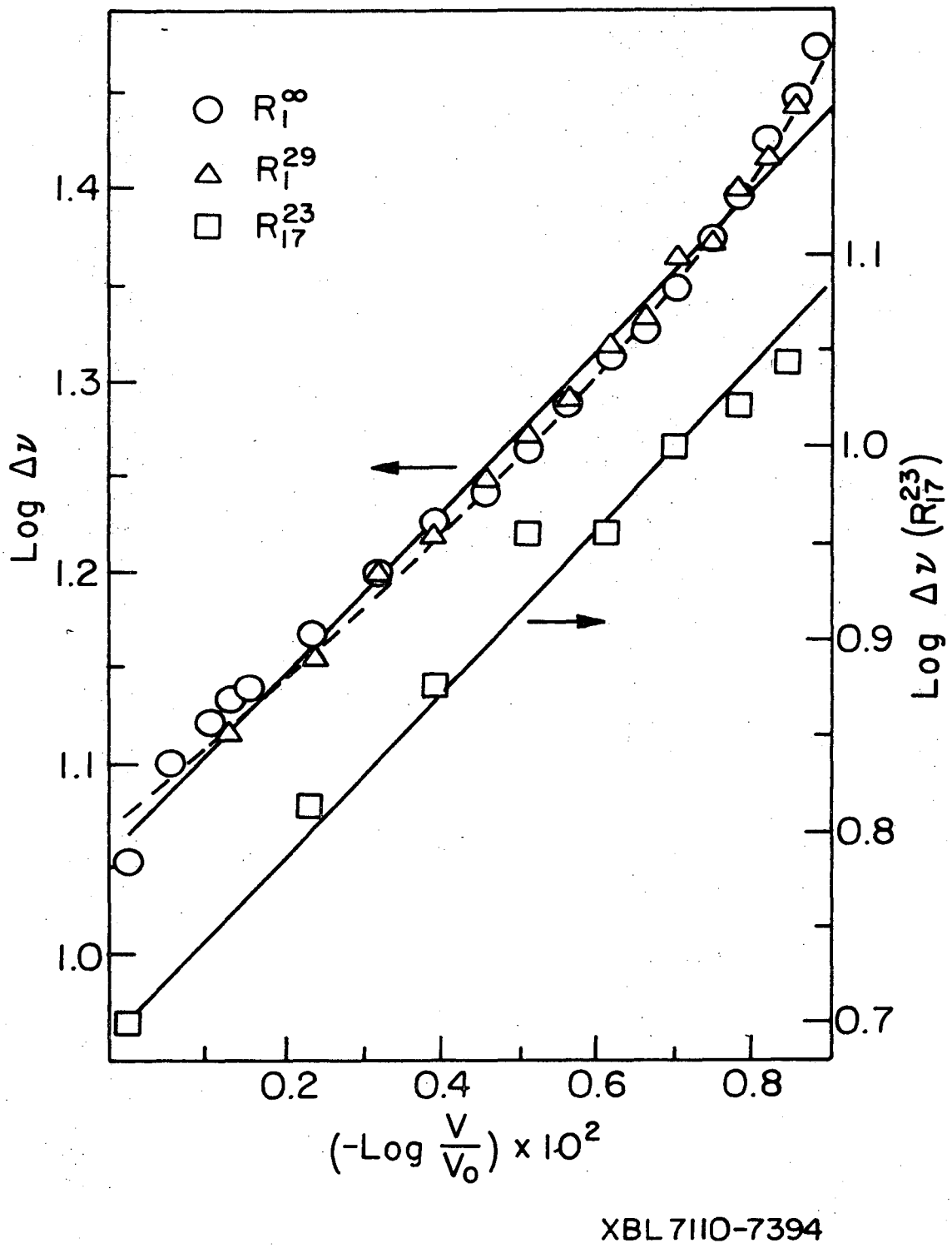

Fig. 27 Log Δν vs Log(v_o/v) for three rocking modes.

In comparing this equation with that obtained by De Bore[59] for the hydrogen repulsion potential, it is significant to look into the implications of this excellent agreement as shown in Fig. 28. Since these two equations are derived from different systems with various assumptions, the agreement is beyond expectation. As was mentioned, the exponential, B, obtained in this study also agrees with Amdur's result from his scattering experiment. However, the coefficient A is off by a factor of two.

2. Volume and Wave Vector Dependence of Gruneisen Parameters

If one defines a CH_2 molecular crystal as a hypothetical crystalline polyethylene with no chemical bond between methylene groups, the vibrational energy levels of this hypothetical crystal, plotted in an extended zone scheme, would consist of nine energy bands corresonding to three translational phonon, three rotational phonon and three internal vibrational exciton bands. The six phonon bands would be distributed in the frequency range from zero to approximately 200 cm^{-1}. The exciton bands could be approximated by Einstein model and have a great density of state at approximately 1400, 2850 and 2900 cm^{-1} for bending, symmetric and asymmetric stretching modes respectively. The heat capacity of this hypothetical substance would approach a constant value of 6R as temperature increasingly approaches 300°K. All of the external modes contribute to the heat capacity at room temperature. However, for crystalline n-paraffins or polyethylene, the strong C-C bond along the chain direction causes the upper energy limit for the external (refer to methylene group) energy levels to reach the value for bending modes. That is, there is no band gap between external and internal energy levels. One would then expect that the heat capacity

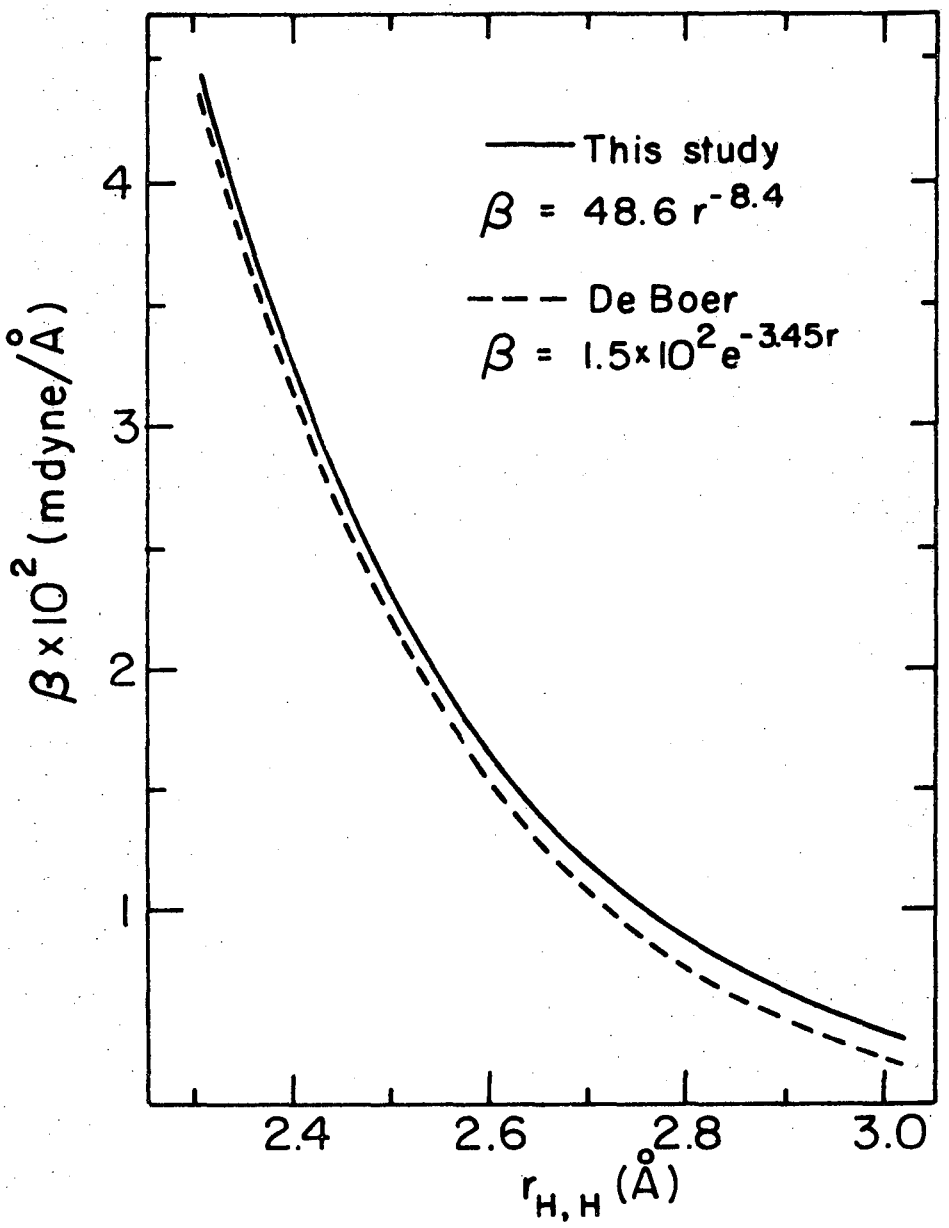

XBL7110-7395

Fig. 28 Second derivative of the interaction potential between non-bonded hydrogens vs $r_{H,H}$.

of n-paraffins and polyethylene would not level off at room temperature and increase with temperature (up to 2100°K, C_v could approach 7R asymptotically if crystalline n-paraffins did exist at this temperature). At room temperature, not all of the external modes of methylene groups contribute to the heat capacity of n-paraffins. Similary, not all of the external modes contribute significantly to the thermal pressure (to be defined later) of n-paraffins or polyethylene. However, there is no clear cut number of normal modes which contribute to the thermal pressure at any temperature.

A significant portion of external (refer to methylene group) energy levels are observed in the IR spectra of n-paraffins. Gruneisen parameters defined as $d \ln\nu / d \ln V$ may readily be calculated from Tables 7,8 and 9 for rocking, wagging, and bending modes. These parameters may give us an idea about the relative contribution of various normal modes to the thermal pressure at a given temperature.

The wave vector as well as the volume dependence of Gruneisen parameters is essential to the understanding of the Mei-Gruneisen equation of state. Since both wave vector and volume dependence of Gruneisen parameters for some vibration modes can also be calculated from our high pressure data presented in Tables 7, 8 and 9, n-paraffins offer us a very rare example for studying these dependences.

The Gruneisen parameters as well as their volume and wave vector dependence to be presented below is applicable to the study of the equation ofstate for crystalline polymers. The Mei-Gruneisen equation of state was originally derived for metals and alkali halide crystals[60] and is not yet familiar in the field of polymers. Therefore, we will re-define the Gruneisen parameters to a greater detail and illustrate

the significance for obtaining their volume and wave-vector dependence.

One may write the Mei-Gruneisen equation of state for the extended crystalline polyethylene or n-paraffins as

$$P = -\frac{dU_o}{dV} + \frac{1}{V}\sum_{i}^{9}\sum_{j}^{N}\gamma_{ij}\left(\frac{1}{e^{h\nu_{ij}/kT}-1} + \frac{1}{2}\right)h\nu_{ij} \tag{66A}$$

$$\gamma_{ij} = -\frac{d\mathrm{Log}\nu_{ij}}{d\mathrm{Log}V} \tag{66B}$$

The observed (external) pressure P is equal to the internal pressure (defined as the first term on the right side of Eq. (66A)) plus thermal pressure (second term). U_o is the static lattice potential defined in Eq. (28) of Chapter II. An isolated polyethylene chain may be considered as a one dimensional crystal of the methylene groups and the crystalline polyethylene as a very anisotropic three dimensional crystal of the methylene groups. There are nine degrees of freedom for an isolated methylene group. In the crystalline state, each of the nine modes of motion splits into N normal modes of the crystal and forms one band of energy levels. N is equal to the number of methylene groups in the entire crystal. As we have mentioned before, only part of the 6N external modes (refer to methylene group) contributes significantly to the thermal pressure. We could replace the upper limit of the summation 9N by 6xN, where $x < 1$. However, x is unknown and is temperature dependent. We shall keep the more general form and leave 9N in the following equations. Each of the N normal modes in the ith energy band have a vibrational frequency ν_{ij} and is specified by a unique phase difference between the vibrational motion of neighboring methylene groups. The frequency-phase relationship is usually unknown

and is generally approximated by the Einstein model for the optical bands and by the Debye model for the acoustic bands. To this approximation, Eq. (66A) is reduced to

$$P = -\frac{dU_o}{dV} + \frac{1}{V}\sum_{i=1}^{9}\gamma_i\sum_{j=1}^{N}\left(\frac{1}{e^{h\nu_{ij}/kT}-1} + \frac{1}{2}\right)h\nu_{ij} \tag{67A}$$

$$\gamma_i = -\frac{dLog\theta_i}{dLogV} \tag{67B}$$

Where θ_i is either an Einstein or Debye temperature for the ith band of energy levels. If it is proper to represent all nine bands with a single Debye temperature, one can further reduce Eq. (67A) to

$$P = -\frac{dU_o}{dV} + \frac{\gamma}{V}\sum_{i=1}^{9}\sum_{j=1}^{N}\left(\frac{1}{e^{h\nu_{ij}/kT}-1} + \frac{1}{2}\right)h\nu_{ij} \tag{68A}$$

$$\gamma = -\frac{dLog\theta}{dLogV} = \frac{V\alpha}{C_v\chi} \tag{68B}$$

Where α, C_v and χ are thermal expansion coefficient, heat capacity and compressibility respectively. γ_{ij} is to be called a microscopic Gruneisen parameter and γ as a macroscopic Gruneisen parameter. The knowledge of the macroscopic Gruneisen parameter as a function of volume and temperature is necessary for the calculation of the equation of state. However, the volume and temperature dependence of α, C_v and χ are very seldom available for any substance. Therefore, the macroscopic Gruneisen parameter γ is usually regarded as a constant.

To the first order perturbation treatment, vibrational frequency, and thus the microscopic Gruneisen parameter are independent of temperature, i.e. $(\delta\nu_{ij}/\delta T)_v = (\delta\gamma_{ij}/\delta T)_v = 0$. The volume dependence of microscopic Gruneisen parameters is readily obtained for optical active modes, when the vibrational frequencies as a function of unit cell dimension are measured with good precision. As shown in Fig. 29, $\nu_a(R_1^{\infty})$ is plotted as a function of volume, pressure and temperature. The open circles represent our compression data. Pastine's P-V relation[57] is used and is indicated in the upper and lower abscissa. The closed circles are low temperature data at 1 atm. by M. Shen, et al.[61] Their T-V relation from x-ray measurement is also included. The very good agreement in slope for these two sets of data may imply the following: (1) Microscopic Gruneisen parameter for R_1^{∞} is independent of temperature. (2) Pastine's theoretical P-V relation is quite good.

The volume dependence of Gruneisen parameters (e.g. the slopes of the curve in Fig. 29 at various volumes) is obatined for $\nu_a(R_1^{\infty})$ and $\nu_a(B_1^{\infty})$ as shown in Fig. 30. The microscopic Gruneisen parameter for both the in-phase bending B_1 and rocking R_1 modes increase with decreasing unit cell volume. The smaller γ_{ij} value for the bending mode is increased faster with pressure than that of the rocking mode which has a larger γ_{ij} value. This might be a general trend. At infinite pressure, one would imagine all the molecular crystals to become atomic crystals or metal and thus, the Gruneisen parameters of internal modes could approach the values for the external modes.

In addition to the volume dependence, if the wave vector dependence of the microscopic Gruneisen parameters were known, the

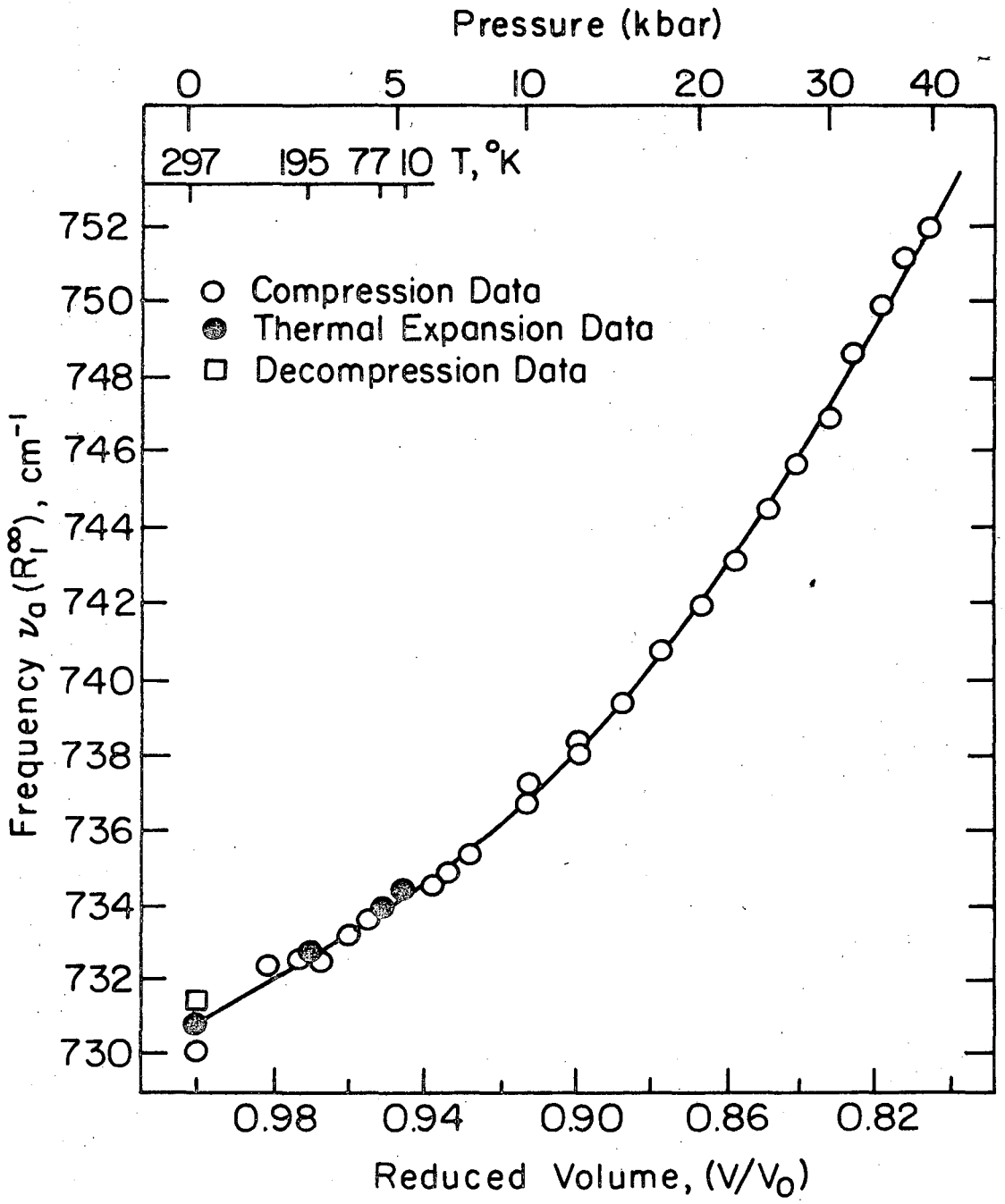

XBL 7110-7396

Fig. 29 $\nu_a(R_1^\infty)$ vs pressure, volume and temperature.

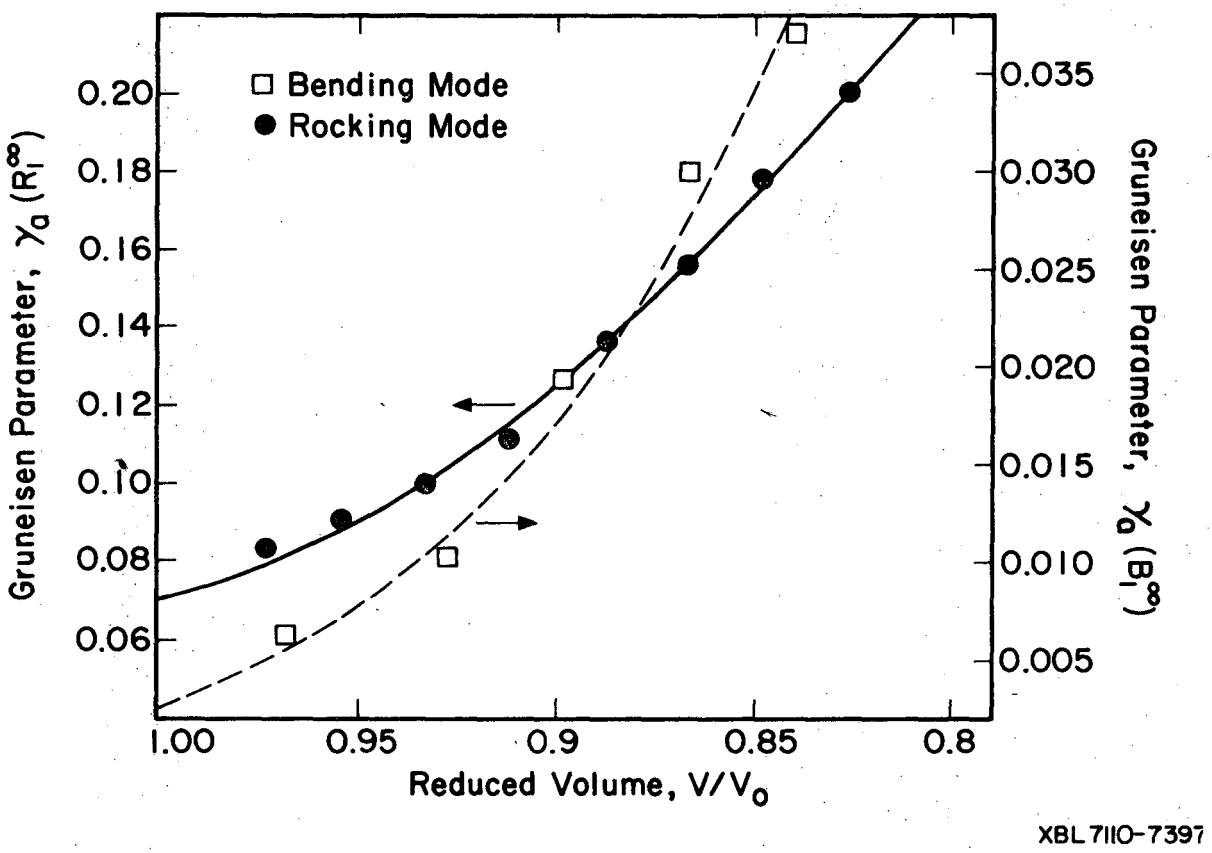

Fig. 30 Gruneisen parameters of polyethylene rocking and bending modes vs volume.

more general equation of state, Eq. (66A), can be readily applied to any substance. The high pressure IR measurement of n-paraffins offers us a starting point along this direction, since dispersion curves (e.g. Fig. 13) are obtained at various pressures. The phase dependence of $\gamma_a(R_m^{23})$ and $\gamma_b(R_m^{23})$ is calculated and shown in Fig. 31. The Gruneisen parameter of b-factor group component is nearly phase-independent. This can be understood from Eq. (35) as due to the cancellation of two dynamic force constants. The Gruneisen parameter of a-factor group component is strongly phase dependent owing to the addition of two resonance interaction force fields. In conjunction with this plot, it is obvious that for a substance with more than one molecule per unit cell, the Gruneisen parameters of those vibration modes which show no factor group splitting are phase independent. In such a case, the Gruneisen parameter for the whole branch may be determined from the observed in-phase mode alone.

Although the volume and wave vector dependences of Gruneisen parameters are obtained for the first time for n-paraffins and polyethylene, a number of values were reported for Gruneisen parameters at 1 atm. in the literature as a result of various types of measurements, e.g. ultrasonic, thermal conductivity, and far infrared measurements. It is not surprising that various measurements give very different values (e.g. 0.25 to 11 for polyethylene), since properties of different vibrational modes are measured. Namely, an Avogadro number of γ_{ij} values could be different from each other. The macroscopic γ differs from the value for any of γ_{ij} or γ_i in general. However, this was not yet familiar in the field of polymer science. γ_{ij}, γ_i and γ were not distinguished. Questions as to why one value is different from those

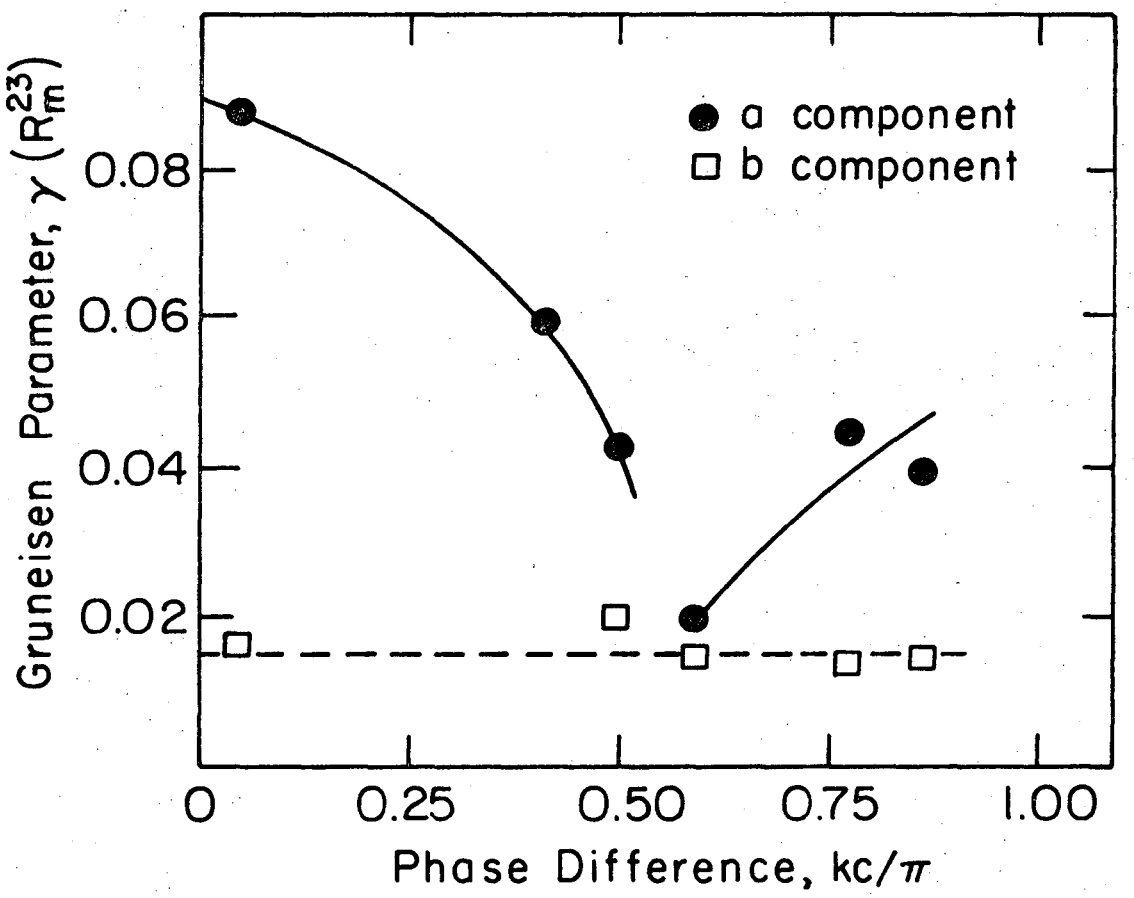

XBL7110-7398

Fig. 31 Gruneisen parameters of n - $C_{23}H_{48}$ rocking modes vs phase difference kc/π.

obtained by others were open in the literature of polymers. This question was presented and discussed by the author to the polymer section at the ACS meeting of April, 1971.

We shall end this section with a discussion on Table 10, which was presented in the ACS meeting to compare our calculated Gruneisen parameters for various normal modes. γ_{ij} for the bending and rocking modes are obtained from our high pressure infrared data (e.g. Fig. 30). The γ_{ij} value for the 71 cm^{-1} translational lattice mode is calculated* from Bank and Krimm's[62] low temperature measurement. The Gruneisen parameter for the translational mode is larger than that for the libration mode (rocking mode). In turn, this is larger than the value obtained for the internal mode. This is expected for the following reason. The smaller the frequency of a normal mode, the larger is its amplitude of vibration at a given temperature. The normal mode is thus affected more by the change of intermolecular distances and has a larger γ_{ij} value.

Owing to recent calculations of P-V relation by Pastine[57] and thermal expansion coefficient by Shen,[61] it becomes possible for us to calculate the macroscopic Gruneisen parameter from Eq. (68B). The macroscopic Gruneisen parameter calculated from the value of C_v by Wunderlich,[63] α by Shen and χ by Pastine, has a value of 1.3. This value is probably more reasonable than the value of 0.25[61] or 7.5[64] in the literature.

---

* γ_{ij} value for 71 cm^{-1} translational mode was calculated to be 0.43 by Barker and Chen. They also used the far infrared data of Bank and Krimm. However, they defined $\gamma = d \ln \nu(x)/d \ln (\rho(x))$ where ν and ρ are vibration frequency and the density for polyethylene. Instead of using pressure or temperature as an independent variable, they changed the crystallinity (x). This is obviously unacceptable.

Table 10. Gruneisen Parameters of Crystalline Polyethylene

$\gamma_{ij} = d \ln \nu / d \ln V$	Bending Mode $\nu_a(B_1^{\infty})$	Rocking Mode $\nu_a(R_1^{\infty})$	Translational Optical Mode
Melt Grown	0.0024	0.070	1.525
Solution Grown			1.28

$\gamma = V\alpha/C_v\chi = 1.3$

ACKNOWLEDGMENTS

The author wishes to thank Professor George Jura for his supervision, guidance and encouragement during the course of this work. Furthermore, for his patience in correcting may English grammar which was a problem for me as a foreign student.

The author appreciates Professor George C. Pimentel's interest in this work, especially the careful reading of this manuscript and the most stimulating discussions and suggestions.

The author also wishes to thank Professors Malcolm Nicol, B. J. Alder, H. L. Strauss, and M. Shen for their helpful discussions.

Special acknowledgment to Mr. D. Newhart for the design and consturction of the high pressure apparatus, without whose help this work could not have been accomplished.

To my wife, whose patience and encouragement have been a source of inspiration throughout my graduate career.

The author also wishes to thank his colleagues, Drs. R. Powell and J. L. Przybylinski, Mr. A. Yee, T. W. Chen and B. Jurado for many interesting and useful lunch hour discussions.

Special thanks to Dr. Malcolm Nicol for furnishing the sample cell and to Dr. A. F. Smith for the pure n-paraffin samples.

This work was done through the auspices of the United States Atomic Energy Commission.

APPENDIX I

Overtone and Combination Transitions

The potential energy surface of a system which has only two vibrational degrees of freedom is a two dimensional surface. A paraboloid surface is the so called harmonic potential. The energy levels of the stationary states as solved from the Schrodinger equation are

$$E(v_1, v_2) = h\nu_1(v_1 + \frac{1}{2}) + h\nu_2(v_2 + \frac{1}{2}) \qquad \text{(A-I.1)}$$

The energy levels as well as the allowable transitions are indicated in Fig. A-1. It is seen from Eqs. (6), (7), (8) and (9) that in order to excite the system to energy levels (0,2) (2,0) or (1,1) from (0,0), two photons are required. This is because

$$\sum_{i}^{2} \left(\frac{\partial\mu}{\partial Q_i}\right) \int_{o} \Phi_{v'}^{*} Q_i \Phi_v dQ_1 dQ_2 = 0$$

Unless

$$|\Delta v_1| + |\Delta v_2| = 1$$

When the system has either electrical or mechanical anharmonicity, the above restirction no longer exists. A single photon with energy of roughly $(h\nu_1 + h\nu_2)$ could excite the system from ground state to energy level E(1,1).

Classically, the relative motion of the atoms in the system can be represented by the motion of a single mass point under the action of

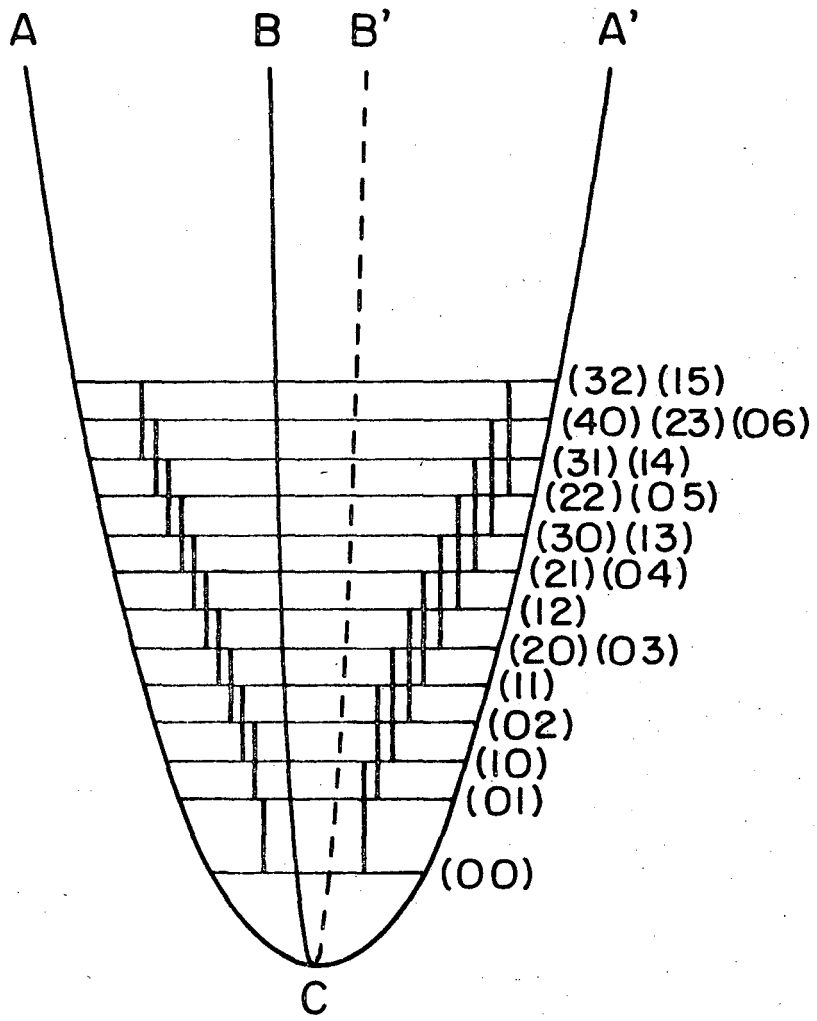

XBL 7110-7399

Fig. A-1. The energy levels (each horizontal line represents a horizontal energy surface $E(v_1, v_2)$ and the allowable transitions for a two-dimensional harmonic oscillator ($\nu_1 = 3/2\ \nu_2$)

gravity on the potential surface. When the mass point starts from any point on the paraboloid surface, the motion can be resolved into two normal motions along ACA' and BCB'. Each one of the normal motions is a simple harmonic motion of all atoms with a single frequency. If the normal motion ν_1(ACA') is connected with a change of dipole moment of the system, the amplitude of the normal motion may be increased by absorbing the radiation of frequency ν_1.

If the paraboloid surface is distorted in such a way that when the mass point starts at A, it will carry out a Lissajous motion and will fill a larger and larger area about ACA'. This distorted surface is a potential surface with slight anharmonicity. Now the motion of each atom is no longer periodic. The normal coordinate η(ACA')(a loose term representing motion around ACA') may be expressed as

$$\begin{aligned}\eta(ACA') = {} & \eta_{10}\cos(2\pi\nu_1 t + \theta_1^{10}) + \eta_{20}\cos(2\pi 2\nu_1 t + \theta_1^{20}) \\ & + \eta_{30}\cos(2\pi 3\nu_1 t + \theta_1^{30}) + \ldots\ldots \\ & + \eta_{11}\cos(2\pi\nu_1 t + \theta_1^{11})\cos(2\pi\nu_2 t + \theta_2^{11}) \\ & + \eta_{21}\cos(2\pi 2\nu_1 t + \theta_1^{21})\cos(2\pi\nu_2 t + \theta_2^{21}) + \ldots \qquad \text{(A-I.2)}\end{aligned}$$

The vibrational motion contains the frequencies $2\nu_1$, $3\nu_1$, $\nu_1 \pm \nu_2$, $2\nu_1 \pm \nu_2$ and so forth. The system can thus also absorb photons of these frequencies. The probability of absorbing the $(2\nu_1)$ photon is proportional to $(\eta_{20})^2$ which is very much smaller than $(\eta_{10})^2$. The amplitude of ACA' normal motion which has a major component of η_{10} is increased irrespective of the energy of the photon abosrbed.

APPENDIX II

An Estimation of the Separation of an Unresolved Doublet

Two factor group components of $\nu(R_{17}{}^{23})$ are observed at various pressure (See Fig. 15 and 23). The doublets are not entirely resolved. However, the peak positions of this doublet may be determined by assuming a Gaussian band shape for each component. The separation $\Delta\nu_{splitting}$ (P), for the doublet at each pressure is plotted vs. the half width $\Delta\nu_{1/2}(P)$ of the doublet at the corresponding pressures in Fig. 33. A linear relationship is obtained between $\Delta\nu_{splitting}$ (P) and $\Delta\nu_{1/2}(P)$. Namely

$$\Delta\nu_{splitting}(P) = (0.91 \pm 0.05)\,[\Delta\nu_{1/2}(P) - \Delta\nu_{1/2}(P=0)] + \Delta\nu_{splitting}(P=0) \qquad \text{(A-II.1)}$$

In the progression of absorption bands for rocking modes, the intensity ratio of two factor group components is nearly unity for all of the doublets. Therefore, one may expect Eq. (A-II.1) to hold equally for all the doublets in this series. The doublets for $\nu(R_{11}{}^{23})$ and $\nu(R_{13}{}^{23})$ are resolved[50] at -180°C and atmospheric pressure with a Beckman IR 7 spectrophotometer. However, even at 40 kb, they are not resolved with a dispersion system of a sodium chloride prism alone. The separations of these two doublets tabulated in Table 7 are calculated from Eq. (A-II.1) by assuming that $\Delta\nu_{splitting}$ (P=0) is independent of temperature.

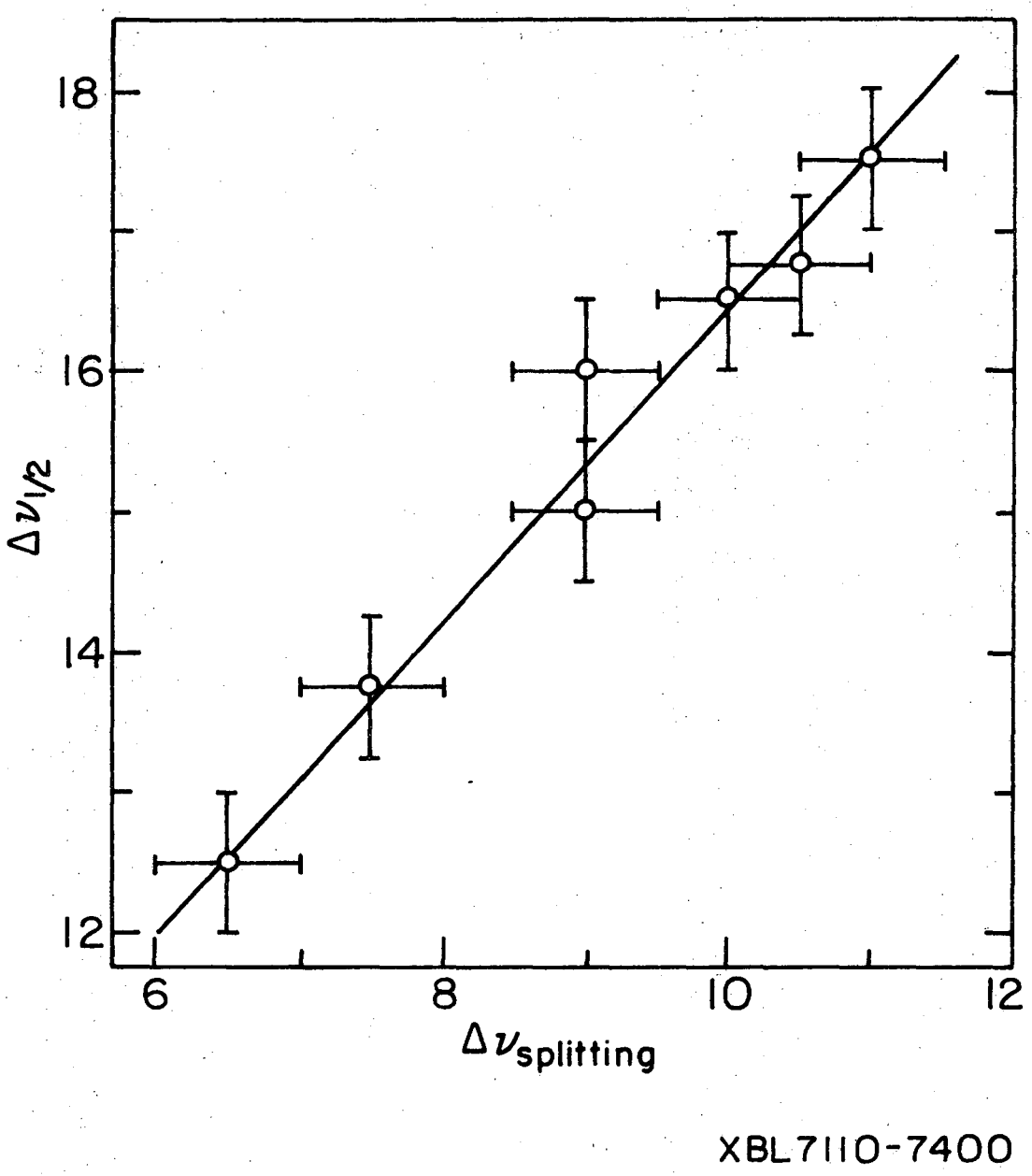

Fig. A-2. Experimental relation between the separation and half width of a doublet.

REFERENCES

1. J. Frankel, Phys. Rev. 37, 17, 1276 (1931).

2. A. S. Davydov, Theory of Molecular Excitons [translated by M. Kasha and Max Oppenheimer, Jr.] (McGraw-Hill, N. Y., 1962).

3. D. P. Craig and S. H. Walmsley, Excitons in Molecular Crystals (W. A. Benjamin, Inc., 1968).

4. D. L. Dexter and R. S. Knox, Excitons

5. D. Fox and O. Schnepp, J. Chem. Phys. 23, 767 (1955).

6. D. S. McClure, Solid State Phys. 8, 1 (1959).

7. D. F. Hornig, J. Chem. Phys. 16, 1063 (1948); Discussions Faraday Soc. 1950, 115

8. H. Winston and R. S. Halford, J. Chem. Phys. 17, 607 (1949).

9. R. M. Hexter, J. Chem. Phys. 33, 1833 (1960).

10. C. Hass, Spectrochim Acta, 8, 19 (1956).

11. R. S. Halford, Ann. N. Y. Acad. Sci. 69, 63 (1957).

12. G. Duyckaerts, Analyst, 84, 201 (1959).

13. R. M. Hexter, Ann. Rev. Phys. Chem. 10, 389 (1959).

14. W. Vedder and D. F. Hornig, Advance Spectra 2, 189 (1961).

15. D. A. Dows, Phys. Chem. Org. Solid State 1, 657 (1963); 2, 881 (1965); J. Chim. Phys. 168 (1966).

16. Any Quantum Mechanical book on time dependent perturbation theory.

17. E. B. Wilson, J. C. Decius, and P. C. Cross, Molecular Vibrations (McGraw-Hill, N. Y., 1955).

18. R. S. Halford, J. Chem. Phys. 14, 8 (1946).

19. D. P. Graig, J. Chem. Soc. 539, 2302 (1955).

20. W. B. Person, G. C. Pimentel, and O. Schnepp, J. Chem. Phys. 23, 230 (1955).

21. W. Kauzmann, Quantum Chemistry (Academic Press, N. Y., 1957) p. 583.

22. N. Q. Chako, J. Chem. Phys. 2, 644 (1934).

23. J. M. Ziman, Principles of the Theory of Solids (Cambridge University Press, 1965).

24. R. de L. Kronig, J. Opt. Soc. Am. 12, 547 (1926).

25. T. S. Robinson and W. C. Price, Proc. Phys. Soc. B66, 969 (1953).

26. E. Fishman and H. G. Drickamer, Anal. Chem. 28, 804 (1956).

27. C. E. Weir, E. R. Lippincott, van Valkenburg and E. N. Bunting, J. Res. Nat'l. Bur. Standards A63, 55 (1959).

28. A. S. Balchan and H. G. Drickamer, Rev. Sci. Instr. 31, 511 (1960).

29. C. K. Wu, M. S. Thesis, University of Hawaii (1967).

30. C. K. Wu and G. Andermann, J. Opt. Soc. Am. 58, 4, 519 (1968).

31. G. Andermann, C. K. Wu and E. Duesler, J. Opt. Soc. Am. 58, 12, 1663 (1968).

32. D. W. J. Cruickshank, Acta Cryst. 10, 504 (1957).

33. N. Claverie, J. Chim. Phys. 61 (6), 889 (1964).

34. G. C. Pimentel and A. L. McClellan, J. Chem. Phys. 20, 270 (1952).

35. R. R. Wiederkehr and H. G. Drickamer, J. Chem. Phys. 28, 311 (1958).

36. G. Herzberg, Infrared and Raman Spectra of Polyatomic Molecules (Van Nostrand Reinhold Company, 1945).

37. E. Fermi, Z. Physik 71, 250 (1931).

38. G. Herzberg, Spectra of Diatomic Molecules (Van Nostrand Reinhold Company, 1950).

39. S. S. Mitra and H. J. Berstein, Can. J. Chem. 37, 533 (1959).

40. H. Luther and H. J. Drewitz, Z. Electrochemie 546 (1962).

41. A. D. Dows, J. Chem. Phys. 36, 2836 (1962); 32, 1342 (1960); 35, 282 (1961).

42. A. D. Dows, Molecular Crystals 5, 111 (1968).

43. G. C. Pimentel, Pure and Appl. Chem. 4, 61 (1962).

44. J. C. Decius, J. Chem. Phys. 23, 1290 (1955).

45. H. Primas and H. H. Gunthard, Helv. Chim. Acta 36, 1659 (1953).

46. H. Primas and H. H. Gunthard, Helv. Chim. Acta 36, 1791 (1953).

47. J. K. Brown, N. Sheppard, and D. M. Simpson, Trans. Roy. Soc. A247 35 (1954).

48. J. K. Brown, N. Sheppard, and D. M. Simpson, Disc. Faraday Soc. 9, 261 (1950).

49. R. G. Snyder, J. Mol. Spectroscopy 4, 411 (1960).

50. R. G. Snyder, J. Mol. Spectroscopy 7, 116 (1961).

51. M. Tasumi and T. Shimanouchi, J. Mol. Spectroscopy 9, 261 (1962).

52. M. Tasumi and T. Shimanouchi, J. Mol. Spectroscopy 11, 422 (1963).

53. M. Tasumi and T. Shimanouchi, J. Chem. Phys. 43, 1245 (1965).

54. M. Tasumi and S. Krimm, J. Chem. Phys. 46, 755 (1967).

55. R. S. Stein, J. Chem. Phys. 23, 734 (1955).

56. P. R. Swan, J. Polymer Sci., 56, 403 (1962).

57. D. J. Pastine, J. Chem. Phys. 49, 3012 (1968).

58. I. Amdur and M. S. Longmire, J. Chem. Phys. 35, 895 (1961).

59. J. de Boer, Physica 9, 363 (1942).

60. M. Born and K. Huang, Dynamical Theory of Crystal Lattices

61. M. Shen, W. N. Hansen, and P. C. Romo, J. Chem. Phys. 51, 425 (1969).

62. M. I. Ban and S. Krimm, Bull. Am. Phys. Soc. 13, 354 (1968).

63. B. Wunderlich, J. Chem. Phys. 37, 1203 (1962).

64. M. G. Broadhurst and F. I. Mopsik, J. Chem. Phys. 52, 3634 (1970).

65. A. E. Smith, J. Chem. Phys. 21, 2229 (1953).

66. M. Nicol, J. Opt. Soc. Am. 55, 1176 (1965).

67. M. Y. Fong and M. Nicol, J. Chem. Phys. 54, 579 (1971).

LEGAL NOTICE

This report was prepared as an account of work sponsored by the United States Government. Neither the United States nor the United States Atomic Energy Commission, nor any of their employees, nor any of their contractors, subcontractors, or their employees, makes any warranty, express or implied, or assumes any legal liability or responsibility for the accuracy, completeness or usefulness of any information, apparatus, product or process disclosed, or represents that its use would not infringe privately owned rights.

TECHNICAL INFORMATION DIVISION
LAWRENCE BERKELEY LABORATORY
UNIVERSITY OF CALIFORNIA
BERKELEY, CALIFORNIA 94720